COAL FIRED POWER PLANT WATER CHEMISTRY ISSUES: AMINE SELECTION AT SUPERCRITICAL CONDITIONS AND SODIUM LEACHING FROM ION EXCHANGE MIXED BEDS

By

JOONYONG LEE

Bachelor of Science in Chemical Engineering
Kangwon National University
Chuncheon, South Korea
1995

Master of Science in Chemical Engineering
Kangwon National University
Chuncheon, South Korea
1997

Submitted to the Faculty of the
Graduate College of the
Oklahoma State University
in partial fulfillment of
the requirements for
the Degree of
DOCTOR OF PHILOSOPHY
May, 2012

COAL FIRED POWER PLANT WATER CHEMISTRY ISSUES: AMINE SELECTION AT SUPERCRITICAL CONDITIONS AND SODIUM LEACHING FROM ION EXCHANGE MIXED BEDS

Dissertation Approved:

Dr. Gary L. Foutch

Dissertation Adviser

Dr. AJ Johannes

Dr. Martin S. High

Dr. Josh D. Ramsey

Dr. Allen Apblett

Outside Committee Member

Dr. Sheryl A. Tucker

Dean of the Graduate College

TABLE OF CONTENTS

Chapter Page

LIST OF TABLES

Table Page

Table Page

LIST OF FIGURES

Figure Page

Figure Page

Figure Page

CHAPTER I

INTRODUCTION

The primary goal of the power generation industry is to produce electricity at the lowest cost without interruptions. Electrical power generation facilities require a significant amount of high purity water for the steam cycle. The presence of impurities in the steam may result in scale and corrosion. Consequently, it is important that the water be maintained at a quality to reduce the potential of corrosion and scale, thereby reducing the possibility of a reduction in boiler efficiency, unscheduled outages and expensive repairs. Appropriate water treatment is essential to ensure that contaminants and corrosion products do not deposit on the boiler tubes or carryover to the steam turbine. Methods to reduce corrosion, such as water pretreatment, pH control within the steam cycle, and replacement of piping to less impacted materials are worth investigating.

1.1. Coal-Fired Power Plants

Coal has a major role in electricity generation worldwide. According to U.S. Energy Information Administration (http://www.eia.gov, 2010), coal-fired power plants generate 44.9% for global electricity, followed by 23.8% for natural gas, and 19.6% for nuclear.

A, typical coal-fired steam cycle is shown in Figure 1-1. Basically, the heated water generates steam and runs the turbine which produces electricity. The steam is condensed and polished before liquid water is returned to the boiler.

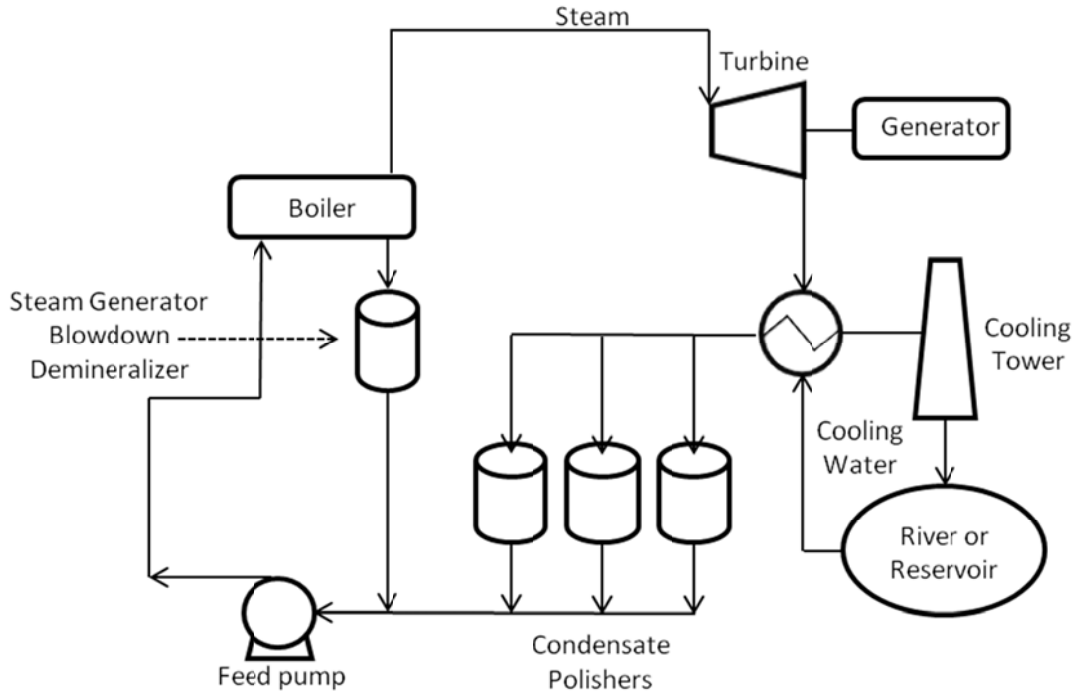

Figure 1-1. Schematic diagram of coal-fired power plant

Water as a working fluid is subjected to wide variations in temperature and pressure in the cycle by compression, heating, expansion, and heat rejection. Temperature may range from 21 to 650°C with pressure from 0.5 to 5000 psi (Flynn, 2009). Drum-type boilers operate normally below the critical pressure of water. At these conditions, the steam is two phase (quality less than 100%). The mixture exiting the boiler is separated in the drum so that steam is transferred to the turbine. In general, the concentrated impurities dissolve in the denser water phase and volatile contaminants can be removed by blowdown. The suspended and total dissolved solids can be removed as

sludge from the bottom of the boiler. It is possible to control purity by steam separation. Therefore, a condensate polisher is not necessary in drum-type boilers. However, blowdown is less effective at the critical point because of the narrow difference in densities between steam and water; so supercritical steam generators (once-through plants), require additional purification steps, such as condensate polishers. Pocock (1979) reported that vaporous carryover is predominant in the drum above 2800 psig. Cooper and Dooley (2008) also reported that vaporous carryover becomes significant for the solids dissolved in the boiler water about 2300 psig.

Thermodynamic efficiency of a coal-fired boiler describes how much thermal energy fed into the cycle is converted into electrical energy. Conventional subcritical coal fired power plants operating at the steam pressure and temperature below 22.0 MPa (~3200 psi) and about 550°C typically achieve 34-36% thermal efficiency. The first coal-fired supercritical cycle began operation in 1957 in the U.S and the demand for supercritical units will expand (Ness et al., 1999). In order to improve efficiency, supercritical coal fired power plants, operating at 565°C and 24.3 MPa, have efficiencies in the range of 38-40%. Most supercritical units operate at a nominal 3800 psig and have a turbine throttle inlet pressure of 3500 psig. The highest design pressure for a unit is about 5000 psig with actually operation at about 4500 psig (Flynn, 2009).

1.2. Ultrapure water

All power cycles require relatively high purity water although the degree of purity depends on operating conditions. Although numerous contaminants are found in water, most may be removed with unit operations such as reverse osmosis, ion exchange,

electrodeionization, activated carbon adsorption, and ultra-filtration addressed in Table 1-1.

Table 1-1. Ionic impurities removal in UPW manufacture (Hussey, 2000)

Unit operations	Advantages	Disadvantages
Reverse Osmosis	No chemical Useful for high ionic concentration waters	Limited removal efficiency Brine product stream
Ion Exchange	**Highest removal efficiency** **Relatively economical (high volumetric production rates)**	Regeneration chemicals and system required Generates particles and bacteria
Electrodeionization	No regeneration chemical required High removal efficiency	Fouling potential

Ultrapure water is essential to several industries, including microchip manufacturers (rinse water), electrical generators (make-up, condensate polishing and reactor-water cleanup), chemical companies (ammonia producers), environmental processors (recovery of heavy metals and radioisotopes) and pharmaceutical processing (pharmaceutical grade water production) (Foutch, 1991). In particular, microchip manufactures for microelectronics rinsewater may require sub ppt (part per trillion, ng/L) concentration. This level of purification can only be achieved with mixed bed ion exchange.

Although standards vary among industries, ultrapure water is typically defined as having electrolytic conductivity less than 0.1 micro Seimens per centimeter (μS/cm); whereas theoretical conductivity for absolutely pure water is 0.054 μS/cm (18mΩ, 25°C). To be classified as ultrapure water, the ionic concentrations of sodium, chloride, and sulfate are less than 20 μg/L (Hussey et al., 2008).

1.3. Mixed-Bed Ion Exchange (MBIE)

Mixed-bed ion exchange (MBIE) is an intimate mixture of cationic and anionic resins used to deionize water. A particular advantage of ion exchange is that both cationic and anionic resins can be used together for simultaneous removal of all charged species. MBIE was introduced by Kunin and McGarvey (1951) for the deionization of boiler feed water (Helfferich, 1965). The process is a convenient and economical method for deionization of water to ultrapure concentrations. A mixed bed has cationic and anionic resins generally in the hydrogen and hydroxyl forms, respectively (Helfferich, 1965).

The principal of MBIE is to obtain a charge coupling and neutralization reaction which makes the exchange irreversible according to LeChatlier's principle. It enables the attainment of extremely low impurity levels with a neutralized effluent, as indicated by the following reactions.

$R–OH^- + X^- \rightarrow R–X^- + OH^-$ (anion exchange)

$R–H^+ + M^+ \rightarrow R–M^+ + H^+$ (cation exchange)

$H^+ + OH^- \leftrightarrow H_2O$ (neutralization)

where M^+ is dissociated arbitrary alkali cation and X^- is an arbitrary halide anion. The net effect results in decreasing concentration of hydrogen and hydroxide in the bulk-phase and increasing the driving force across the film for other ions.

For the steam cycle, mixed bed polishers accomplish several goals. Mixed bed polishers reduce the total electrolyte concentration in makeup or boiler feedwater to nearly 0.04 - 0.09 mg/L and silica to 0.01 - 0.05 mg/L. MBIE reduces sodium and silica leakage that occurs at the beginning and end of each operating cycle to provide a more consistent, uniform feedwater quality. These units provide protection against breakthrough of the primary demineralizer units (Hussey et al., 2008).

The service life of MBIE is determined by monitoring the effluent concentration. This includes both equilibrium leakage from residual ionic loading and kinetic leakage from ions entering with the feed solution. In economic aspects, an advantage of ion exchange resins is that they can be regenerated and reused. Resin regeneration efficiency is critical to ultrapure water production because, in most cases, the initial ionic loading caused by inefficient regeneration determines the service life and operating performance.

1.4. Objective

The main objective of this research is to investigate the thermal stability of various amines alternative to ammonia commonly used at high temperature and pressure. An assessment of the amines for their degradation characteristics in supercritical water will be performed. While degradation leads to ineffective pH control, the breakdown products may generate concentrations of undesirable organic acids that may damage materials of construction. Amines with minimal degradation and low undesirable

products will be the best choices for the next generation of steam cycle power plants. As a result, degradation kinetics of alternative amines in water at supercritical conditions will be evaluated.

REFERENCES

Energy Information Administration (EIA), Annual Report, 2010

Pocock, F. J. "Corrosion and Contaminant Control Concerns in Central Station Steam Supply Systems", Presented at the American Society for Metals Conference, Atlanta, Georgia, May 1979.

Cooper, J.R. and Dooley, R.B. "Procedures for the Measurement of Carryover of Boiler Water into Steam," The International Association for the Properties of Water and Steam, Berlin, Germany, September 2008.

Ness, H.N., Kim, S.S., and Ramezan, M. "Status of Advanced Coal-Fired Power Generation Technology Development in the U.S." 13th U.S/Korea Joint Workshop on Energy and Environment, September 1999.

Flynn, D. "The Nalco Water Handbook" New York, McGraw-Hill, 2009.

Hussey, D.F., Foutch, G.L., and Ward, M.A. "Ultrapure Water," Ullmann's Encyclopedia of Industrial Chemistry, 7th Edition, Revision, September 2008.

Katzer, J. "The Future of Coal," Massachusetts Institute of Technology (MIT) Coal Energy Study Advisory Committee, 2007.

Kunin R. and McGarvey, F. ”Mixed bed deionization,” 1951, United States Patent 2578937

Helfferich, F. “Ion-Exchange Kinetics. V. Ion Exchange Accompanied by Reactions,” J. Phys. Chem., 1965, 69 (4), 1178–1187.

Foutch, G. L., "Ion Exchange: Predictive Modeling of Mixed-bed Performance,” *Ultrapure Water,* 8, 47 (1991).

CHAPTER II

WATER CHEMISTRY IN POWER PLANTS

2.1. Introduction

High purity water is used in conventional coal-fired power plants as the working fluid. The proper chemistry to manage water and steam purity is essential to availability and reliability. Normally, feedwater contains impurities such as alkalinity, silica, iron, dissolved oxygen, calcium and magnesium that cause deposits or corrosion in the steam cycle. The major contaminant sources are cooling water inleakage, air inleakage, makeup water, corrosion and combustion products, demineralizers, water treatment chemicals, oils, greases, paints, preservatives, solvents, construction debris, and radioisotopes. There are several ways to purify water in the system. Deaeration is used to strip dissolved gases and filtration is used for removal of insoluble solid impurities; however, undesirable ionic impurities related to corrosion or deposit are removed by ion exchange.

The history of steam cycle chemistry shows ineffective water technology or quality control may lead to corrosion in the system resulting in reduction of efficiency, loss of capability, and outage for cleaning. Chemical treatment can be applied to both

the feedwater and boiler water to minimize corrosion potential, however the first requirement is for high-purity feedwater recycled from the condenser, or added as makeup because it may include corrosive species such as chloride, sulfate, carbon dioxide and organic anions (Friend and Dooley, 2010).

2.2. Corrosion

Corrosion is the disintegration of metal or alloy from exposed to an acidic environment. Steam and water are aggressive fluids at high pressure and temperature because of the tendencies of water to combine with reactive metals to form metal hydroxides, oxides, and hydroxides (DOE, 1993). Corrosion is a complicated combination of various factors and can be controlled by factors; such as pH, temperature, water purity, oxygen concentration and flow rate.

Although corrosion occurs slowly in pure water at room temperature, rate increases at elevating temperature because the properties of the corrosive species such as oxygen, carbon dioxide, chlorides, and hydroxides, are functions of temperature. The reduction step of the oxidation-reduction process is where a positively-charged ion gains an electron. For most metals in an aqueous environment reduction is by hydronium ions. The following reactions apply to pure water without oxygen at room temperature and approximately neutral pH. In case of corrosion in water in the absence of oxygen;

$$Fe \rightarrow Fe^{2+} + 2e^{-}$$

$$2H_3O^{+} + 2e^{-} \rightarrow 2H_2O + H_2$$

The overall reaction is the sum of oxidation and reduction.

$$Fe + 2H_3O^+ \rightarrow Fe^{2+} + 2H_2O + H_2$$

The presence of the ferrous ion (Fe^{2+}) relies on operation temperature, pH and flow rate. For instance, the ferrous ion combines with water to form insoluble ferrous hydroxide ($Fe(OH)_2$) at the metal surface at low temperature. However, the ferrous hydroxide reacts to form magnetite (Fe_3O_4) at temperature above 120°F. Furthermore, the ferrous ion forms magnetite without the ferrous hydroxide formation at higher temperature above 300°F (GE energy, http://www.gewater.com).

$$Fe^{2+} + 2OH^- \rightarrow Fe(OH)_2 \rightarrow FeO + H_2O$$

$$2FeO + H_2O \rightarrow Fe_2O_3 + H_2$$

$$3Fe(OH)_2 \rightarrow Fe_3O_4 + 2H_2O + H_2$$

$$3Fe^{2+} + 4H_2O \rightarrow Fe_3O_4 + 4H_2$$

Oxide film layers, such as wustite (FeO), hematite (Fe_2O_3), and magnetite (Fe_3O_4), form on the metal surface through oxidation and reduction. The metal surface is no longer in contact with acidic aqueous environment because of the magnetite layer, the layer slows down further oxidation reaction by diffusion of the ferrous ions (DOE, 1993).

In general, the corrosion rate, especially for iron, is relatively independent of the pH in the range of 4 to 10. The corrosion rate is governed largely by the rate at which oxygen reacts with hydrogen, thereby depolarizing the surface and allowing reduction to continue.

$$Fe \rightarrow Fe^{2+} + 2e^-$$

$O_2 + 2e^- \rightarrow O^{2-}$

$Fe + O_2 + 2H^+ \rightarrow Fe^{2+} + H_2O$

Copper is also oxidized by hydrogen and oxygen. The overall corrosion reactions are follows;

$2Cu + 2H^+ \rightarrow 2Cu^+ + H_2$

$2Cu + H_2O \rightarrow Cu_2O + H_2$

In general, the stability of both of iron and copper is depending on pH because the oxide layers dissolution occur lower pH with unexpected contaminations. Carbon dioxide is the primary contaminant for pH decrease due to dissolving in water and forming carbonic acid which is a weak acid which dissociates by hydrolysis. Carbon dioxide is removed by degas units in most plants; however, bicarbonate and carbonate in the make-up water remain and are sources of carbon dioxide.

$2NaHCO_3 + Heat \rightarrow Na_2CO_3 + CO_2 + H_2O$

$Na_2CO_3 + H_2O + Heat \rightarrow 2NaOH + CO_2$

Hydrogen (H^+), by dissociation of water with carbonic acid, lowers pH in water with carbon dioxide. One ppm (part-per-million) of dissolved carbon dioxide at 60°C can lower pH from 6.5 to 5.5, approximately (Chen et al., 1998).

$CO_2 + H_2O \rightarrow H_2CO_3$

$H_2CO_3 \rightarrow H^+ + HCO_3^-$

$$HCO_3^- \rightarrow H^+ + CO_3^{2-}$$

Corrosion of iron in carbonic acid can be represented as:

$$Fe + 2HCO_3^- + 2H^+ \rightarrow Fe(HCO_3)_2 + H_2 \rightarrow Fe^{2+} + 2HCO_3^- + H_2$$

This reaction is accelerated at pH of 5.9 or less (Dunham, 1988). If oxygen dissolves in water, then the corrosion reactions are

$$2Fe + 2H_2O + O_2 \rightarrow 2Fe(OH)_2$$

$$4Fe(OH)_2 + 2H_2O + O_2 \rightarrow 4Fe(OH)_3$$

$$2Fe(OH)_3 \rightarrow Fe_2O_3 + 2H_2O$$

$$4Fe + 3O_2 \rightarrow 2Fe_2O_3$$

2.3. Water Technology in Power Plants

Historically, there are five possible choices for power plant water treatment; all volatile treatment (AVT), oxygenated treatment (OT), equilibrium phosphate control (EPT), phosphate treatment (PT) and caustic treatment (CT). These choices consist of two categories such as solids treatments (EPT, PT and CT) and no solids treatments (AVT) (Flynn, 2009).

For boiler water treatments, OT and AVT(O) are only applicable to units with all-ferrous feedwater systems, but AVT(R), EPT, PT and CT are applicable to both all-ferrous and mixed-metallurgy. OT and AVT(O) are the most reliable and best performing treatments (Dooley et al., 2002). Typical steam cycle treatments are addressed at Table 2-1.

Table 2-1. Characteristics of the leading boiler-water chemical treatment programs (Jonas, 1983; Kritzer, 2004)

Program	Advantages	Disadvantages
Conventional phosphate Na_3PO_4 (+NaOH)	Hardness salts removal by blowdown Control high levels of suspended solid Acids neutralized;	Not prefer at the high pressure boilers above 10.4 MPa (1500 psig); Possible caustic cracking by excessive concentrated NaOH.
Coordinate phosphate $Na:PO_4 < 3:1$	Caustic corrosion prevention Easy removable deposit form High steam purity Acids neutralized	Concentrated phosphate may dissolve the protecting iron oxide film Possible corrosion by phosphoric acid at very low $Na:PO_4$ molar ratios (<2.1)
Congruent phosphate, $2.6:1 < Na:PO_4 < 2.8:1$	Caustic and acid corrosion prevention Easy removable deposit form High steam purity Acids neutralized	Difficulty of control $Na:PO_4$ molar ratio because of low solubility of phosphate in low density water Continuous feed / blowdown required.
All-Volatile (AVT)	No precipitation in boiler water High purity steam at feedwater conditions No carryover of solids, Easy removable boiler deposition of corrosion products by chemical cleaning.	Boiler corrosion by Exceed inhibiting ability of volatile feed High feedwater purity required Interference with condensate polishing, Possible corrosion of stainless steels and copper alloys by NH_4OH and oxygen.
Neutral, oxygen added at about 100 ppb O_2	No chemical additives Low corrosion rates of ferritic steels.	High feedwater purity required Corrosion of copper alloys and some valve seats

The chemicals in AVT are based on pH control and corrosion inhibition. A corrosion inhibitor is defined as a chemical additive which, when added in small concentration, prevents or minimizes the reaction with metal. pH control minimizes corrosion and amines are broadly classified as acid-neutralizing and filming (Dooley and Chexal, 1999).

Amines are nitrogen-containing in which one or more of the hydrogen has been replaced by an alkyl or aryl group. Amines are broadly classified as primary, secondary, or tertiary based on the number of organic groups that attach to the nitrogen atom. In general, boiling points are higher than those of alkanes but lower than those of alcohols of comparable molecular weight. Molecules of primary and secondary amines can form strong hydrogen bonds with each other and to water. Molecules of tertiary amines cannot form hydrogen bonds with each other; however they can form hydrogen bonds to water molecules or other hydroxylic solvents. As a result, tertiary amines generally boil at lower temperature than primary and secondary amines with comparable molecular weight. All low molecular weight amines are very water soluble.

Amines are widely used in commercial hydrothermal systems as acid neutralization agents and corrosion inhibitors. They have been proven to be effective in stabilization pH of water in boiler and steam condensate system in later sections of the chapter.

Neutralizing amines are used to neutralize the acid generated by the dissolution of carbon dioxide or other acidic process contaminants. These amines hydrolyze when added to water and generate the hydroxide ions required for neutralization.

$R\text{-}NH_2 + H_2O \rightarrow R\text{-}NH_3^+ + OH^-$

The overall neutralization reaction is

$R\text{-}NH_3^+ + OH^- + H_2CO_3 \rightarrow R\text{-}NH_3^+ + HCO_3^- + H_2O$

EPRI has published Secondary Water Chemistry Guidelines recommending operation in the pH range of 8.8 to 9.6 for plants containing copper alloys and in the range of 9.3 to 9.6 for plants with all-ferrous systems (Blomgren et al., 1987, Bilanin et al., 1987). However, it should extend into the 9.8 to 10 pH range for units with air-cooled condenser when the feedwater system is all-ferrous (Dooley, 2009). EPRI's most recent interim guidelines for cycle water chemistry present pH 9.8 to 10 for all-ferrous and mixed-metallurgy for AVT(R), AVT(O), and OT (EPRI, 2008).

The three possible choices employing all volatile chemistries are (Dooley et al., 2002; Flynn, 2009);

1) AVT(R): Ammonia with a reducing agent is added after the condensate pump or polisher to increase pH and remove residual oxygen. This treatment must be used for mixed-metallurgy systems but is also used for all-ferrous systems with poor feedwater cation conductivity (> 0.3 μS/cm).
2) AVT(O): Ammonia is added after condensate pump or polisher. This is the feedwater choice for all-ferrous system.
3) OT: Ammonia with small amount of oxygen is added instead of a reducing agent. This is the feedwater of choice for all-ferrous systems with a condensate polisher or with the ability to maintain feedwater cation conductivity (< 0.15 μS/cm).

Both AVT(R) and AVT(O) treatments require high purity feedwater at all times. The cation conductivity must remain less than 0.2 μS/cm, and dissolved oxygen at the condensate pump discharge must remain less than 10 μg/L. OT needs very high purity water with cation conductivity less than 0.15 μS/cm.

AVT suppresses corrosion by keeping dissolved oxygen in feed water and boiler water close to zero and keeping the pH controlled by weak alkalinity. Although AVT is not acceptable for all units, it may be suitable for use in specific units whenever changes in unit design and operation occur (Dooley, 2002). AVT is the main feed water treatment for once-through boilers in Japan, since they cannot tolerate dissolved solids.

On the other hand, oxygenated treatment (OT) intends to prevent corrosion by allowing traces of oxygen (20-200 ppb) to exist in feed and boiler water and thereby forming a protective film - a dense corrosion product (Fe_2O_3: hematite) - on the metal surface of equipment and piping. Hematite formed by OT has low solubility compared to magnetite (Fe_3O_4) formed in AVT and has features of a smooth protective film (hematite) with fine particle size (Yamagishi and Miyajima, 2004).

2.4. Advanced Amines

Ammonia was the most common pH control agent from the 1970's to mid-1980's (Richardson and Price, 2000). However, ammonia has high volatility and tends to transfer toward the vapor phase so that very little protection is provided in wet steam areas and essentially none at high temperature. Although the presence of NH_3 / O_2 does not cause problems, since oxidation of ammonia is slow, ammonia oxidation is accelerated near supercritical conditions producing N_2 and N_2O and a pH drop (Dooley

and Chexal, 1999; Klimas et al., 2003). Moreover, Nordmann and Fiquet (1996) reported ammonia leads to resin exhaustion or copper alloy corrosion and is insufficient to protect steel components, in liquid phase, from flow-assisted erosion-corrosion.

The ability of amine based on pH elevation depends on basicity, volatility, and thermal stability of the specific amines.

Basicity means the ability to elevate pH after neutralizing acids. According to hydrolysis of amine, the equilibrium constant for this reaction is given by

$$K_b = \frac{[R - NH_3^+][OH^-]}{[R - NH_2]}$$

where K_b is the equilibrium constant for the reaction. High equilibrium constant corresponds to more OH^- formation and pH increase.

Every aqueous species has some finite volatility. The distribution coefficient, K_d is defined as;

$$K_d = \frac{\text{molality in the vapor phase}}{\text{neutral species molality in the liquid phase}}$$

The distribution coefficient is nearly constant over small changes in the total solute concentrations in dilute solution. However, it is hard to estimate the molality of the neutral species so that it is convenient to use the relative volatility where relative volatility is defined as;

$$RV = \frac{\text{molality in the vapor phase}}{\text{Total molality in the liquid phasee}}$$

The relative volatility is highly dependent on concentration or solution pH for the specific solution of interest. Figure 2-1 to 2-4 represent pH, relative volatility, basicity, and distribution coefficient of the particular amines from 25 to 300°C (Cobble and Turner, 1992).

Morpholine was first introduced in the secondary steam cycle in U.S. PWRs in 1986 and proved more effective than ammonia. Based on morpholine experience, Electric Power Research Institute (EPRI) began the advanced amine qualification program to evaluate the most favorable amines as pH control agents and recommended guidelines (1993; 1994; 1997; 2002; 2009). The guidelines have been providing the guidance necessary to complement a program for effective and economical control of corrosion and deposition within the coal-fired power plants and PWRs.

2.5. Literature Review

2.5.1. Thermal Degradation of Aqueous Amines

There are numerous studies on evaluation of various amines and their byproducts at subcritical conditions, as well as the impact on ion exchange beds below 260°C.

Polderman et al. (1955) reported that the major monoethanolamine degradation products are 1-(2-hydroxyethyl)imidazolidone (HEI) and N-(hydroxyethyl) ethylenediamine (HEED). These products were confirmed by Lang and Mason (1958). Samuel (1960) reported that aqueous morpholine decomposed by about 40 wt% at 308°C in 48 h and produced ethanolamine, diethanolamine and other unknown primary amines.

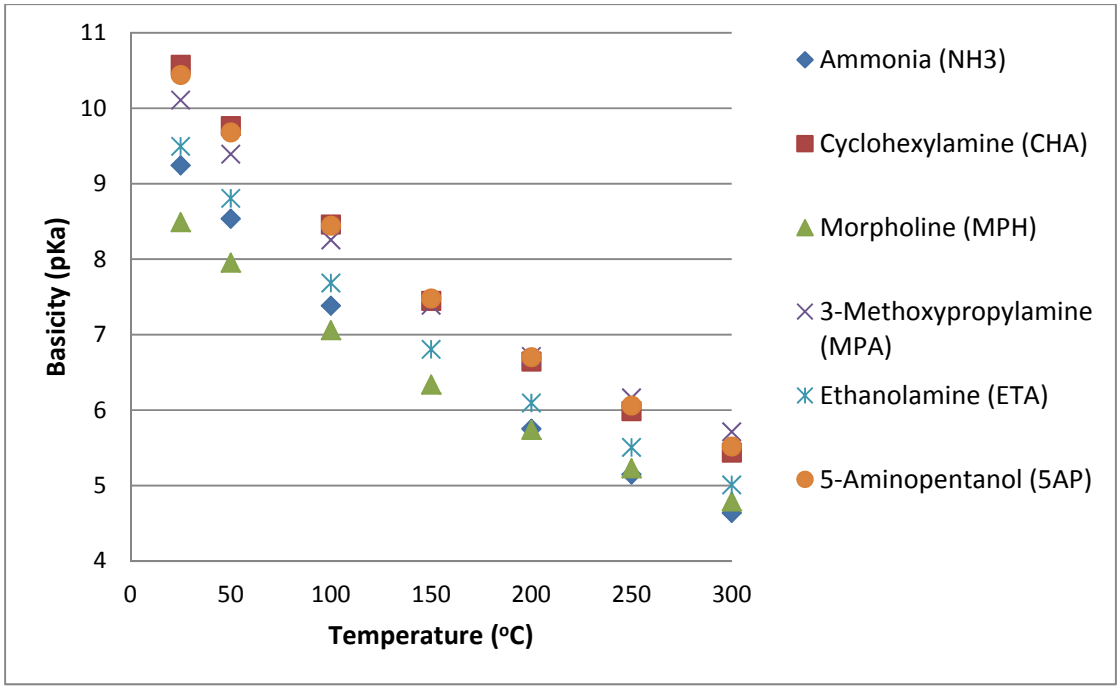

Figure 2-1. Basicity of 10 ppm amines (Cobble and Turner, 1992)

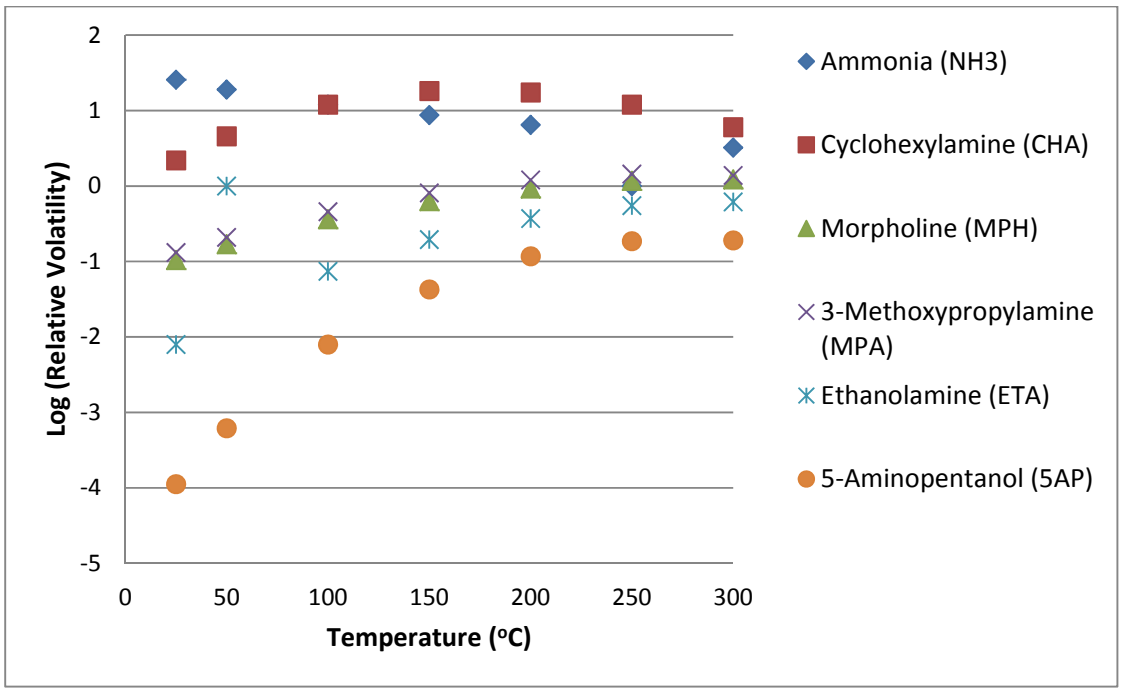

Figure 2-2. Relative volatility of 10 ppm amines (Cobble and Turner, 1992)

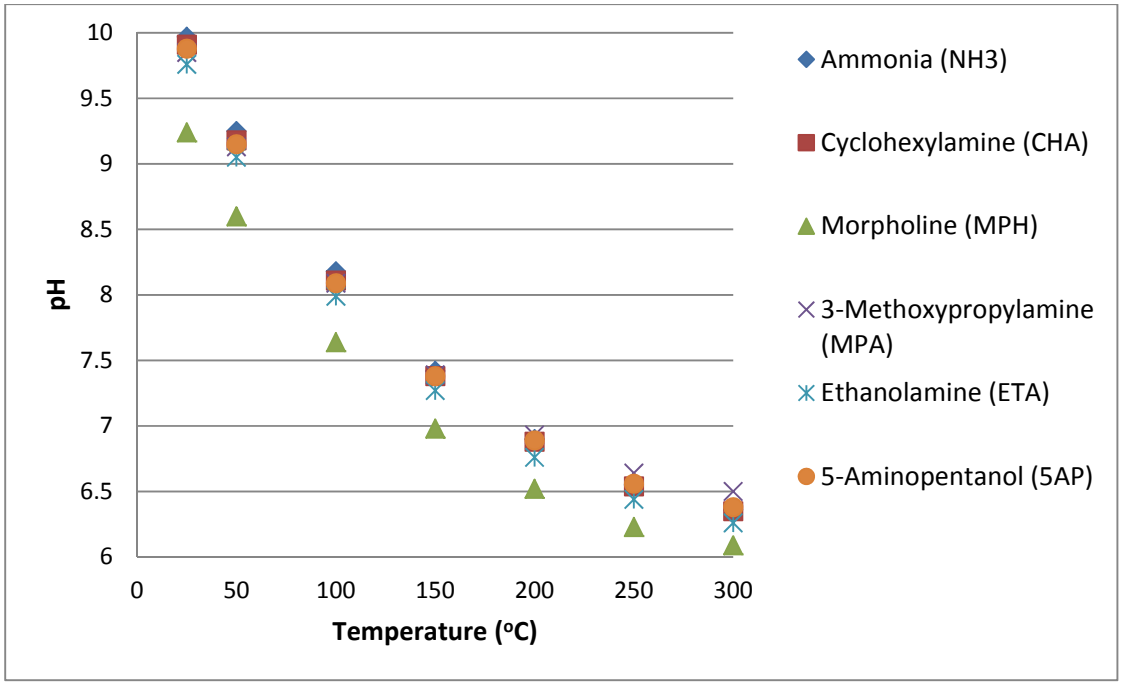

Figure 2-3. pH of 10 ppm amines (Cobble and Turner, 1992)

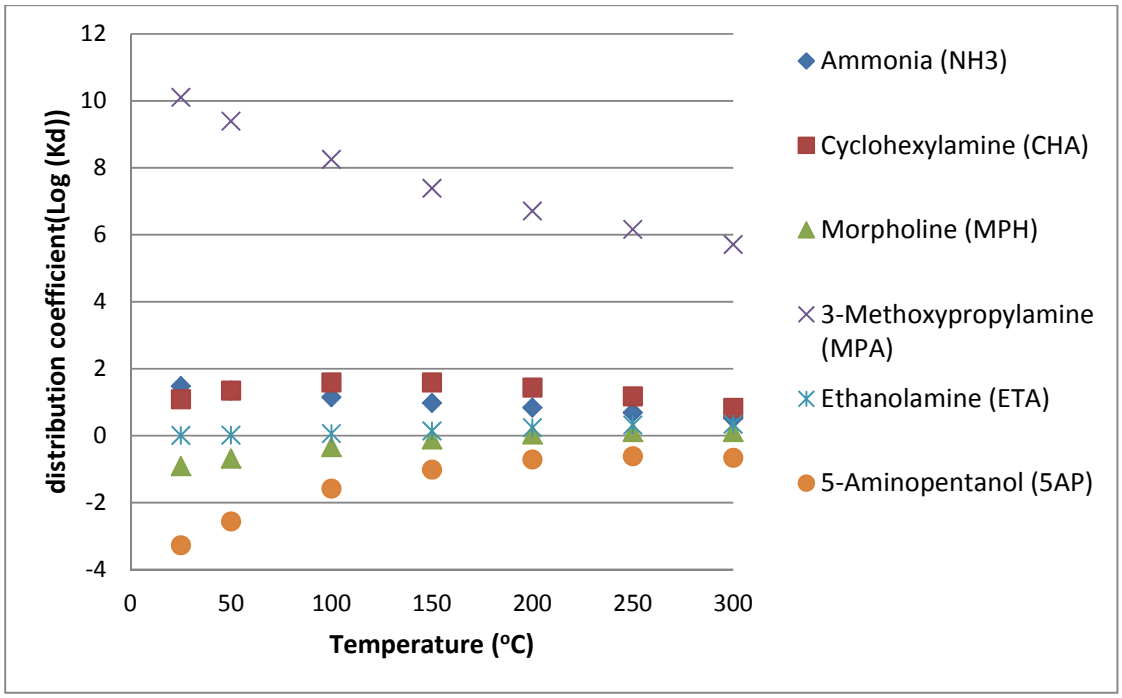

Figure 2-4. Distribution coefficient of 10 ppm amines (Cobble and Turner, 1992)

Yazvikova (1975) studied dehydrated samples of oxazolidone and monoethanolamine at elevated temperatures from 150 to 200°C. The oxazolidone was completely consumed with the formation of an equimolar amount of N,N"-di(hydroxyethyl) urea (DHU). At elevated temperature, above 200°C, DHU, hydroxyethylimidazolidone (HEIA) and hydroxyethylethylenediamine (HEEDA) began to form with the sum of their concentrations equal to the amount of DHU disappearance.

Byproducts such as acetic and formic acids were observed by Burns et al. (1986) when morpholine was added to the secondary cycle at the Beaver Valley Unit 1. Power plant. Dauvois et al. (1986) proposed ammonia, ethylene glycol, and acetic and formic acids as possible byproducts of morpholine degradation.

Gilbert and Saheb (1987) studied the distribution coefficient of morpholine in the steam cycle at Gentilly nuclear power plant and detected the presence of ammonia, methylamine and ethylamine.

Cobble and Turner (1992) calculated pH and volatility as a function of temperature for 96 amines and established criteria for acceptable performance. Ten amines had pH of at least one unit above that of pure water at 10 ppm concentration and 300°C with less volatility than ammonia.

Shenberger et al. (1992) evaluated the degradation of six amines: 1,2-diaminoethane, ethanolamine, morpholine, 2-amino-2-methyl-l-propanol, 3-methoxypropylamine, and 3-hydroxyquinuclidine plus ammonia in a high pressure boiler and feed water heater (FWH). All loop tests were conducted at 286°C (1000 psig) average temperature with 4-5% blowdown with an average steam flow of approximately

90 lbs/hr. First order rate constants were calculated for both the FWH and the boiler and listed in Table 2-2.

Table 2-2. Amine decomposition rate constants (Shenberger et al. 1992)

Amine	k(s^{-1}) FWH	k(s^{-1}) Boiler
DAE	3.55×10^{-4}	1.24×10^{-4}
ETA	5.87×10^{-5}	1.07×10^{-6}
MPH	7.47×10^{-4}	4.08×10^{-6}
AMP	4.68×10^{-4}	2.78×10^{-4}
MPA	2.87×10^{-6}	-
3HQ	-	1.44×10^{-5}

Wesolowski et al. (2002) performed experimentation on the protonation of morpholine, dimethylamine and ethanolamine up to 290°C. Acid dissociation equilibria were measured potentiometrically with a hydrogen-electrode concentration cell in a 1.0 molal ionic strength solution. Degradation products were not measured.

Amine degradation literature addressed two general applications: amines used in the oil and gas industry for H_2S and CO_2 separation and amines used as corrosion inhibitors in water. Data for oil and gas applications were considered only when relevant to this project. For example, Smith et al. (1992) reported degradation of corrosion inhibitors and kinetic analysis up to 240°C. They reported a first order rate constant for 5-aminopentanol at 260°C of 0.77×10^{-5} s^{-1}.

Gilbert and Lamarre (1989) reported the decomposition rate constants of morpholine are 2.67, 8.73 and 21.25×10^{-7} s^{-1} at 260, 280 and 300°C and 4.7, 6.6 and 8.9 MPa, respectively. The kinetics of morpholine were found to be first order with activation energy of 131.9 kJ/mol. Ammonia, ethanolamine, 2-(2-aminoethoxy) ethanol,

methylamine, ethylamine, ethylene glycol, and acetic and glycol acids were found as byproducts of morpholine by thermal degradation. They reported morpholine had decomposed around 7% after 3 days of testing at 260°C, around 15% after 7 days, and around 50% after 30 days. At 300°C, the morpholine decomposition increased exponentially with the test duration (around 8% after 0.66 days and 59% for 5 days).

Kennard and Miesen (1985) evaluated diethanolamine (DEA) degradation. Experiments were at 30 wt% at 4137 kPa (~600 psi). They presented data and rate constants at 205 and 250°C. The respective k values were 0.00365 hr^{-1} (1.014 x 10^{-6} s^{-1}) and 0.033 hr^{-1} (9.167 x 10^{-6} s^{-1}) with assuming a pseudo first-order reaction. They observed N,N-Bis(hydroxyethyl)piperazine (BHEP) and N,N,N-tris(hydroxyethyl) ethylenediamine (THEED) as major degradation products.

Feron and Lambert (1992) compared the decomposition rates for ammonia, morpholine and 2-methyl-2-amino-1-propanol. Morpholine appears relatively stable, with 50% decomposition occurring after more than three weeks. Ammonia and acetate were decomposition products of 2-methyl-2-amino-1-propanol. From the information presented, reaction rate constants are not estimable. Ammonia and morpholine showed less than 2% decomposition at 282°C. 2-methyl-2-amino-1-propanol showed 22% degradation at the same conditions without oxygen. In laboratory tests at 300°C, 2-methyl-2-amino-1-propanol was completely destroyed in less than 2 hours. In short resident time studies at 400°C, decomposition products of 2-methyl-2-amino-1-propanol were identified as ammonia, acetate, hydrogen and methane.

Rossi and McDonald (1994) patented a corrosion inhibitor. Experimentation was performed with a nitrogen sparged test boiler. They presented data for 61 ppm of 3-methoxypropylamine at 1500 and 2500 psig of 4.9 and 24.6 % decomposition, respectively. These represent temperatures of 314 and 354°C, respectively. Rate constants are not calculated and, since the reactor residence times are not presented, they cannot be estimated.

For instance, it was noted that acetic, formic, glycolic, glyoxalic, and oxalic acids are shown in the following oxidation reaction of MEA (Rooney and Daniels, 1998).

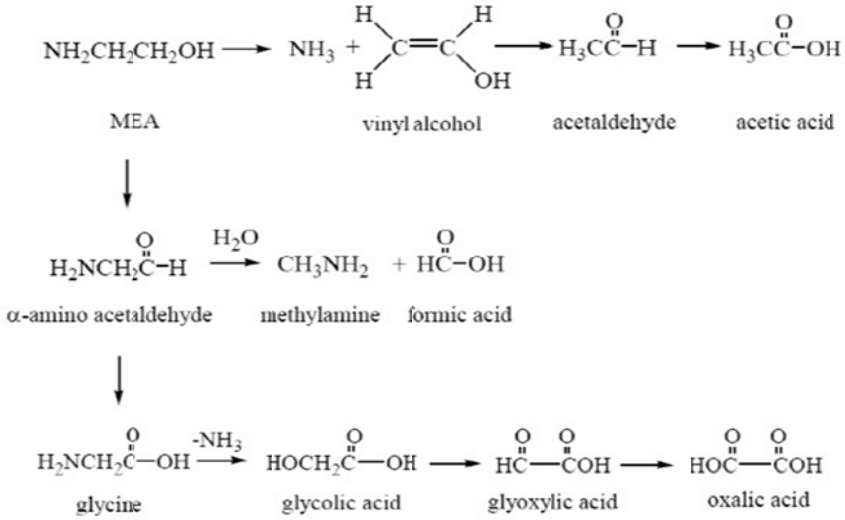

There are numerous papers that discuss the decomposition of specific amines. Domae and Fujiwara (2009) presented data for the decomposition of 3-methoxypropylamine at 280°C for two hours. They noted that 9 to 15% of 10 ppm of 3-methoxypropylamine decomposed to 110 ppb formate, 260 ppb acetate and 400 ppb propionate when dissolved oxygen was less than 5 ppb.

Trace and Walker (1980) studied hydrolytic thermal stability of 1000 ppm of amines, which are 3-methoxypropylamine, morpholine, cyclohexylamine, diethylaminoethanol, and aminomethylpropanol, at 600 psi (489°F) for 24 hours. The ammonia concentrations of 3-methoxypropylamine was below 1.0 ppm. Ammonia was found as 1.6, 3.3, 2.4, and 124 ppm for morpholine, cyclohexylamine, diethylaminoethanol, and aminomethylpropanol, respectively.

Davis and Rochelle (2009) reported thermal degradation of monoethanolamine as a function of initial concentration, carbon dioxide loading, and temperature. N,N'-di(2-hydroxyethyl)urea, 1-(2-hydroxyethyl)-2-imidazolidone, and N-(2-hydroxyethyl)ethylenediamine were found as byproducts with monoethanolamine loss. In the presence of carbon dioxide, the temperature dependent rate constant was approximately 29 kcal/mol and the degradation rate was 2.5 to 6% per week at 135°C.

More information about filming amines is present in the patent literature. These amines are used to protect equipment in transit or downtime. Examples of filming amine references include Walker et al. (1975 and 1976).

Table 2-3 summarizes the kinetic analysis of amine degradation data in sub-critical condition.

2.5.2. Impact of Chemicals on Ion Exchange Resins

It is known that amines degrade at high temperature to lower molecular weight chemicals and carboxylic acids; such as acetic, formic and oxalic acids. Impurities, including amine degradation products are considered when managing ion exchange resin

Table 2-3. Amines references of rate constant at different conditions

Amine	Pressure, psi	temp. °C	temp. K	1/K	conc. ppm	rate const s^-1	ln(rate const)	Reference
DAE		286	559.15	1.788E-03	10	0.000124	-9.00E+00	Shenberger et al.
ETA		286	559.15	1.788E-03	10	0.00000107	-1.37E+01	Shenberger et al.
MPH		286	559.15	1.788E-03	10	0.00000408	-1.24E+01	Shenberger et al.
AMP		286	559.15	1.788E-03	10	0.000278	-8.19E+00	Shenberger et al.
MPA		286	559.15	1.788E-03	10			Shenberger et al.
3HQ		286	559.15	1.788E-03	10	0.0000144	-1.11E+01	Shenberger et al.
DAE		140-280	413.15-553.15	2.43E-03-1.808E-03	10	0.000355	-7.94E+00	Shenberger et al.
ETA		140-280	413.15-553.15	2.43E-03-1.808E-03	10	0.0000587	-9.74E+00	Shenberger et al.
MPH		140-280	413.15-553.15	2.43E-03-1.808E-03	10	0.0000747	-9.50E+00	Shenberger et al.
AMP		140-280	413.15-553.15	2.43E-03-1.808E-03	10	0.000468	-7.67E+00	Shenberger et al.
MPA		140-280	413.15-553.15	2.43E-03-1.808E-03	10	0.00000287	-1.28E+01	Shenberger et al.
MPH		260	533.15	1.876E-03	150	0.000000267	-1.51E+01	Gilbert and Lamarre
MPH		280	553.15	1.808E-03	150	0.000000873	-1.40E+01	Gilbert and Lamarre
MPH		300	573.15	1.745E-03	150	0.00000213	-1.31E+01	Gilbert and Lamarre
MPH		300	573.15	1.745E-03	4.7	0.000000775	-1.41E+01	Mckay
AMP		280-295	553.15-568.15	1.808E-03-1.76E-03	1	0.000497	-7.61E+00	Feron
DEA		205	478.15	2.091E-03	300000	1.01111E-06	-1.38E+01	Kennard and Melsen
DEA		250	523.15	1.911E-03	300000	9.16667E-06	-1.16E+01	Kennard and Melsen
ETA		300	573.15	1.745E-03	100	0.000299	-8.12E+00	OSU
			573.15	1.745E-03	100	0.000425	-7.76E+00	OSU
					100	0.000258	-8.26E+00	OSU
MPA	1500	314	587.15	1.703E-03	61			Rossi et al.
	2500	354	627.15	1.595E-03	61			Rossi et al.

performance. Fouling, poisoning, precipitation, absorption, de-crosslinking, swelling and degradation of ion exchange caused by chemicals have been studied.

Watkins and Walton (1961) studied adsorption of amines on cation exchange resins. They used aniline, benzylamine, pyridine, piperidine and n-butylamine in various solvents such as water, glacial acetic acid, methanol, ethanol, isopropanol and dioxane. The results show amines are adsorbed in excess of ion exchange resin capacity in water however they are not in methanol, acetic acid or dioxane. They found the degree of adsorption in different solvents depend on swelling of resins in the solvents.

Gorden et al. (1966) introduced rejuvenation of poisoned strong base anion exchange resins which were fouled by anions such as titanates, molybdates and silicates or ionic complex of iron with chloride, fluoride, or phosphates. Metals may also deposit as soluble precipitates such as phosphates, oxychlorides, and hydroxides through hydrolysis. They also mentioned colloidal or soluble silicic acid or silicates as natural sources of fouling.

Puri and Costa (1986) studied impacts of common foulants on cation resins. Organic fouling on anion resins will progressively intensify when the ratio of total organic carbon to total anion is greater than 1.7×10^{-3} and simultaneously reduce strong-base-resin capacity. Iron, silica and aluminum were reported to reduce capacity and cause poor quality, especially iron migrating to inner matrix of resin bead; causing cracking and fragmentation. Duke et al. (2000) indicated that iron fouling is a widespread and difficult problem for industrial ion exchange resins. They introduced

fouling using geothermal brines which are containing large amounts of dissolved ions such as iron, manganese, silicate, zinc and other metals.

Lewis et al. (1993) and Fountain et al. (1990) reported resin cracking and break-up of macroporous cation resins when morpholine, 2-aminomethylpropanol and 5-aminopentanol were used in steam cycle. They found large bead size and high cross-linkage resin lead to severe bead cracking. Furthermore, resin cracking causes elevated pressure drop and poor condensate polisher performance.

Abrams et al. (1958) studied the effects of dissolved oxygen on weak and strong base anion exchanges. They introduced organic fouling and chemical attack which causes resin deterioration. Strong oxidizing agents such as chromic acid, chlorine or hypochlorites may cause resin degradation, discoloration, swelling, attrition and capacity loss.

Harries and Tittle (1986) studied deterioration of exchange kinetics and reported factors that cause deterioration in anion exchange resin. Organic fouling by naturally occurring species such as humic and fulvic acid was proposed as a possible reason along with cross contamination by acid regenerant.

Stahlbush and Strom (1990) proposed five kinds of decomposition mechanisms of strong-acid cation exchange resins resulting in release of both inorganic sulfate and organic sulfonates as well as desulfonation of the resin; also inorganic sulfate is released when cation resins are heated with air or oxygen above 120°C.

More studies have been performed to investigate the interactions with chemicals and ion exchange resins and the database of chemicals fouling impact to ion exchange resins is summarized in Table 2-4.

2.6. Supercritical Water

Supercritical water may be defined when either its temperature or pressure exceeds critical values (374°C and 3200 psia). Near the critical point, water has unique vapor and liquid properties, such as viscosity and dielectric constant. Hydrogen bonding is almost entirely disrupted, so that the water molecules lose the ordering responsible for many of liquid water's characteristic properties. In particular, solubility is closer to that of high-pressure steam than to liquid water. The loss of bulk polarity by the water phase has striking effects on normally water-soluble salts. No longer readily solvated by water molecules, they frequently precipitate out as solids (Hong and Spritzer, 2002).

Supercritical water provides the enhanced solubilities of organic reactants, a single phase environment free of inter-phase mass transfer limitation, and faster reaction kinetics. Also, water may be involved in overall kinetics and mechanism in a hydrothermal system as a solvent (Savage et al., 1995; Akiya and Savage, 2002).

A key property of water in many applications is the dissociation equilibrium which is characterized by equilibrium constant (K) and ionic product (Kw);;

$$H_2O = H^+ + OH^-$$

$$K_w = a(H^+)a(OH^-)$$

There equations are formulated with hydronium (H_3O^+) rather than hydrogen ion (H^+) at normal temperature however, hydrogen ion is noted at supercritical states (Weingartner and Franck, 2005).

Benjamin and Savage (2004) studied the reaction rate of methylamine in supercritical water at temperature between 386 and 500°C, densities of 0.04 to 0.54 g/cm^3 and pressure less than or equal to 250 atm. In the low density region, the effect of water is negligible with major products of ammonia and methanol. The rate constant for methylamine disappearance in this region has the activation energy of 38 ± 7 kcal/mol. At higher water densities, above 9.28 g/cm^3, hydrolysis is important and methanol yield increases. They reported pyrolysis and hydrolysis were dominating at low and high density, respectively. Different products were created in sub and supercritical water (Abraham and Klein, 1985; Townsend et al., 1988; Torry et al., 1992).

Table 2-4. Fouling impact of chemicals on ion exchange resin

Chemicals / ions	Resin type	Effect on resin	References
•Ionic complex Colloidal silica, Calcium sulfate, Calcium phosphates	Anion and cation	Reduces capacity	Kunin(1996)
•Amines Aniline, Benzylamine, Pyridine, Piperidine n-butylamine	Cation	Reduces capacity Swelling in water not acetic acid, methanol, ethanol, isopropanol, dioxane	Watkins and Walton (1961)
•Anion Titanates, Molybdates, Silicates, •Ionic complex Iron chloride, Iron fluoride, •Soluble precipitates Phosphates, •Metals through Hydrolysis, Oxychlorides, Hydroxides •Colloidal or soluble silicic acid or silicate	Strong-base anion	Reduces capacity	Goren et al. (1966)
•Calcium, Magnesium, Iron, Aluminum, Barium,. •Organics, Iron, Aluminum, Suspended matter •Silica, Oil / grease.	Cation Anion Cation / Anion	Reduces capacity Poor quality	Puri and Costa (1986)
•Strong oxidizing agents Chromic acid, Chlorine, Hypochlorites	Weak / strong base anion	Reduces capacity degradation, discoloration, swelling, attrition	Abrams et al.(1958)
•Natural species Humic and Fulvic acid	Anion	Reduces capacity	Harries and Tittle (1986)
•Ethanolamine	Anion	Reduces capacity Physical deterioration	Miller (1997) Foutch et al. (2002) Raught (2005)
•AMP (2-Amino-2-methyl-propan-1-ol) •5AP (5-aminopentanol)		Cracking, fracturing, cleaving, excessive fines observed	Richardson and Price (2000)

Lee and Gloyna (1992) examined hydrolysis of methylamine at supercritical conditions between 400 and 525°C and 230 and 335 atm with water densities from 0.1 to 0.28 g/cm^3. First-order kinetics with respect to the methylamine described both hydrolysis and overall reaction rates. Ammonia was the major product at low density (<0.26 g/cm^3) but overall reactivity increases while methylamine yield decreases at high density (>0.28 g/cm^3). Hydrolysis proceeded faster than oxidation. They also noted the methylamine selectivity increases with density increases but unknown nitrogen-containing products other than ammonia were produced at low density.

In order to understand solvent effects of water, specific water properties can be justified in supercritical conditions. Figure 2-5 to Figure 2-8 show variance of unique thermodynamic properties of water at high temperature and pressure, which came from literature, based on vapor liquid equilibrium (VLE) data (NIST; Marshall and Franck, 1981).

Figure 2-5 shows the isothermal water density variation with pressure change. The most rapid density change is observed near 4000 psi for 400°C about 0.24 to 0.3 g/cm^3. On the other hand, the density of water does not exceed 0.15 g/cm^3 at 500 and 600°C. It means that hydrolysis dominates above 4000 psi for 400°C.

The heat capacity defines how much heat is required to raise the temperature of water from hydrogen bonding. The acid-base behavior of molecules dissolved in supercritical water is an important part of their reactivity. Since acid-base reactions involve charge separation and association, their reaction kinetics and equilibrium are affected by the dielectric constant and hydrogen bonding of water. At constant

temperature, increasing density favors increasing charge separation (Akiya and Savage, 2002). The isobaric variation of heat capacity is presented in Figure 2-6. According to the definition of heat capacity, hydrogen bonding of water molecules is strongest near 4000 psi for 400°C.

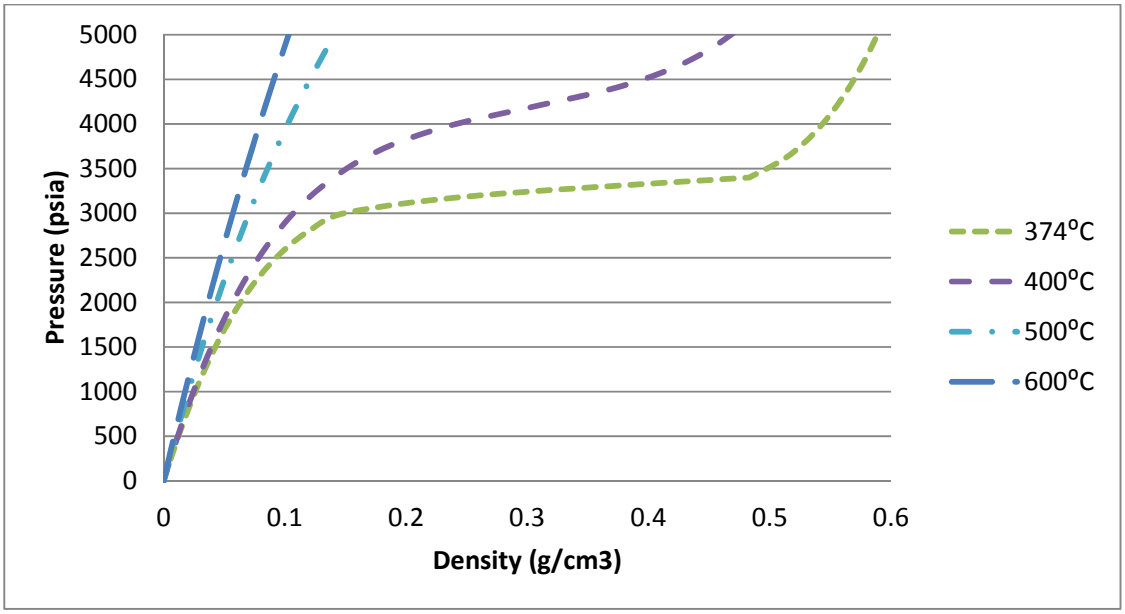

Figure 2-5. Isothermal variation of pressure with density (NIST).

The ionic product of water is defined as the product of hydrogen and hydroxide ion concentrations and Kw value is 1.0×10^{-14} $(mol/l)^2$ at 25°C. Figure 2-7 shows the isobaric ion product of water variation with temperature. Hydrogen bonding characterizes the change in solubility properties of supercritical water. At constant density, as the temperature is increased, the dielectric constant decreases due to the breakage of hydrogen bonds (Cochran et al, 1992).

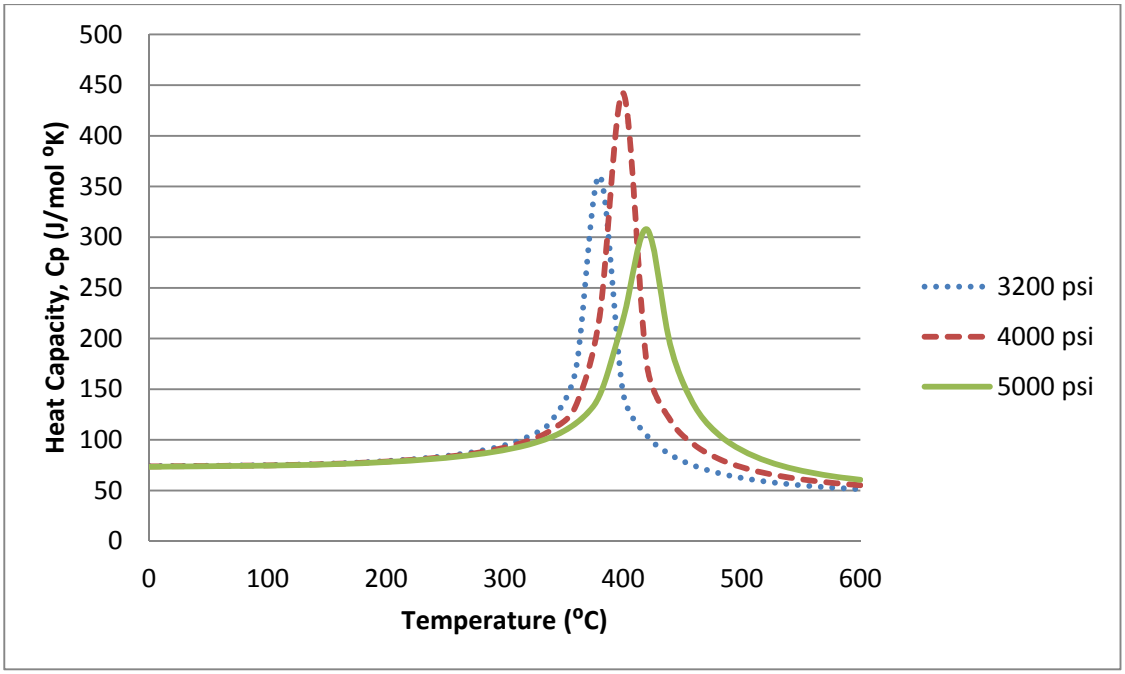

Figure 2-6. Isobaric heat capacity variation with temperature (NIST).

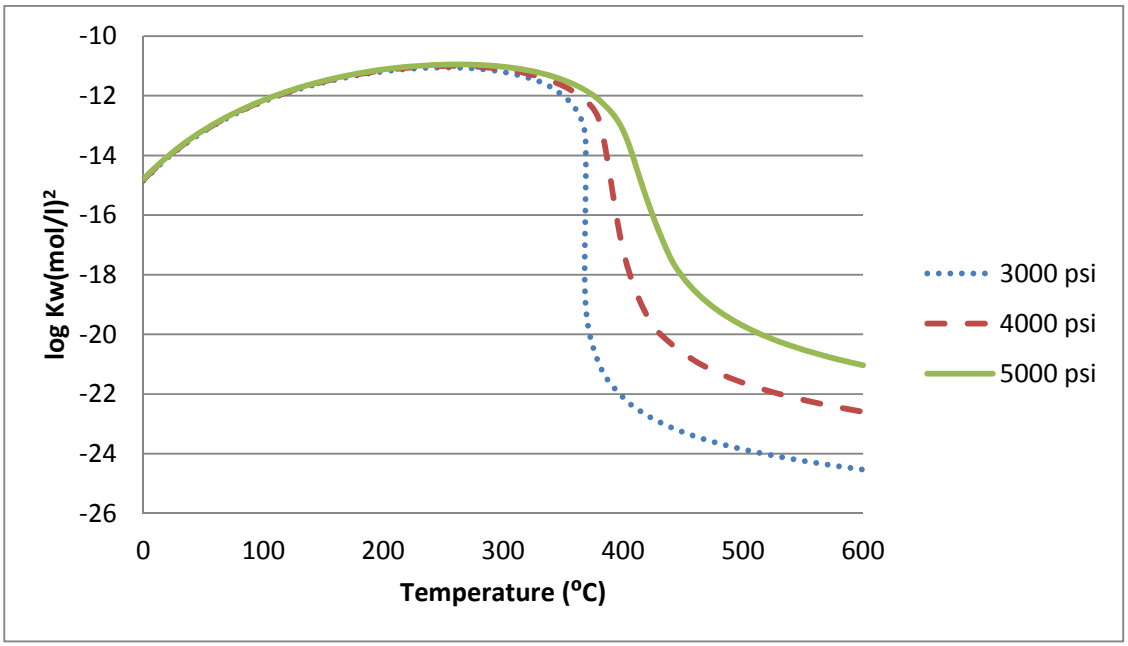

Figure 2-7. Isobaric ion product of water variation with temperature

(Marshall and Franck, 1981)

Figure 2-8 shows the isobaric dielectric constant variation with temperature. Dielectric constant (ε) decreases with increasing temperature. It is defined as the degree of non-conductivity of a substance, for instance, the value is zero at vacuum and controls the solvent behavior and the ionic dissociation salt. Notice the steep change of dielectric constant near critical temperature. In this region, water is a low dielectric fluid, a poor solvent for electrolytes and a good solvent for organic compounds (Levelt Sengers, 1988).

Weingartner and Franck (2005) simulated the dielectric constant in high density supercritical region has values of 10 to 25 which are similar to those of dipolar liquids, such as acetonitrile or acetone under ordinary conditions. These values are sufficiently high to dissolve and ionize electrolyte, but also enable miscibility with nonpolar solutes.

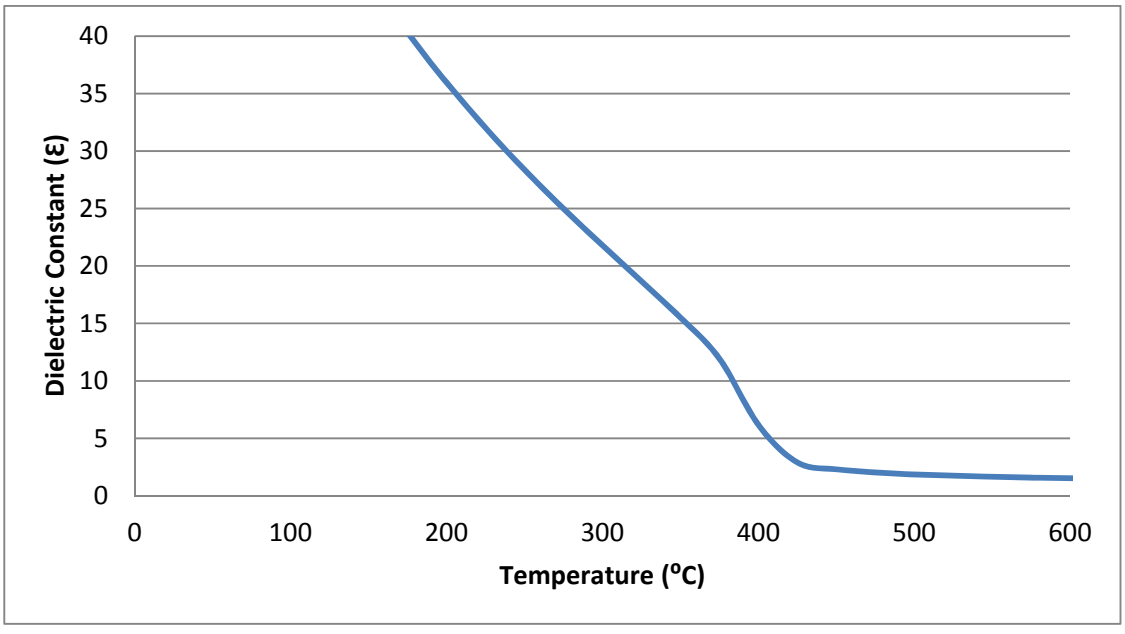

Figure 2-8. Isobaric dielectric constant variation with temperature at 30 MPa (Archer and Wang, 1990)

Kritzer (2004) reported rapid change in physical properties such as density, pH value and electrochemical potential at the critical point makes water a highly corrosive fluid in supercritical water system. Temperature will plays a role influence of solvent properties as well as stability of chemical additives involving in corrosion.

REFERENCES

Friend. D.G. and Dooley, R.B."Volatile treatments for the steam-water circuits of fossil and combined cycle/HRSG power plants," International Association for the Properties of Water and Steam, Niagara Falls, Canada July 2010

U.S. Department of Energy (DOE), "Fundamentals Handbook Chemistry volume 1 of 2," Washington, D.C. 20585 (1993)

Cobble, J.W. and Turner, P.J. "PWR Advanced All-Volatile Treatment Additives, By-Products and Boric Acid," EPRI report TR-100755, 1992.

Chen, T., Robert, D.P., Carol, B.B., and Cicero, D.M. "Condensate Corrosion in Steam Generating Systems." CORROSION 98, March 22 - 27, 1998, San Diego CA.

Dunham, M. "Corrosion in Dry Kiln Piping," Western Dry Kiln Association Proceedings. 1988, Reno, Nev.

Blomgren, J.C., Carr, W.C., Eaker, R.W., Frieling, G.D., Gould, A.J., Green, S.J., Harhay, A.J., Koch, D.W., Lurie, S.W., Rootham, M.W., Sawochka, S.G., Svenson, J.G., and Welty, C.S. "PWR Secondary Water Chemistry Guidelines". *Electric Power Research Institute Report NP-5056-SR*, (1987) May.

Bilanin, W., Cubicciotti, D., Green, S.J., Jones, R.L., Santucci, J., Shaw, R.A., Welty, C.S., and Wood, C.J. "LWR Water Chemistry Guidelines" *Progress in Nuclear Energy*, **20** (1987), pp. 1–42.

Dooley, R.B., Shields, K.J., Aspden, J.D., Howell, A.K., Dupreez, F., and Mathews, J.A. "*EPRI's Guideline on Chemistry for Fossil Units with Air-cooled Condensers (ACCs)*" EPRI 9th Ninth International Conference on Cycle Chemistry in Fossil and Combined Cycle Plants with Heat Recovery Steam Generators, Westin Copley Place Hotel, Boston, Massachusetts, June 29-July 1, 2009.

EPRI, "Interim Guidelines for Control of Steamside Corrosion in Air-cooled Condensers of Fossil Unit" Electric Power Research Institute, Palo Alto, CA: 2008. 1015655.

Flynn, D. "The Nalco Water Handbook" New York, McGraw-Hill, 2009

Dooley, R. B., Shields, K., Aschoff, A., Ball, M., and Bursik, A. "*Cycle Chemistry Guidelines for Fossil Plants: All-Volatile Treatment: Revision 1,"* Electric Power Research Institute, Palo Alto, CA: 2002. 1004187.

Jonas, O. "Steam." In Kirk-Othmer Encyclopedia of Chemical Technology, 3rd ed. Vol. 21, 1983, 507-551. New York: John Wiley & Sons.

Kritzer, P."Corrosion in High-Temperature and Supercritical Water and Aqueous Solutions: a Review." J. of Suprecritical Fluids 29 (2004) 1-29.

Matsubara, M., Itaba, S., and Miyajima, M. "The Results of Chemical Cleaning by Organic Chemicals of Boiler Tubes of a Plant Operated on OT " PowerPlant Chemistry 2006, 8 (4)

Richardson, J.A and Price, S.G. “A Review of the Morpholine Form Condensate Polishing System at Oldbury-On-Severn Nuclear Power Station.” Ion Exchange at the Millennium: Proceedings of IEX 2000, 35-43

Dooley, R.B. and Chexal, V.K. ”*Flow-Accelerated Corrosion*” CORROSION 99, NACE International, Houston, 1999, Paper#347.

Klimas, S. J., Fruzzetti, K., Turner, C.W., Balakrishnan, P.V., Strati, G.L., and Tapping, R.L. "Identifcation and Testing of Amines for Steam Generator Corrosion and Fouling Control," 2003 ECI Conference of Heat Exchanger Fouling and Cleaning: Fundamentals and Applications, Santa Fe, NM, 2004, paper 37, 271-278

Yamagishi, M. and Miyajima, M. “Evaluation of Oxygenated Water Treatment,” Proceedings of 14th International Conference on the Properties of Water and Steam in Kyoto, 2004, 461-466.

Burns, G.D. “Advanced Amine Application Guidelines Revision 0,” Electric Power Research Institute, Palo Alto CA., September 1993, TR-102952.

Burns, G.D. “Advanced Amine Application Guidelines Revision 1,” Electric Power Research Institute, Palo Alto CA., December 1994, TR-102952-R1.

Miller, A.D. “PWR Advanced Amine Application Guidelines Revision 2,” Electric Power Research Institute, Palo Alto CA., October 1997, TR-102952-R2.

Polderman, L.D., Dillon, C.P., and Steele, A.B., “Why MEA Solution Breaks Down in Gas Treating Service.” Oil and Gas Journal, 54 (2), 180, 1955

Yazvikova, N.V., Zelenskaya, L.G., and Balyasnikova, L.V. "Mechanism of Side reactions During removal of Carbon Dioxide from Gases by Treatment with Monoethanolamine." *Zhurnal Prikladnoi Khimii*, 1975. 48(3): 674-676.

Agarwala, K.K. "Study on stability of morpholine in high pressure boiler system," Fertil Technol, 19: 73-75, 1982.

Burns, G.D., Crutchfield, J.E., Nolan, R.C., and Passell, T.O. "*On-line Analysis of Fluoride, Acetate, Formate, Chloride, Carbonate, and Sulfate in a Single Run Using Gradient Ion Chromatography*" 47th Ann. Meeting Int. Water Conf., Paper IWC-86-12, Pittsburgh, Pennsylvania, October 27-29, 1986.

Dauvois, V., Desmoulins, D., Lambert, I., and Nordmann, F. "*Laboratory and Plant Investigations on Decomposition Products of Morpholine in the Secondary system of French PW,*" Proc. of Water Chemistry of Nuclear Reactor System Conf., Bournemouth, England, October 13-17, 1986

Gilbert, R. and Saheb, S.E. "Field measurement of the distribution coefficients of chemical additives used for corrosion control in steam-water cycles," Mater Perform, 26: 30-36, 1987.

Cobble, J.W. and Turner, P.J. "PWR Advanced All-Volatile Treatment Additives, By-Products and Boric Acid," EPRI report TR-100755, 1992.

Shenberger, D.M., Zupanovich, J.D., and Walker, J.L. "Loop testing of alternative amines for all-volatile treatment control in PWRs," Electric Power Research Institute, Palo Alto CA., June 1992, TR-100756.

Wesolowski, D.J., Benezeth, P., Palmer, D.A., and Anovitz, L.M. “Protonation Constants of Morpholine, Dimethylamine and Ethanolamine to 290C and the Effect of Morpholine and Dimethylamine on the Surface Charge of Magnetite at 150-250C, Electric Power Research Institute, Palo Alto CA., TR-1003179, 2002.

Smith, J.R.L., Smart, A.U., and Twigg, M.V. "The Reactions of Amine, Polyamine and Amino Alcohol Corrosion Inhibitors in Water at High Temperature," J. Chem. Soc. Perkin Trans. 2, 939-947, 1992.

Gilbert, R. and Lamarre, C. "Thermal Stability of Morpholine Additive in the Steam-Water Cycle of CANDU-PHW Nuclear Power Plants," Can J Chem Engr., 67, 1989, 646-651.

Kennard, M. L. and Melsen, A. "Mechanisms and Kinetics of Diethanolamine Degradation," Ind. Eng. Chem. Fundam., 1985, 24, 129-140.

Feron, D. and Lambert, I. “Thermal stability of three amines in pressurized water reactor secondary systems. Laboratory and loop experiments” Journal of Solution Chemistry, Vol. 21, No. 8, 1992.

Rossi, A.M. and McDonald, A.C. “Corrosion control composition and method for boiler/condensate steam system,” United States Patents, 1994, #5368775.

Domae, M. and Fujiwara, K. "Thermal Decomposition of 3-Methoxypropylamine as an Alternative Amine in PWR Secondary Systems," J Nucl. Sci. and Tech, 46(2) 210-215, 2009.

Trace, W.L. and Walker, J.L. “Methoxypropylamine and Hydrazine Steam Condensate Corrosion Inhibitor Compositions and Methods,” United States Patents, 1980, # 4192844.

Davis, J. and Rochelle, G. “Thermal degradation of monoethanolamine at stripper conditions,” Energy Procedia 1 (2009) 327–333.

Walker, J.L.C, PA, Cornelius III, Thomas Edward (Coraopolis, PA), Filming Amine Emulsions. 1975, Calgon Corporation (Pittsburgh, PA): United States.

Walker, J.L.C, PA, Cornelius III, Thomas Edward (Coraopolis, PA), Filming Amine Emulsions. 1976, Calgon Corporation (Pittsburgh, PA): United States.

Watkins, S.R. and Walton, H.S. “Absortion of Amines on Cation Exchange Resin,” *Anal. Chim. Acta* 1961, *24*, 334-342.

Goren, M.B. “Rejuvenation of poisoned ion exchange resins,” United States Patents, 1966, # 3252920.

Puri, V.K. and Costa, S.T. “Treat resins properly to drive full benefits of ion exhcnage,” *Power*, 1986, 130 (9), 43-47.

Duke, H., Featherstone, J.L., and Marston, C.R. “Method for cleaning fouled ion exchange resins,” United States Patents, 2000, # 6080696.

Lewis, G.G., Greene, J.C., Tyldesley, J.D., Wettom, E.A., and Fountain, M.J. Proceedings of Conference on the Use of Amines in Conditioning Steam/Water Cycles, 1993. Electric Power Research Institute, Palo Alto, CA.

Fountain, M.J., Greene, J.C., and Jones, M.G. Proceedings of Conference on the Use of Amines in Conditioning Steam/Water Cycles, 1993. Electric Power Research Institute, Palo Alto, CA.

Abrams, I.M. and Benezra, L. "Ion Exchange Polymers," Reprinted from Encyclopedia of Science and Technology, 1967. John Wiley and Sons, Inc.

Harries, R.R. and Tittle, K. "Deterioration of exchange kinetics in condensate purification plant," Water Chemistry of Nuclear Reactor Systems 4, British Nuclear Energy Society, London, 1986 (1) 309-317.

Stahlbush, J.R. and Strom, R.M. "A decomposition mechanism for cation exchange resins," *Reactive Polymers,* 13 (1990) 233-240.

McKay, M. "Morpholine Decomposition Studies in a Model Boiler at Dissolved Oxygen Concentration up to 500 ppb" presented at EPRI Workshop on Use of Amines in Conditioning Steam/Water Cycles, Sept. 25-27, 1990, Tampa, FL.

Kunin, R. "Amber-Hi-Lites," 1996, ISBN 0-927188-07-4, Tall Oaks Publishing Inc.

Foutch, G.L. and Apblett, A. "Investigation of ETA Interactions in Mixed Bed Ion Exchange System-Phase 1," Electric Power Research Institute, Palo Alto CA., August 2002, TR-1003599.

Raught, D.P., Foutch, G.L., and Apblett, A. "Ion Exchange Resin Fouling by Organic Amines in Secondary Systems at U.S. Nuclear Power Plants," PowerPlant Chemistry 2005, 7(12) 741-747.

Richardson, J.A. and Price, S.G. “A Review of the Morpholine Form Condensate Polishing System at Oldbury-On-Severn Nuclear Power Station.” Ion Exchange at the Millennium: Proceedings of IEX 2000 Cambridge, UK 16 T 20 July 2000.

Hong, G.T. and Spritzer, M.H. “Supercritical Water Partial Oxidation” Proceedings of the 2002 U.S. DOE Hydrogen Program Review, NREL/CP-610-32405

Savage, P.E., Gopalan, S., Mizan, T.I., Martino, C.S., and Brock, E.E. “Reactions at supercritical conditions: applications and fundamentals.” AIChE J. 41, (1995),1723

Akiya, N. and Savage, P.E. “Roles of Water for Chemical Reactions in High-Temperature Water.” Chem. Rev. 2002, 102, 2725.

Weingartner, H. and Franck, E.U. “Supercritical Water as a Solvent” Angew. Chem. Int. Ed. 2005, 44, 2672-2692.

Benjamin, K.M. and Savage, P.E. “Hydrothermal reactions of methylamine.” Journal of Supercritical Fluids 31, 301-311, 2004.

Abraham, M.A. and Klein, M.T. “Pyrolysis of benzylphenylamine neat and with tetralin, methanol, and water solvents” Ind. Eng. Chem. Prod. Res. Dev. 24 (1985) 300.

Townsend, S.H., Abraham, M.A., Huppert, G.L., Klein, M.T., and Papsek, S.C. “Solvent effects during reactions in supercritical water.” Ind. Eng. Chem. Res. 27 (1988) 143.

Torry, L.A., Kaminsky, R., Klein, M.T., and Klotz, M.R. “The effect of salts on hydrolysis in supercritical and near-critical water: reactivity and availability.” Journal Supercritical Fluids 5 (1992) 163.

Lee, D. and Gloyna, E.F. “Hydrolysis and oxidation of acetamide in supercritical water,” Environ. Sci. Technol. 26 (1992) 1587.

NIST, http://webbook.nist.gov

Marshall, W.L and Franck, E.U. “Ion Product of Water Substance, 0 – 1000^{o}C, 1 – 10,000 Bars New International Formulation and Its Background.” *J. Phys. Chem. Ref. Data* 1981, *10*, 295.

Cochran, H.D., Cummings, P.T, and Karaborni, S. “Solvation in supercritical water,” Fluid Phase Equilibria, (1992) 71: 1-16

Levelt Sengers, J.M.H. “Supercritical Fluids: Their properties and applications.” In *Supercritical Fluids Fundamentals and Applications*, Proceedings of NATO Advanced Study Institute on Supercritical Fluids, December 01, 1998

.

CHAPTER III

AMINE SELECTION FOR USE IN POWER PLANTS

3.1. Introduction

Most hydrothermal systems use stainless steel or metal alloy with Iron (Fe) and Copper (Cu) materials; these are pH sensitive so that management of alkalinity and acidity, as well as impurities in feedwater, is considered to reduce various forms of corrosion potential (Dooley and Chexal, 1999).

Ammonia, a popular pH control agent, is not adaptable for use near the critical point. Ammonia has no effect on pH in the boiler at these operating conditions because it is not hydrolyzed to ammonium (NH_4^+), but exists as NH_3.

Alternative amines require base strength, volatility, concentration requirements, no corrosion by degradation products, safety in use and low cost. However, all amines break down into organic acids which contribute to cation conductivity of the feedwater and steam.

Degradation of carbonic-containing molecules forms carbonic acid which reduces the pH of steam. It is noted that the three typical treatments in feedwater, such as AVT(R), AVT(O), and OT, are capable of operating in the sub-critical region. On the other hand, these treatments may not be effective in keeping the pH high and reducing the corrosion potential in systems that exceed the critical point because of weak thermal stability and undesired byproducts such as carboxylic acids.

Amine use in plants operating at supercritical conditions (greater than 374°C and 22.1 MPa) has been debated. The literature shows very little experimental data above 260°C. Therefore, amine degradation to organic acids and subsequent impact of byproducts on the performance of the ion exchange beds is of interest.

To evaluate the impact of higher temperatures and pressures, five amines were evaluated as to whether they are candidates for use at supercritical conditions. Related performance factors, including partition coefficients and pH variability, are not part of this work.

3.2. Neutralizing Amines Selection

Degradation tests were performed on five amines: ethanolamine (ETA), cyclohexylamine (CHA), morpholine (MPH), 3-methoxypropylamine (MPA) and 5-aminopentanol (5AP). Chemical structures are presented in Figure 3-1. Ammonia was tested for comparison.

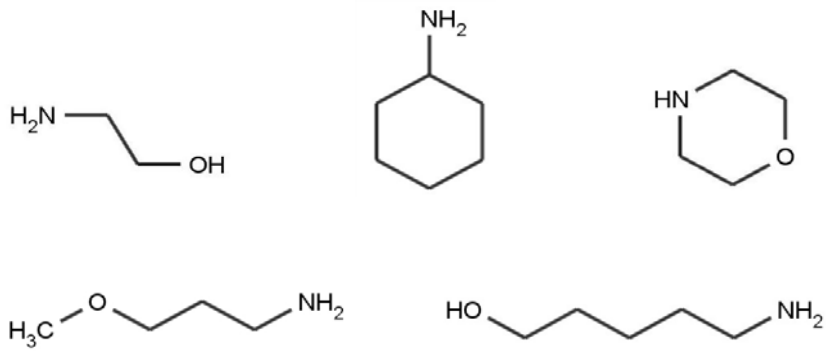

Figure 3-1. Chemical structures of the amines used for the degradation test

Ammonia is the most common pH control agent. However, it has drawbacks such as high volatility, tendency to transfer to the gas phase and low base strength (pH of 9.57 in 2 ppm and 9.97 in 10 ppm of aqueous solution at 25°C): so it has limited ability to protect surfaces exposed to wet steam. As a result, it is difficult to control steam-cycle pH by ammonia addition , especially under two-phase conditions (Domae and Fujiwara, 2009).

The Central Electricity Generating Board (CEGB) tested 5-aminopentanol (5AP) at the Wylfa station. 5AP has excellent low relative volatility as measured up to 240°C. The base strength, calculated from low temperature data, is good. 5AP was selected as a compromise between increasing base strength and increasing molecular weight for its structure type (Fountain, 1993).

3-methoxypropylamine (MPA) has good base strength and very good volatility, being slightly more volatile than water at 300°C and substantially less volatile below 150°C. High temperature volatility studies show no tendency to decomposition, but some tarring occurred on long exposure at 300°C. MPA has been added to secondary

systems of commercial PWR plants in the United States (Wilson and Bates, 2005). It has slightly strong basicity and low volatility, so lower concentration is required to adjust pH in steam.

Ethanolamine (ETA) is a moderately weak base of low volatility. ETA is a hydrolytic decomposition product of morpholine (MPH) and appears to have good thermal stability. Field tests conducted by EPRI showed that ETA was more effective than morpholine in maintaining pH and, therefore, was expected to result in lower steel corrosion rates (EPRI, 1994). ETA and MPH are the most commonly used organic amines in European Union (EU) and U.S. Nuclear Power Plants (NPP)., for applications that require pH between 9.5 and 9.8 (Nordmann, 2003; Millett and Fruzzetti, 2005).

Morpholine (MPH) is widely used in the steam cycle of fossil and nuclear power plants to increase pH of the condensate, feedwater and drainwater to 9.0-9.5. MPH is a weak base, giving nominally unacceptable pH control at 300°C. MPH appears to be stable in aqueous solution and is commonly used in coal-fired boilers at dosages of 10 ppm. With regard to morpholine, 5-9 mg/L is usually used to raise pH to 9.0-9.5 in steam (Gilbert and Lamarre, 1989). MPH distributes into liquid phase because of smaller relative volatility than other amines. For the several condensate units, the high concentration of MPH causes a high pH in liquid phase at the first condensate unit. However, little MPH is left in the next steam. In a result, cyclohexylamine (CHA) corresponding to high tendency to distribute into the steam is popular used in the system by blending with morpholine.

For the amines mentioned above, information on degradation at temperatures higher than 300°C and pressures in the supercritical region is limited. Table 3-1 shows properties of selected amines for the experiments conducted. The amines have a purity of more than 99%: MPH, CHA, ETA, 5AP, and MPA. A 10 ppm of ammonia standard (NH_3Cl) was purchased from Ricca Chemistry Company, while MPH, CHA, ETA, 5AP and MPA were purchased from Acros Organics and 5-aminopentanol was purchased from Aldrich Chemical Company.

Table 3-1. Properties of selected amines (Cobble and Turner, 1992)

Amine	Mw	pH (25°C)	pKa (25°C)	Log RV (25°C)
Morpholine (MPH)	87	9.24	8.491	-0.98
Cyclohexylamine (CHA)	99	9.91	10.577	0.34
Ethanolamine (ETA)	61	9.76	9.496	-2.10
3-methoxypropylamine	89	9.85	10.107	-0.88
5-aminopentanol (5AP)	103	9.88	10.443	-3.95
Ammonia (NH_3)	17	9.97	9.244	1.41

3.3. Experimental Apparatus and Procedures

3.3.1. Apparatus

Five ml batch reaction tubes were made of 316 stainless steel, capable of withstanding high pressure and temperature and resists corrosion by acid (Gilbert and Lamarre, 1989). The dimension of the reaction tube is 0.56 inch OD with a 0.31 inch ID and 0.125 inch wall thickness. Physical properties are shown at Table 3-2.

Table 3-2. Physical properties of 316 stainless steels

Chemistry Data		Physical Data	
Carbon	0.030-0.080 %	Density (lb /in^3)	0.288
Chromium	16 – 18 %	Specific Gravity	7.95
Iron	Balance	Specific Heat (Btu/lb/°F - [32-212°F])	0.12
Manganese	2 % max	Electrical Resistivity (mΩ-cm (at 68°F))	445
Molybdenum	2-3 %	Melting Point (°F)	2550
Nickel	10-14 %	Modulus of Elasticity Tension	28
Phosphorus	0.045 % max		
Silicon	1 % max		
Sulphur	0.03 % max		

High pressure reaction tubes are filled with a precise mixture of 10 ppm amine and water. Ammonia at 2 ppm has a pH of 9.57, while 10 ppm has a pH of 9.97 at 25°C. Using Steam Tables from the NIST database, the pressure, specific volume, and temperature conditions are defined within the reaction tube. This requires accurate measurement of the reaction tube volume and mass of water. These two values give the specific volume. For example, 0.1 Liter at 600°C and 10 MPa contain 2.6 grams of water. If the volume and temperature are fixed, adjusting the mass adjusts the pressure. In this way a direct measure of temperature, mass and volume gives an indirect pressure value. It means the degradation experiment is controlled by only temperature and injection mass / volume of aqueous amine solution. For precise calculation of amine solution, the volume of each reaction tubes was measured and indicated in Table 3-3.

Figure 3-2 shows the schematic diagram of the reaction tube for amine degradation. Additional components include a vacuum pump to reduce oxygen and a syringe for sample injection.

Table 3-3. Actual volume of batch reaction tubes

Number of reaction tubes	Volume (ml)
1	5.20
2	5.21
3	5.11
4	5.24
5	4.99

The model FA1730 oven (~1200°C) manufactured by Sybron Thermolyne Corporation was used for degradation experiments. The aqueous amine solution (10 ppm) was loaded into the tube using a vacuum pump and two valves, as seen in Figure 3-2. The vacuum pump removed air and minimized oxidation in the reactor tubes. To further avoid oxidation, nitrogen gas was purged with 10 psi of pressure into the tube for 2 minutes prior to solution injection. After nitrogen purging, the tube opening was blanked and the tube was vacuumed by the pump to assure air removal. The valve of the pump was closed, and then an amount of aqueous amine solution was loaded by opening the valve. The tube was capped with a sealing ball and screw. The filled tubes were placed in the oven at a specific isothermal temperature from 400 to 600°C for 10 minutes. Tubes were removed from the oven then cooled in iced water for 6 hours which was sufficient for complete condensation before collecting samples. Tubes were opened and samples were collected in 1 ml conical glass vials and analyzed by IC to identify and quantify the amine degradation products, such as organic acids, and remaining amine.

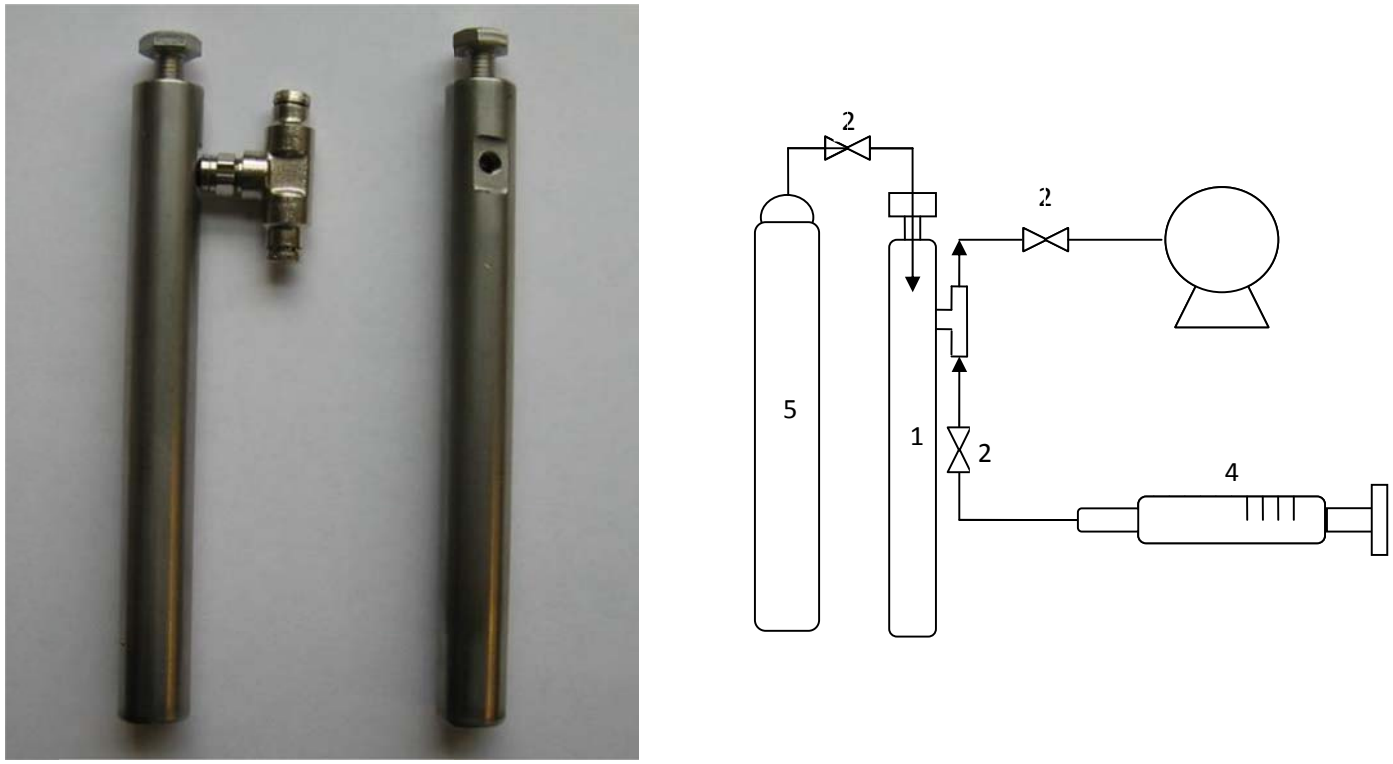

Figure 3-2. Schematic of amine degradation test system

(1, 316 stainless reaction bomb; 2, valve; 3, vacuum pump; 4, injection syringe; 5, nitrogen gas bomb)

3.3.2. Ion Chromatography (IC)

Analysis of amine in aqueous media is difficult because of its high volatility. Most of the common amine detection / measurement methods count on the concepts used in chromatography, where the amines are separated for identification and compared to standards. So, direct gas chromatographic analysis of the amines needs packed or capillary columns coated with thick films of special materials due to high volatility (Gronberg and Jonsson, 1992; Tsukioka et al., 1993).

The original analytical method was gas chromatography (GC). An Agilent 6890 series gas chromatography and an Agilent 5973 mass selective detector (MSD) were used with a Restek Rtx-5 (30m×0.25mm ID×0.25μm thickness) capillary column, split flow injection and flame ionization detector. However, the direct GC analysis shows insignificant peaks and poor repeatability because of high reactivity and the formation of thermal degradation products at high column operating temperatures (Saha et al., 1977).

Derivatization steps were introduced in several GC and high pressure liquid chromatography (HPLC) methods in order to analyze high volatility chemicals, such as amines (Sacher et al., 1997). The derivatization methods for GC and HPLC are presented for amine analysis by Vatsala et al. (1994) and Joseph et al. (1993), respectively. However, their derivatization methods require complicated steps and long measurement time. In recent years, ion chromatography (IC) has been widely used in the industry because GC provides unreliable results with over-predicted rates. IC is capable of ionic analysis while HPLC is capable of nonionic analysis (Davis, 2009).

Cation chromatography was the analytical method for amines and anion chromatography was used for degradation byproducts. A model 790 Personal IC (Metrohm Corp.) system, with a high performance conductivity detector, IC pump and IC-Net 2.1, was used for separation of common cations and selected amines. A metrosep C 2 150 cation column packed with silica gel with carboxyl groups that separates cationic species based on their affinity for the resin was used for the separation. A Metrosep A Supp 5 150 anion column packed with polyvinyl alcohol with quaternary ammonium groups and suppressor module were used for degradation byproducts such as organic acids. The major components of this instrument were an eluent, a high pressure pump, an injection loop (10µl of cation and 20µl of anion), a separator column, eluent suppressor and a conductivity cell detector. Commercially available reagent-grade chemicals were used to prepare eluents; 0.05mmol of HNO_3 plus 0.75 mmol of cation analysis and 3.2 mmol sodium carbonate plus 1.0 mmol sodium bicarbonate for an eluent, 100 mmol of H_2SO_4 for regeneration of suppressor and ultrapure water for anion rinsing. The columns and suppressor were regenerated before the IC analysis to make results clear. Columns were equilibrated with each eluent by keeping a pump flow rate of 1.0 ml/min for 30 min for cation and 0.8 ml/min for 45 minutes for anion, respectively.

3.3.3. Aqueous Amine Solution Preparation

All 10 ppm aqueous amine solutions were prepared by dilution with 18 mΩ deionized (DI) water from 99% amine at room temperature (25°C). Experimental conditions of thermal degradation in supercritical water were designated by vapor-liquid equilibrium (VLE) data from NIST database at the specific temperature and pressure (http://webbook.nist.gov). Mass of aqueous amine solutions in each reaction tube was

evaluated for temperature from 400 to 600°C and pressure from 1000 to 5000 psi (Table 3-4 and Figure 3-3).

Table 3-4. Amount of amine solution (mL) for each operating temperature added to each 5 ml reaction tube

Temperature (°C)	Pressure (psia)				
	1000	2000	3000	4000	5000
300	0.166				
350	0.139	0.367			
400	0.123	0.284	0.535	1.205	2.339
500	0.102	0.218	0.352	0.512	0.705
600	0.088	0.183	0.286	0.396	0.516

The reaction tubes were filled with an amount of aqueous amine solution. All reaction conditions were double checked with both the calculated VLE at given pressure and temperature and by direct mass measurement of the reaction tube before and after aqueous amine solution addition. A leak test was also performed at the maximum temperature and pressure, 600°C and 5000 psia and no leaks were observed before and after heating in the oven.

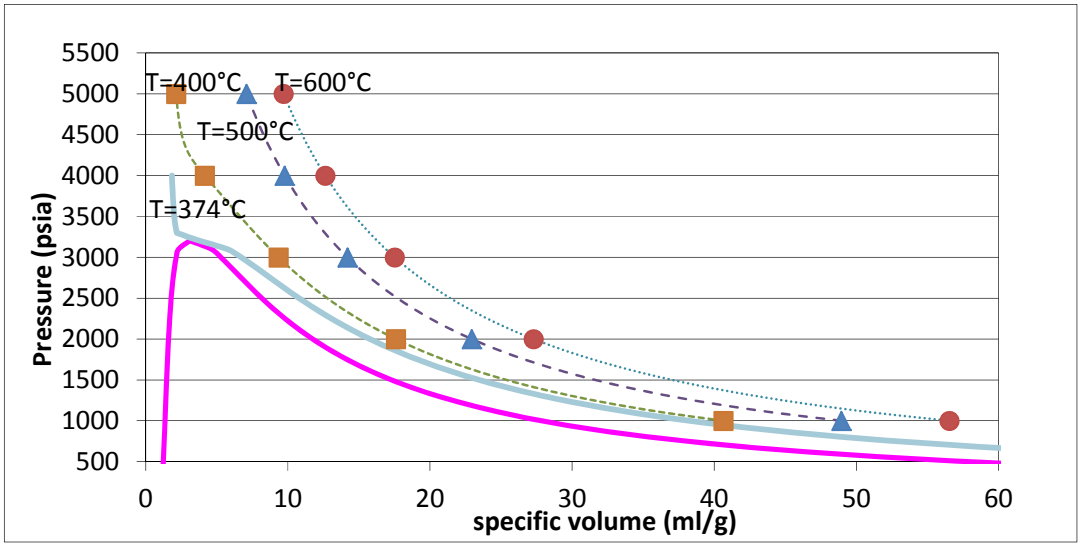

Figure 3-3. VLE diagram of experiment conditions

In addition, the total amounts of initial amine loading should be different at certain temperature and pressure. Figure 3-4 to 3-6 show the total moles of each amine in 5 mL of reactor volume based on Table 3-4.

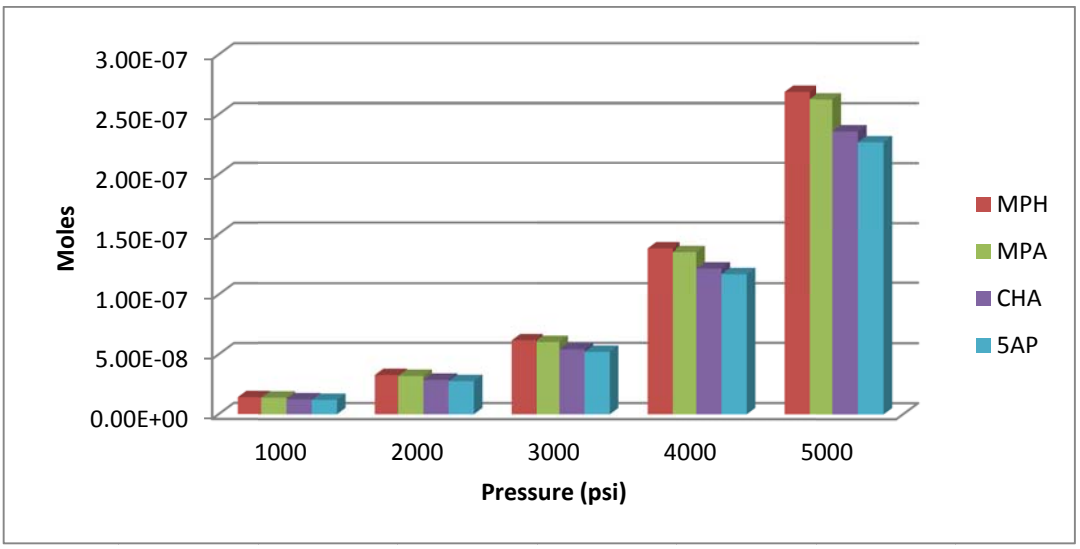

Figure 3-4. Total amounts (moles) of amines initial loading in 5 mL of reactor volume at 400°C

The difference of molecular weight results in the difference amount of initial loading (5AP:103.17 > CHA:99.18 > MPA:89.14 > MPH:87.17 g/mol). In the same reason, total loaded amounts of amines are significantly larger than those at lower pressure, lower temperature and lower molecular weight of amines. The differences of initial loading amount also increase at the higher pressure through Figure 3-4 to 3-6.

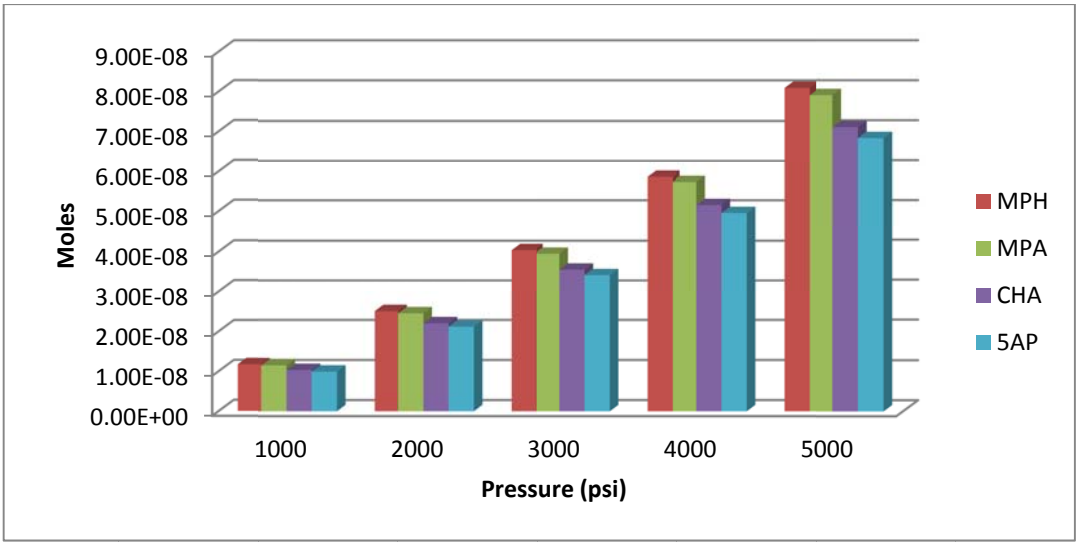

Figure 3-5. Total amounts (moles) of amines initial loading in 5 mL of reactor volume at 500°C

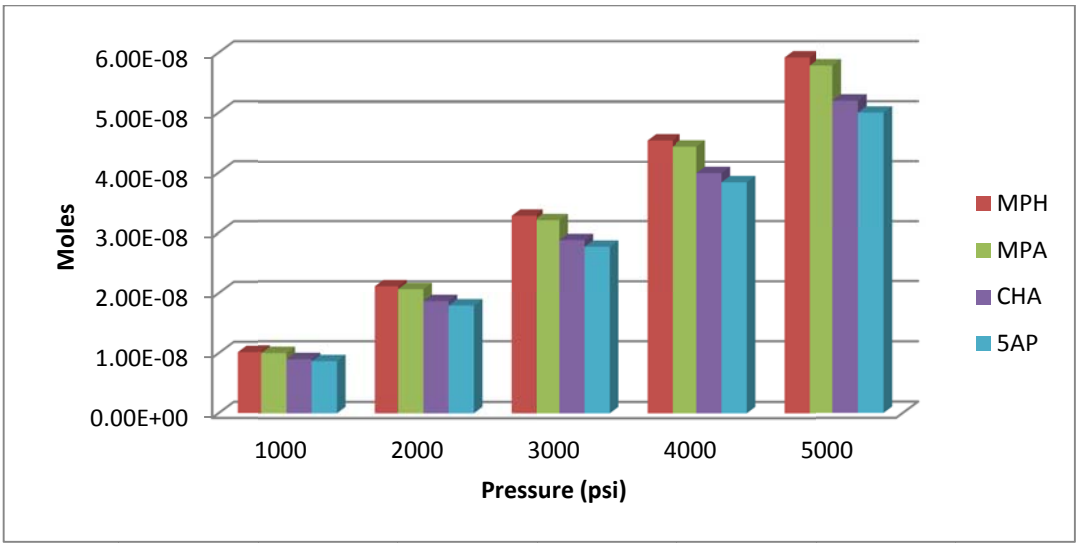

Figure 3-6. Total amounts (moles) of amines initial loading in 5 mL of reactor volume at 600°C

3.3.4. Kinetics Model

The amines that have relatively high decomposition rates would be unsuitable for use in power plants. To predict the degradation more accurately, kinetic rate constants are determined. Gilbert and Lamarre (1989) and Mckay (1990) assumed all the amines

degrade according to first order or pseudo-first order reaction kinetics. This assumption was likely for diaminoethane (DAE), ethanolamine (ETA), and 2-amino-2-methyl-propanol (AMP) which undergoes hydrolysis and is consistent with morpholine degradation. Mckay (1990) reported that morpholine decomposition is pH, or at least composition, dependent. Moreover, thermal degradation might show a similar dependence since experimentation was conducted at a constant concentration and pH.

Kinetic information for the rate of amine degradation to byproducts is defined with concentration, temperature, and time. The rate expression may be either mechanistic or a pseudo first-order equation. The approach used is as described by Foutch and Johannes (1992). By repeating experiments at different times at the same temperatures, the degradation rate constants can be obtained. Arrhenius constants are determined from the data over the temperature range. Experimental data are evaluated along with comparable literature data. A first order rate law is

$$\frac{dC_A}{dt} = -kt$$

where C_A represents the concentration of remaining amine after 10 minutes heating, t is the time in seconds, and k is the rate constant in second^{-1}.

Arrhenius equation provides dependence of the rate constant *k* of chemical reactions on the temperature T and activation energy E_a and Arrhenius constants and activation energy can be determined by assuming pseudo-first order reaction.

$$\ln\frac{C_A}{C_{A0}} = -kt = -A\exp\left(\frac{-Ea}{RT}\right)t$$

where A is the Arrhenius constant and E_a is activation energy. In the meaning of constants, A is the total number of collisions per second and it will vary depending on the order of the reaction. It is known that either increasing the temperature or decreasing activation energy will result in an increase in rate of reaction. Both the activation energy and rate constant represent macroscopic reaction-specific parameters that are not simply related to threshold energies and the success of individual collisions at the molecular level. Temperature effect on the rates of chemical reaction can be analyzed by the Arrhenius equation, which is usually expressed in terms of ln(k) versus 1/K and should be a straight line. The Arrhenius constant and activation energy can be determined from the plot without additional manipulation. Normally, operating the reaction at a constant temperature for a finite amount of time would be best.

3.3.5. Oven Calibration

Although the Arrhenius equation needs constant temperature, significant time is required for temperature to ramp up and down due to heat transfer resistance of the reaction tube. To compensate for this fact, temperature profiles within the tubes were determined for each operating condition. Each temperature inside the tube was measured by a thermocouple and target temperature indicated the temperature in the oven. The operating temperature cited for the data is the maximum temperature that the solution attained during the experiment. These are presented in Figure 3-7.

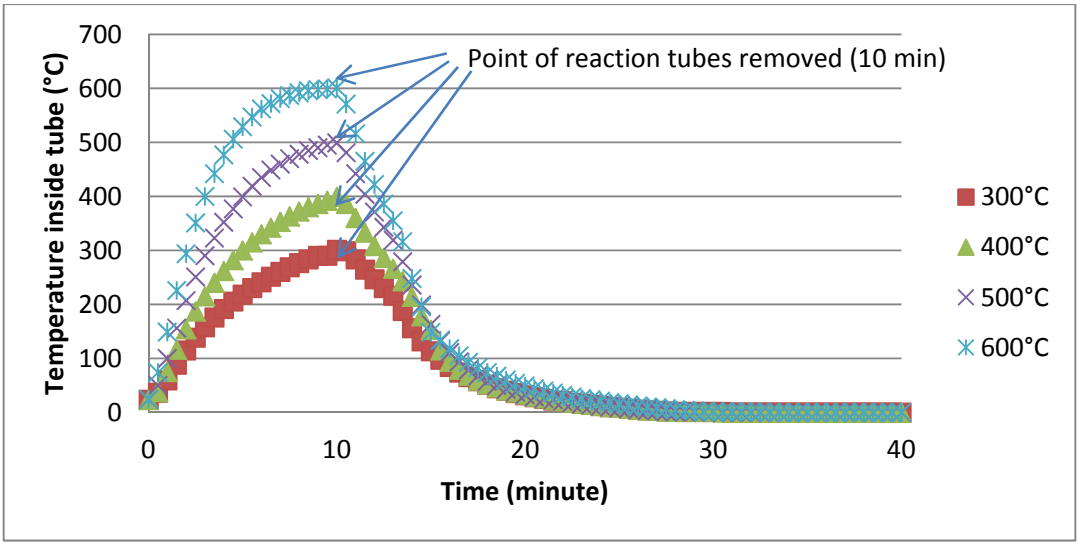

Figure 3-7. Measured temperature profile inside reaction tube at each temperature

The profile is based on the temperature inside the tube for 10 minutes of heating along with 6 hours cooling in iced water for complete sample condensation. The experiment shows that the maximum temperature was reached at 10 minutes; the time the tubes were removed from the furnace. The area below the curve was integrated by Numerical Evaluation of Integrals for solving first-order differential equations. Arrhenius equation with an assumption of pseudo first order is applied over the profiles for each temperature presented in Figure 3-7 and the constants are extracted. The general equations are;

1) For N+1 points, where (N/3) is an integer,

$$\int_{X_0}^{X_N} f(X)dX = \frac{3h}{8}[f_0 + 3f_1 + 3f_2 + 2f_3 + 3f_4 + 3f_5 + 2f_6 \cdots + 3f_{N-1} + f_N]$$

2) For N+1 points, where N is an even,

$$\int_{X_0}^{X_N} f(X)dX = \frac{h}{3}[f_0 + 4f_1 + 2f_2 + 4f_3 + 2f_4 + \cdots + 4f_{N-1} + f_N]$$

where $h = \frac{X_N - X_0}{N}$

3.4. Experimental Results and Discussions

The objective of this work is to evaluate the thermal stability of amines by kinetic analysis as well as establishing the material balance with their byproducts at supercritical conditions.

3.4.1. Degradation Fractions

The amine concentrations were measured by IC in the temperature range of 300 to 600°C and the pressure range of 1000 to 5000 psi and compared with literature data in Table 2-3. Ethanolamine and ammonia have almost the same IC retention time; 3.77 minute for ammonia and 4.01 minute for ethanolamine, although each calibration curve was well established. Hence, ethanolamine data indicate area instead of concentration.

Table 3-5. Final concentration and degraded percentage after 10 min reaction as a function of temperature and pressure (Initial concentration=10 ppm)

Temp (°C)	Pressure (psia)	NH3 *	MPH	MPA	CHA	5AP	ETA+NH3 ***
600	5000	8.7 (13.2%)	0.1 (99.5%)	0.1 (99.1%)	0.1 (99.8%)	0.1 (99.1%)	36.7
600	4000	8.8 (12.3%)	BDL**	0.1 (98.9%)	0.1 (99.2%)	0.3 (97.1%)	15.1
600	3000	9.5 (4.9%)	BDL**	0.1 (99.3%)	BDL**	0.5 (95.3%)	14.6
600	2000	8.2 (17.6%)	BDL**	BDL**	0.1 (99.4%)	0.1 (99.3%)	13.2
600	1000	7.9 (21.4%)	0.2 (98.0%)	BDL**	0.0 (99.7%)	BDL**	13.1
500	5000	9.7 (2.8%)	BDL**	0.6 (93.7%)	BDL*	1.4 (86.4%)	13.1
500	4000	9.8 (2.4%)	BDL**	0.6 (93.6%)	1.0 (89.7%)	1.3 (87.1%)	13.5
500	3000	8.8 (12.0%)	BDL**	0.7 (93.3%)	BDL**	1.4 (86.4%)	12.4
500	2000	3.5 (64.6%)	0.7 (93.6%)	0.7 (93.5%)	BDL**	1.4 (86.5%)	13.4
500	1000	5.1 (48.9%)	BDL**	0.6 (93.9%)	1.0 (89.8%)	1.4 (86.3%)	13.6
400	5000	10.0 (0.0%)	0.6 (94.2%)	3.8 (62.5%)	2.4 (76.5%)	7.9 (21.4%)	2.6
400	4000	9.9 (0.2%)	0.6 (94.1%)	4.3 (56.8%)	4.2 (58.3%)	4.3 (56.7%)	13.6
400	3000	9.5 (5.4%)	BDL**	0.9 (90.3%)	2.8 (71.9%)	1.4 (86.2%)	5.4
400	2000	4.5 (54.9%)	0.6 (94.1%)	0.6 (93.6%)	1.8 (82.2%)	1.3 (87.1%)	11.9
400	1000	4.8 (52.5%)	BDL**	0.7 (93.0%)	1.00 (90.1%)	1.4 (86.4%)	8.8
350	1000	4.9 (50.3%)	0.6 (94.2%)	0.7 (92.7%)	3.00 (70.3%)	0.7 (93.0%)	16.7
300	1000	4.1 (59.4%)	4.0 (59.6%)	5.2 (47.9%)	4.4 (56.3%)	2.8 (73.7%)	14.1

* Ammonia(NH_3) tested for comparison with 10 ppm of ammonium chloride solution

** BDL : Below Detection Limit, *** ETA and NH_3 peaks were not completely separated (Area of 10ppm of NH_3 : 57,ETA:20)

Figure 3-8 to 3-12 show the remaining amine concentration in the ranges from 400 to 600°C and 1000 to 5000 psi. The values are the actual remaining concentrations of samples collected from individual reaction tubes.

The sub-critical degradation results from 300 and 350°C are compared with supercritical conditions in Figure 3-8. The largest amounts remain at 300°C with a tendency to decrease above 350°C. MPA shows 48% degradation at 300°C; less than the significant 93% degradation at 350°C. On the other hand, CHA shows 56% degradation at 300°C; less than the 70% degradation at 350°C. Remaining ammonia concentration increased as temperature was raised and there was a significant 50 to 60% ammonia loss below 600°C. All organic amines were more degraded at elevated temperature; however, the difference was not significant at 1000 psi above the critical temperature. In addition, almost all organic amines are totally degraded at 600°C and 1000 psi.

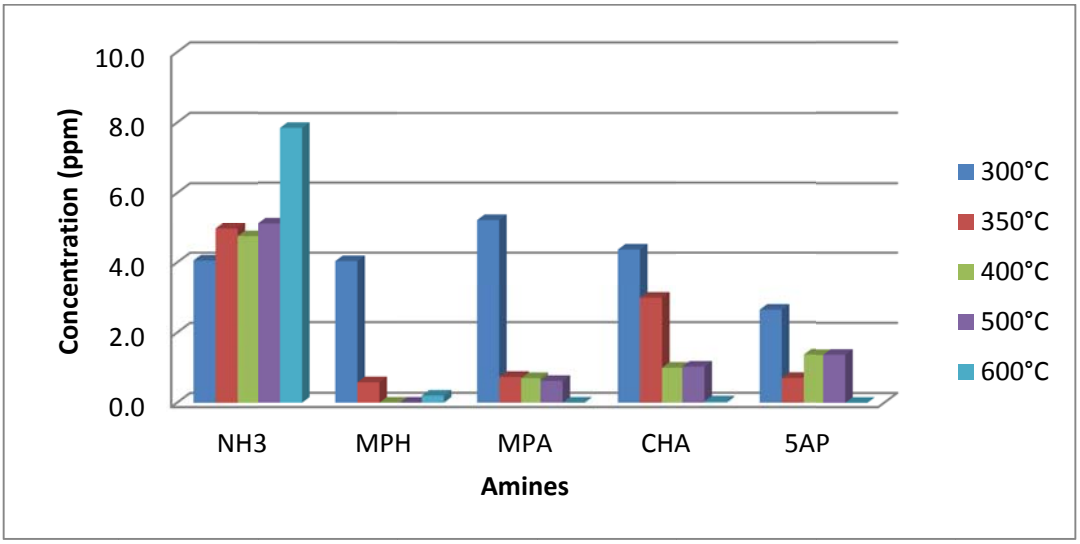

Figure 3-8. Amine concentration at 1000 psi after 10 min in the furnace

Ammonia concentration was slightly increased at elevated temperature at 2000 psi (Figure 3-9). All organic amines were significantly degraded below 1 ppm. CHA shows the highest concentration (1.78 ppm), however CHA is completely decomposed at 500 and 600°C. 5AP maintains 1.3 ppm concentration at 400 and 500°C but also decomposed to zero at 600°C.

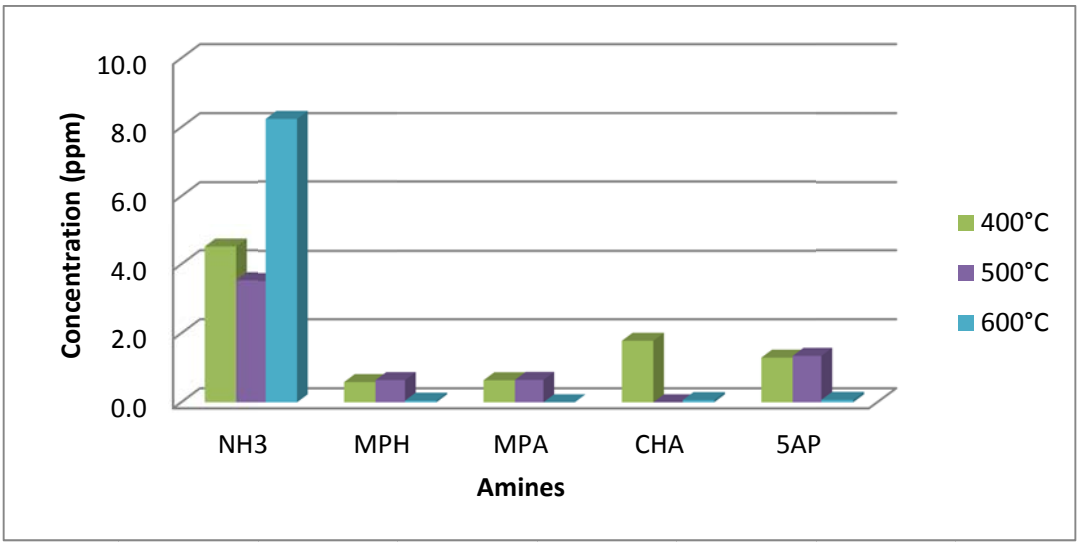

Figure 3-9. Amine concentration at 2000 psi after 10 min in the furnace

For Figure 3-10, remaining ammonia concentrations at 3000 psi were significantly higher than those at 1000 and 2000 psi. All MPH decomposed completely at 3000 psi and CHA shows the highest concentration at 400°C but is significantly decomposed at 500 and 600°C. On the other hand, 5AP was about 86% of degradation until 500°C but steep decomposing to 95% at 600°C.

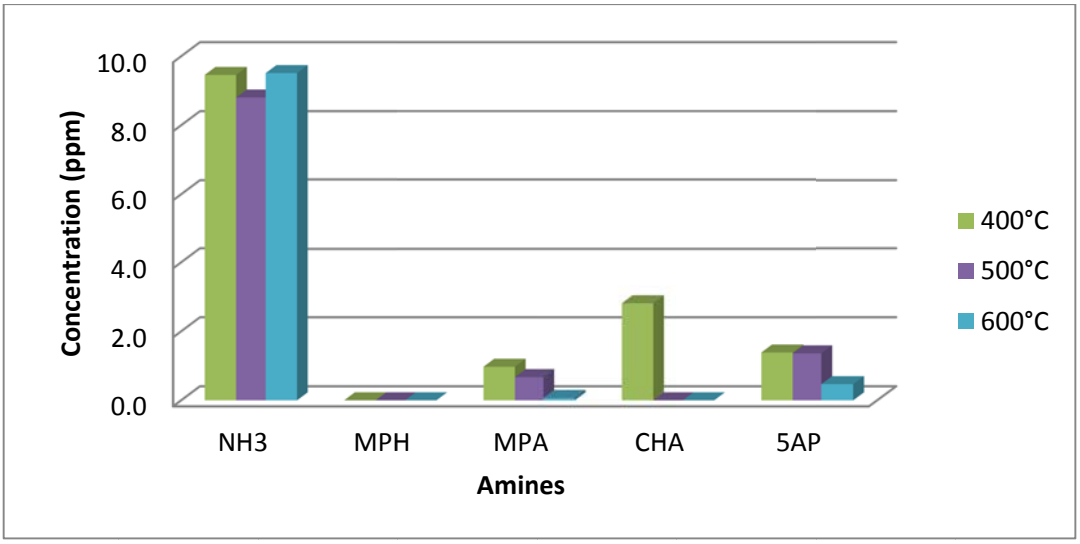

Figure 3-10. Amine concentration at 3000 psi after 10 min in the furnace

Figure 3-11 indicates ammonia concentration decreases with an increase in temperature; however ammonia remained near the initial concentration (8.8 to 10 ppm) with 0 to 12% of reduction. MPA, CHA, and 5AP also had the highest concentration (4 ppm) at 400°C but those significantly decomposed to 0.6, 1.0 and 1.3 ppm at 500°C, respectively and totally decomposed at 600°C.

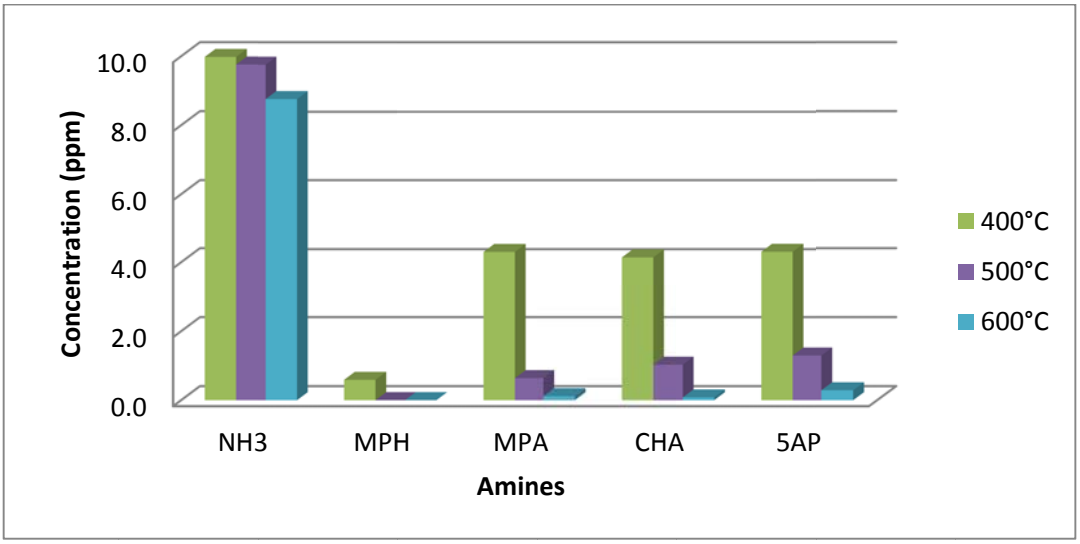

Figure 3-11. Amine concentration at 4000 psi after 10 min in the furnace

In Figure 3-12, remaining ammonia concentration decreases at elevated temperature but the difference was less than 12% between 400 and 600°C. In addition, MPA, CHA, and 5AP show the highest remaining concentration at 400°C in 3.76, 2.35 and 7.86 ppm, respectively. Isothermally, remaining concentration of selected amines (Figure 3-8 to 3-12) shows less degraded at elevated pressure. As a result, pressure is an amine degradation factor; and from Le Chatelier's principle, elevated pressure benefits the direction of reaction that has the fewest number of molecules.

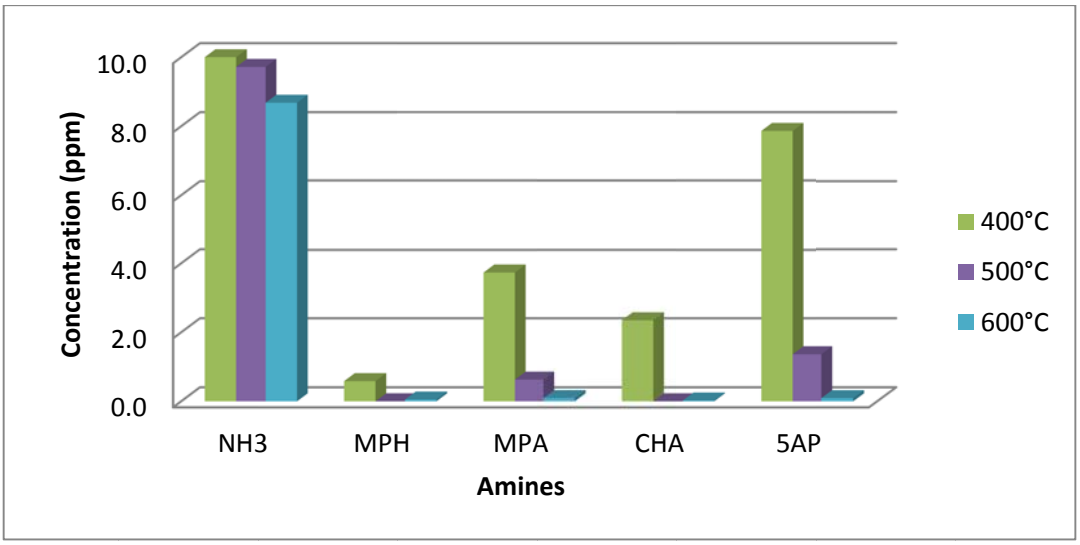

Figure 3-12. Amine concentration at 5000 psi after 10 min in the furnace

Figures 3-13 to 3-15 show the isobaric remaining concentration with temperature in supercritical water. In Figure 3-13, remaining concentrations of MPA, CHA and 5AP increase with pressure. On the other hand, the results of MPA and CHA show the largest amount at 4000 psi and 400°C while MPH is near zero at these conditions.

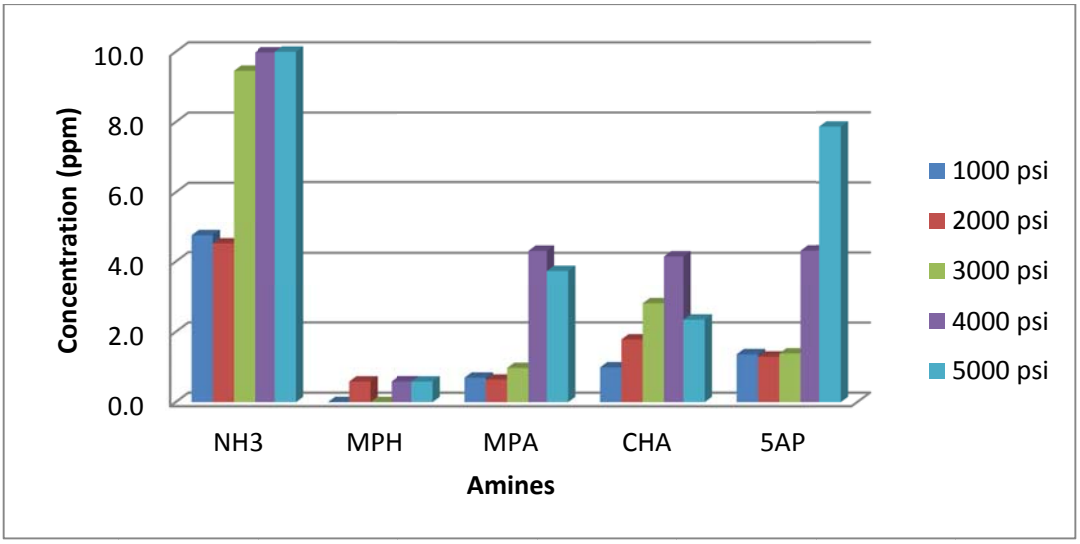

Figure 3-13. Amine concentration at 400°C after 10 minute in the furnace

Figure 3-14 shows that all organic amines were 90% degraded at 500°C over the elevated pressure range. 5AP shows relatively less 85% degradation at these conditions.

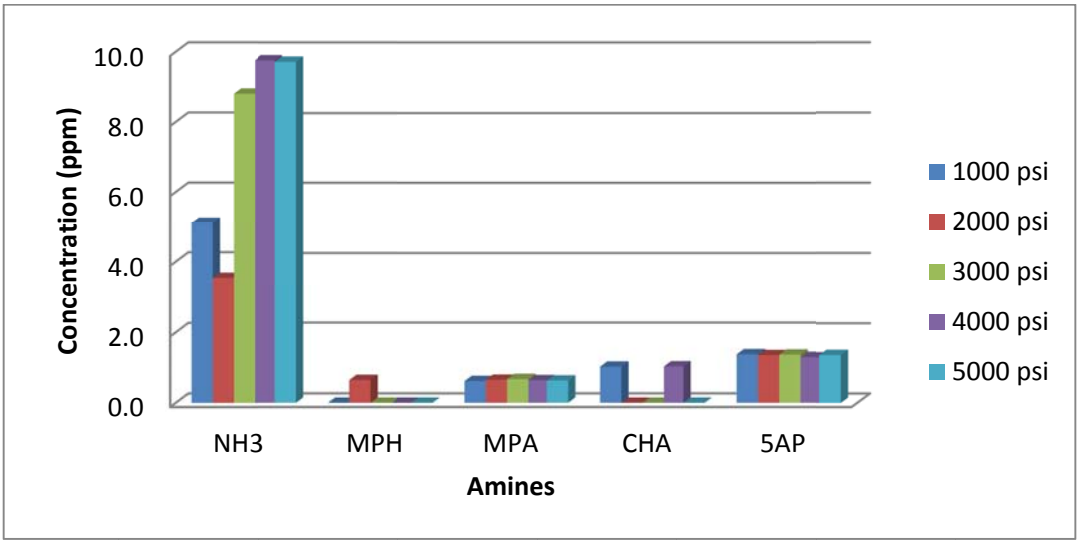

Figure 3-14. Amine concentration at 500°C after 10 minute in the furnace

Figure 3-15 shows that pressure is not a significant degradation parameter at the highest temperature. All organic amines were degraded from 97 to 100% at 600°C.

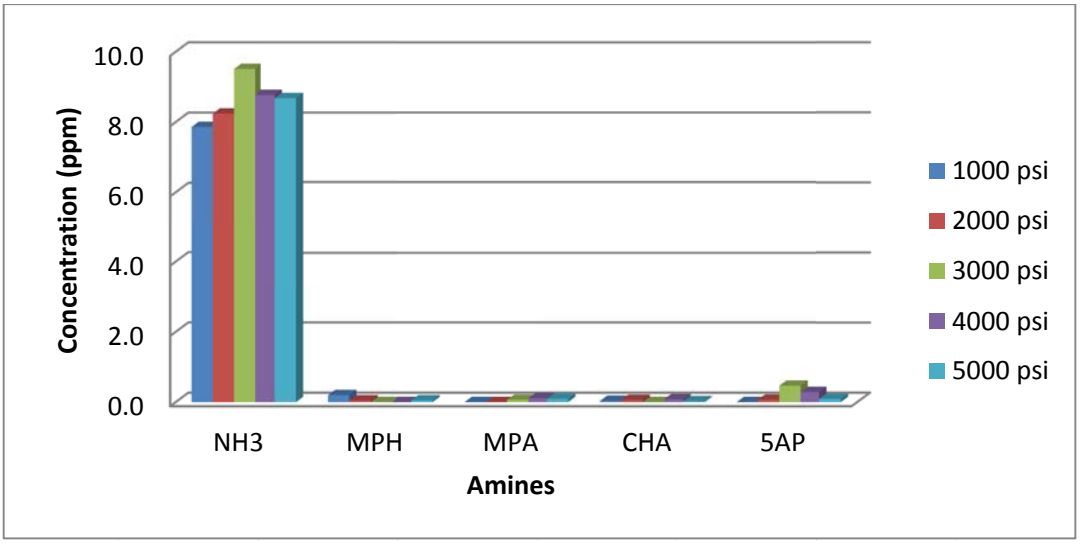

Figure 3-15. Amine concentration at 600°C after 10 minute in the furnace

From Figures 3-8 to 3-15, the most significant findings are that all organic amines degrade significantly at high temperature. Minor variations occur with pressure, but even these short durations at elevated temperature destroy organic amines.

Ammonia remains at relative high concentration over all conditions since ammonia is known to be non-reactive at these conditions. All amounts are less than initial concentration and indicate loss of ammonia by leaks or inaccurate measurements.

3.4.2. Kinetic Analysis

3.4.2.1. Pseudo-First Order Reaction

Pseudo first order reaction was applied for kinetic analysis in case of small amount of amines in excess water surrounding. In general, kinetic measurements of second-order reactions, using an excess of one reactant can yield more accurate rate data than is generally realized. The kinetic of organic amine degradation was evaluated at 400, 500 and 600°C and 1000 to 5000 psi. The rate dependence on temperature was

established by the Arrhenius equation, which is derived into a plot of ln(k) versus 1/T(K). The plot should be linear assuming pseudo-first order as discussed in Chapter 3-5, where remaining concentration of amines were used to calculate the kinetic parameters.

Arrhenius equation was applied in terms of integral expression of time and temperature with pseudo first order reaction based on the result of remaining amine concentrations measurement;

$$\ln\left(\frac{\mathrm{C_A}}{\mathrm{C_{A_o}}}\right) = -\int k\,\mathrm{dt} = -\int \mathrm{A}\exp\left(\frac{-\mathrm{E_a}}{\mathrm{RT_i}}\right)\mathrm{dt}$$

Degradation rate (k) was determined from degradation fraction such as the relation between initial and remaining concentrations.

$$k = \frac{ln\left(\frac{C_A}{C_{Ao}}\right)}{\int dt}$$

Arrhenius constant (A) and activation energy (E_a) were optimized from these two object functions (OF);

$$y_1 = ln\left(\frac{C_A}{C_{A_o}}\right)$$

$$y_2 = -\int A\exp\left(\frac{-E_a}{RT_i}\right)dt$$

$$OF_1 = \sum\left(\frac{y_2 - y_1}{y_1}\right)^2$$

$$OF_2 = \sum(y_2 - y_1)^2$$

The Arrhenius constants and activation energies obtained from linear regression are presented in Table 3-6. However the kinetic data of ETA was not evaluated since ETA and ammonia were not separated completely.

Figures 3-16 to 3-19 show the Arrhenius plots for each organic amine at different temperatures and pressure.

MPH results show the lowest 4.4×10^{-3} s^{-1} of rate constant (k) at 500°C and 2000 psi in Figure 3-16. The activation energy of MPH has the largest value (4.8×10^{4} J/mol) at 4000 psi and the lowest value (3.3×10^{-10} J/mol) at 3000 psi.

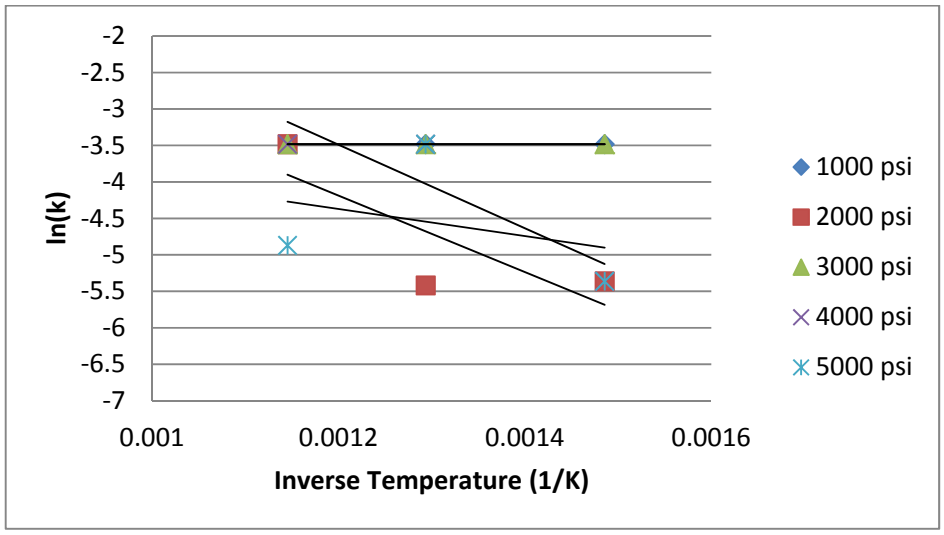

Figure 3-16. MPH Arrhenius plots in the temperature range from 400 to 600°C

Figure 3-17 is the MPA Arrhenius plots. The rate constant (k) has the lowest value at 5000 psi -- 1.6×10^{-3} to 7.8×10^{-3} s^{-1} at 400 to 600°C -- and activation energies were 3.8×10^{4} J/mol. On the other hand, the rate constant shows the highest value (5.4×10^{-2} s^{-1}) at 1000 and 2000 psi and activation energies were calculated as 5.8×10^{4} and 5.7×10^{4} J/mol, respectively.

Table 3-6. Optimized Arrhenius constant (A), activation energy (E) and rate constant (k) at different temperature and pressure conditions considering measured temperature profile.

Temperature (°C)	Pressure (pisa)	MPH			MPA		
		A[s^-1]	E[J/mol]	k[s^-1]	A[s^-1]	E[J/mol]	k[s^-1]
400	1000	3.10×10^{-2}	0.00×10^{0}	3.10×10^{-2}	9.60×10^{1}	5.80×10^{4}	4.40×10^{-3}
	2000	8.20×10^{0}	4.40×10^{4}	4.70×10^{-3}	8.40×10^{1}	5.70×10^{4}	4.60×10^{-3}
	3000	3.70×10^{-2}	3.30×10^{-10}	3.10×10^{-2}	8.90×10^{-2}	1.80×10^{4}	3.90×10^{-3}
	4000	2.95×10^{1}	4.80×10^{4}	4.70×10^{-3}	2.40×10^{0}	4.10×10^{4}	1.40×10^{-3}
	5000	1.20×10^{-1}	1.50×10^{4}	4.70×10^{-3}	1.60×10^{0}	3.80×10^{4}	1.60×10^{-3}
500	1000	3.10×10^{-2}	0.00×10^{0}	3.10×10^{-2}	9.60×10^{1}	5.80×10^{4}	4.70×10^{-3}
	2000	8.20×10^{0}	4.40×10^{4}	4.40×10^{-3}	8.40×10^{1}	5.70×10^{4}	4.60×10^{-3}
	3000	3.70×10^{-2}	3.30×10^{-10}	3.10×10^{-2}	8.90×10^{-2}	1.80×10^{4}	4.50×10^{-3}
	4000	2.95×10^{1}	4.80×10^{4}	3.10×10^{-2}	2.40×10^{0}	4.10×10^{4}	4.60×10^{-3}
	5000	1.20×10^{-1}	1.50×10^{4}	3.10×10^{-2}	1.60×10^{0}	3.80×10^{4}	4.60×10^{-3}
600	1000	3.10×10^{-2}	0.00×10^{0}	1.00×10^{0}	9.60×10^{1}	5.80×10^{4}	5.40×10^{-2}
	2000	8.20×10^{0}	4.40×10^{4}	3.10×10^{-2}	8.40×10^{1}	5.70×10^{4}	5.40×10^{-2}
	3000	3.70×10^{-2}	3.30×10^{-10}	3.10×10^{-2}	8.90×10^{-2}	1.80×10^{4}	8.30×10^{-3}
	4000	2.95×10^{1}	4.80×10^{4}	3.10×10^{-2}	2.40×10^{0}	4.10×10^{4}	7.40×10^{-3}
	5000	1.20×10^{-1}	1.50×10^{4}	7.70×10^{-3}	1.60×10^{0}	3.80×10^{4}	7.80×10^{-3}

Table 3-6. Optimized Arrhenius constant (A), activation energy (E) and rate constant (k) at different temperature and pressure conditions considering measured temperature profile (Continued).

Temperature	Pressure	CHA			5AP		
(°C)	(pisa)	A[s^-1]	E[J/mol]	k[s^-1]	A[s^-1]	E[J/mol]	k[s^-1]
400	1000	1.30×10^{-1}	2.10×10^{4}	3.90×10^{-3}	2.20×10^{2}	6.50×10^{4}	3.30×10^{-3}
	2000	1.40×10^{0}	3.10×10^{4}	2.90×10^{-3}	1.10×10^{-1}	2.00×10^{4}	3.40×10^{-3}
	3000	7.30×10^{3}	8.20×10^{4}	2.10×10^{-3}	1.90×10^{-2}	1.00×10^{4}	3.30×10^{-3}
	4000	2.50×10^{0}	4.20×10^{4}	1.50×10^{-3}	8.10×10^{-1}	3.50×10^{4}	1.40×10^{-3}
	5000	5.80×10^{0}	4.00×10^{4}	2.40×10^{-3}	2.30×10^{2}	7.30×10^{4}	4.00×10^{-4}
500	1000	1.30×10^{-1}	2.10×10^{4}	3.80×10^{-3}	2.20×10^{2}	6.50×10^{4}	3.30×10^{-3}
	2000	1.40×10^{0}	3.10×10^{4}	5.40×10^{-2}	1.10×10^{-1}	2.00×10^{4}	3.30×10^{-3}
	3000	7.30×10^{3}	8.20×10^{4}	5.40×10^{-2}	1.90×10^{-2}	1.00×10^{4}	3.30×10^{-3}
	4000	2.50×10^{0}	4.20×10^{4}	3.80×10^{-3}	8.10×10^{-1}	3.50×10^{4}	3.40×10^{-3}
	5000	5.80×10^{0}	4.00×10^{4}	5.40×10^{-2}	2.30×10^{2}	7.30×10^{4}	3.30×10^{-3}
600	1000	1.30×10^{-1}	2.10×10^{4}	9.40×10^{-3}	2.20×10^{2}	6.50×10^{4}	5.40×10^{-2}
	2000	1.40×10^{0}	3.10×10^{4}	8.40×10^{-3}	1.10×10^{-1}	2.00×10^{4}	8.20×10^{-3}
	3000	7.30×10^{3}	8.20×10^{4}	5.40×10^{-2}	1.90×10^{-2}	1.00×10^{4}	5.10×10^{-3}
	4000	2.50×10^{0}	4.20×10^{4}	8.00×10^{-3}	8.10×10^{-1}	3.50×10^{4}	5.90×10^{-3}
	5000	5.80×10^{0}	4.00×10^{4}	1.00×10^{-2}	2.30×10^{2}	7.30×10^{4}	7.80×10^{-3}

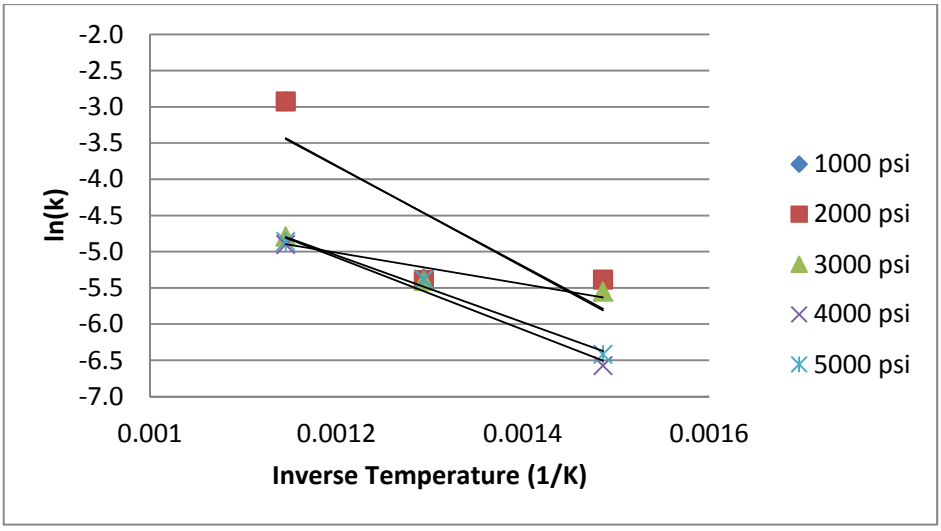

Figure 3-17. MPA Arrhenius plots in the temperature range from 400 to 600°C

CHA results show the lowest rate constant at 4000 psi as 1.5×10^{-3}, 3.8×10^{-3} and 8.0×10^{-3} s^{-1} at 400, 500 and 600°C with 8.2×10^{4} J/mol of activation energy in Figure 3-18. The results show little change in rate constant (k) at 1000 psi from 3.9×10^{-3} to 9.4×10^{-3} s^{-1} with 2.1×10^{4} J/mol activation energy but the overall rates are slightly higher than those at 4000 psi.

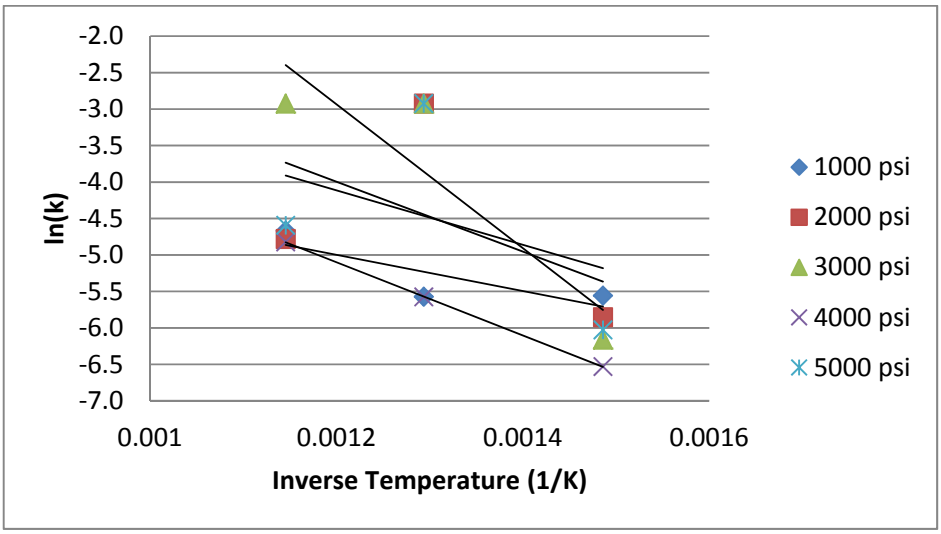

Figure 3-18. CHA Arrhenius plots in the temperature range from 400 to 600°C

Figure 3-19 shows the 5AP Arrhenius plot at supercritical conditions. There is little change in rate constant at 3000 psi from 3.3×10^{-3} to 5.1×10^{-3} s^{-1} with 1.0×10^{4} J/mol activation energy. On the other hand, the lowest rate was found at 5000 psi and 400°C as 4.0×10^{-4} s^{-1} and the difference of rate constants at the highest temperature was not significant. 5AP shows the lowest overall degradation rates (4.0×10^{-4} to 7.8×10^{-3} s^{-1}) with 7.3×10^{4} J/mol activation energy at 5000 psi.

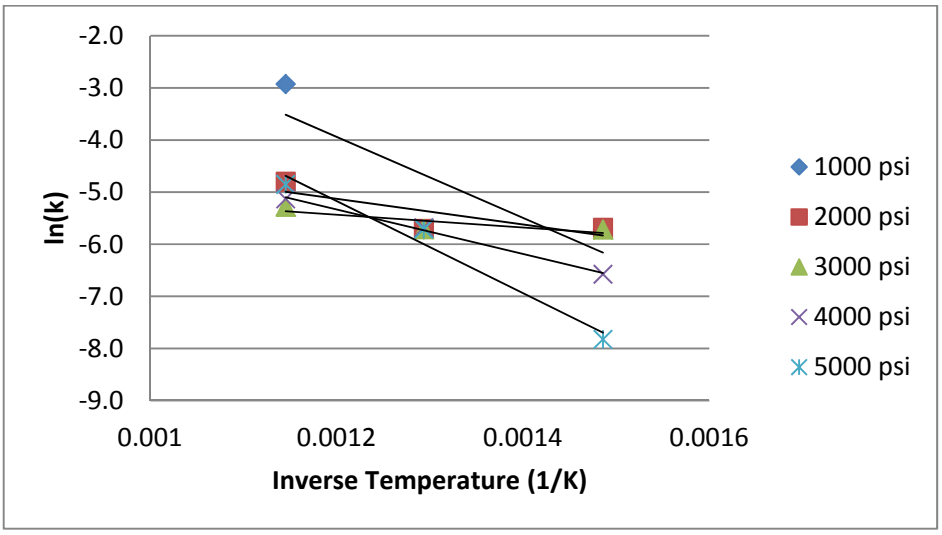

Figure 3-19. 5AP Arrhenius plots in the temperature range from 400 to 600°C

Figure 3-20 to 3-24 show the Arrhenius plots of organic amines at different pressures. Rate constants of amines will be compared at the specific pressure over the range.

5AP shows the lowest rate constant with 6.5×10^{4} J/mol and the largest activation energy followed by 5.8×10^{4} and 2.1×10^{4} J/mol for MPA and CHA, respectively in Figure 3-20.

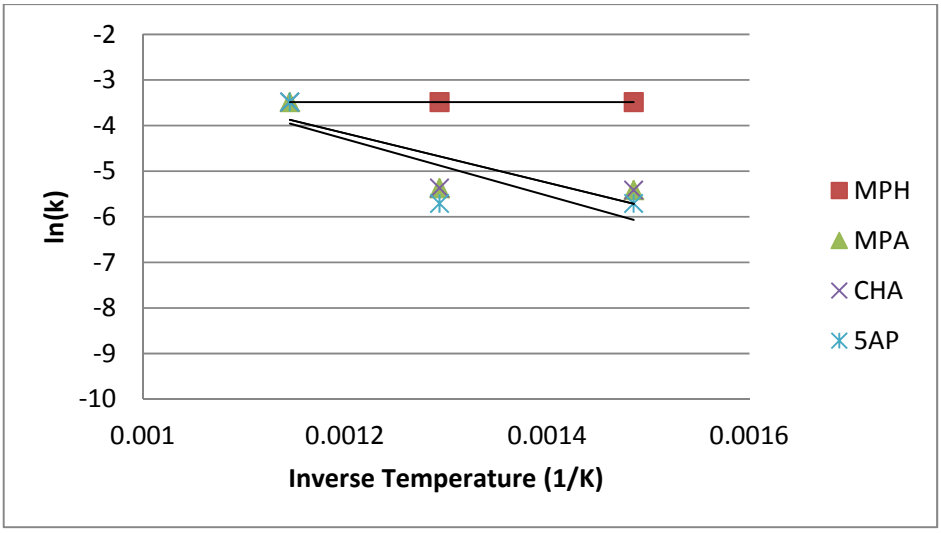

Figure 3-20. Arrhenius plots at 1000 psi in the temperature range from 400 to 600°C

Figure 3-21 shows no significant difference in rate constants for amines at 2000 psi, however 5AP shows that an overall lowest rate constants (3.4×10^{-3} to 8.2×10^{-3} s^{-1}) with 2.0×10^{4} J/mol (the largest activation energy) followed by 5.7×10^{4} and 3.1×10^{4} J/mol for MPA and CHA, respectively.

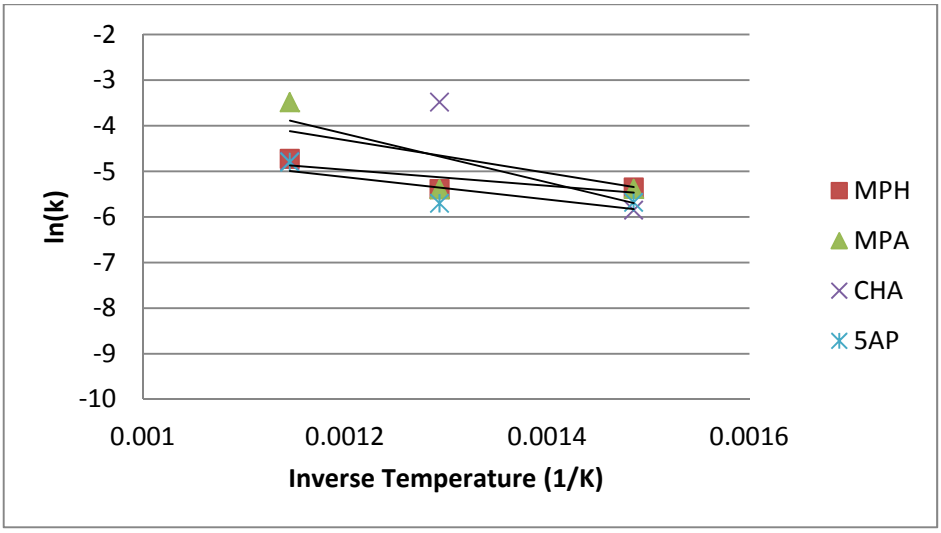

Figure 3-21. Arrhenius plots at 2000 psi in the temperature range from 400 to 600°C

5AP and MPA show low rate constants at 3000 psi in Figure 3-22. The rate constants and activation energy for 5AP were 3.3×10^{-3} to 5.1×10^{-3} s^{-1} and 1.0×10^{4} J/mol, respectively. On the other hand, those for MPA were 3.9×10^{-3} to 8.3×10^{-3} s^{-1} and 1.8×10^{4} J/mol, respectively.

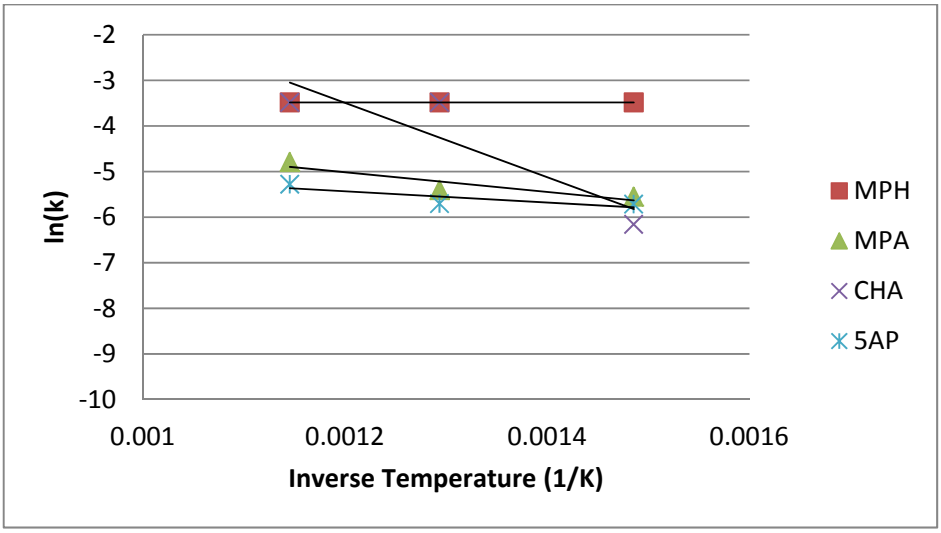

Figure 3-22. Arrhenius plots at 3000 psi in the temperature range from 400 to 600°C

Figure 3-23 shows almost the same rate constants as 5AP, CHA and MPA, however 5AP shows the lowest rate constant of 1.4×10^{-3} to 5.9×10^{-3} s^{-1} with 3.5×10^{4} J/mol activation energy.

Figure 3-24 shows 5AP has overall lowest rate constants (4.0×10^{-4} to 7.8×10^{-3} s^{-1}) with 7.3×10^{4} J/mol activation energy followed by 3.8×10^{4} and 4.0×10^{4} J/mol for MPA and CHA, respectively. Although there was no significant difference of rate constants at the highest temperature (600°C), degradation rate constant of 5AP was 4.0×10^{-4} s^{-1} followed by 1.6×10^{-3}, 2.4×10^{-3} and 4.7×10^{-3} s^{-1} at the lowest temperature (400°C), respectively.

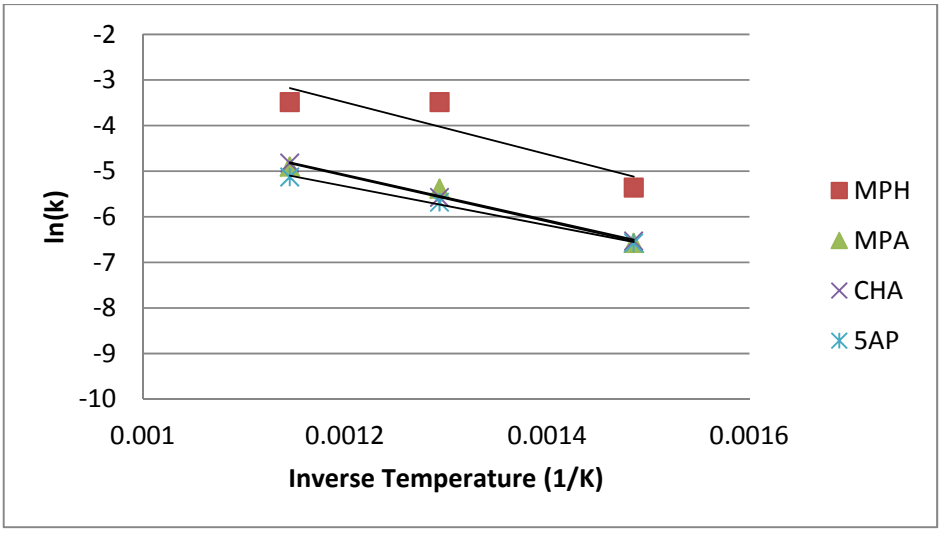

Figure 3-23. Arrhenius plots at 4000 psi in the temperature range from 400 to 600°C

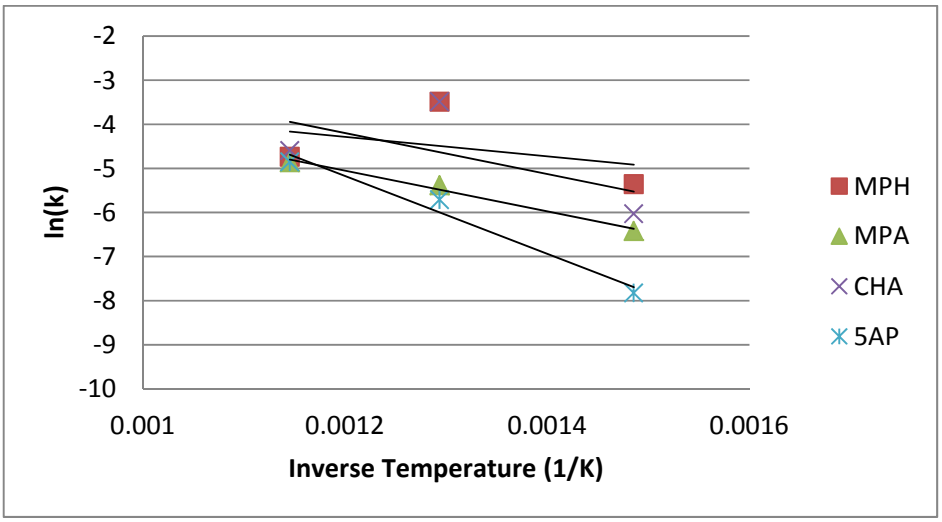

Figure 3-24. Arrhenius plots at 5000 psi in the temperature range from 400 to 600°C

The amine degradation data in this study was limited to high temperature and pressure conditions. The data for 10 ppm initial concentrations of MPH at the ranging from 400 to 600°C were compared with data at 280°C (Cobble and Turner, 1992; Gilbert and Lamarre, 1989). These comparisons are presented in Figure 3-22 along with the relationship of MPH in the temperature range from 280 to 600°C. Both data sets have similar linear trend indicative of pseudo-first order reaction. In addition, relatively high

uncertainty / deviation at higher temperature may be due to high relative volatility in sample preparation and leakage upon heating at high pressure.

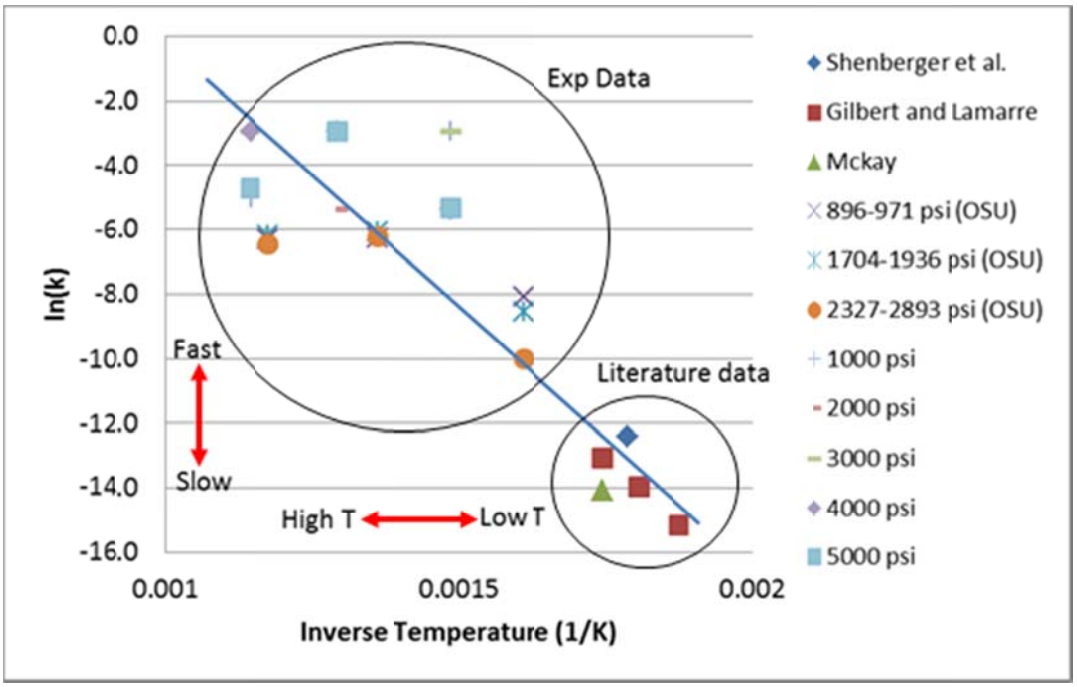

Figure 3-25. Arrhenius plots of MPH for both of experimental and literature data using a pseudo-first order

3.4.2.2. Evaluation of Degradation Order

Degradation kinetics in previous chapter was evaluated by using the pseudo first order and hydrolysis in supercritical water. This chapter will evaluate the reaction order at certain temperature by using the results obtained from the experiments and explain the amines oxidation related to oxygen come from supercritical water itself.

Lee and Park (1996) conducted the reaction kinetics and mechanism of nitrogen compounds in supercritical water in ranging from 440 to 550°C. The decomposition kinetics of nitrobenzene had activation energy of 68.0 ± 9.0 kJ/mol. The decomposition rate was enhanced in the presence of oxygen.

The determining step of reaction order begins from a power law rate expression;

$$r = k[\text{Amine}]^m[H_2O]^n$$

where k, [Amine], m, and n are the rate constant, final concentration of amine, degradation order of amine, and supercritical water. In excess of water;

$$\ln(r) = m \ln[\text{Amine}] + \ln k' \qquad (k' = k\,[H_2O]^n)$$

Figure 3-26 to 3-29 show the straight line with slope m and intercept k' in the plot of ln (final concentration of amines) against ln (r). It was assumed that this kinetic study was considered only temperature, not pressure. The degradation order of MPH were 1.00 and 1.66 for 400 and 600°C, however not evaluated for 500°C due to data limitation.

With the same way, the degradation orders of other amines were evaluated in Table 3-7. Although there was variation of degradation order in supercritical water, the maximum order (1.66) was not limited to second.

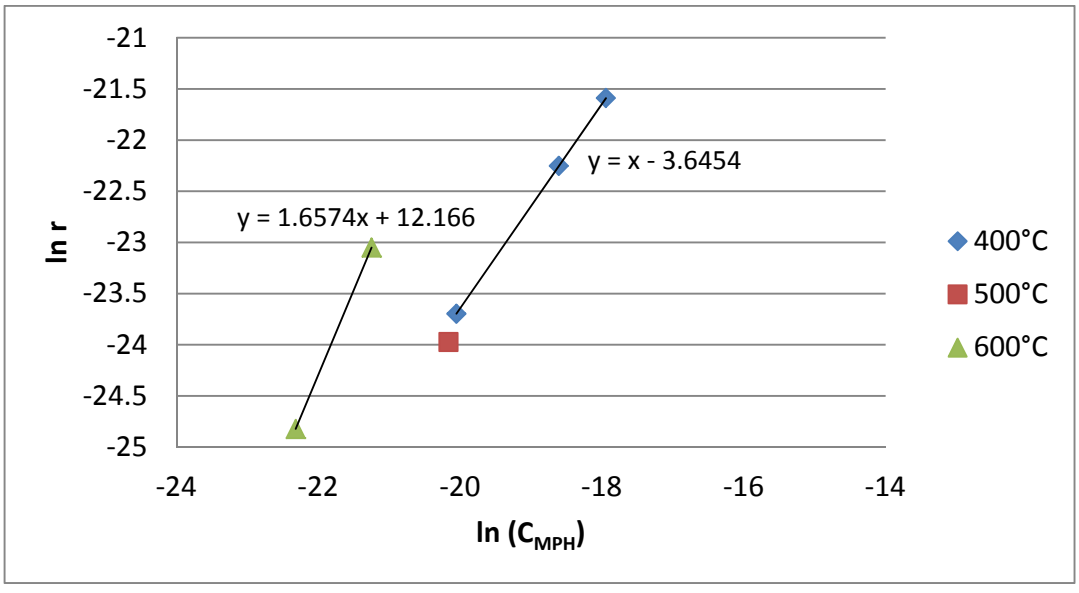

Figure 3-26. Determination of degradation order with MPH

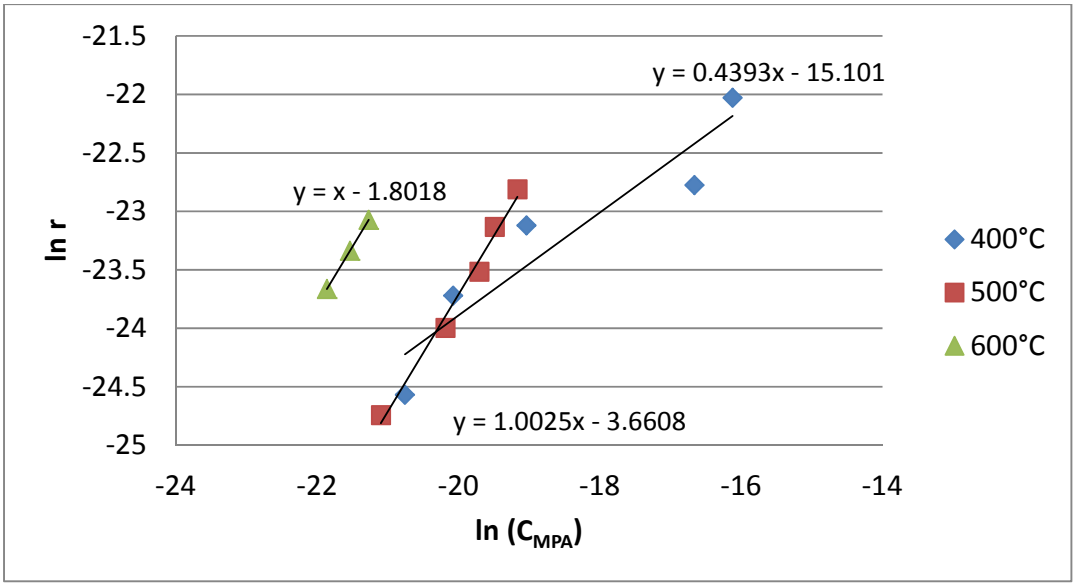

Figure 3-27. Determination of degradation order with MPA

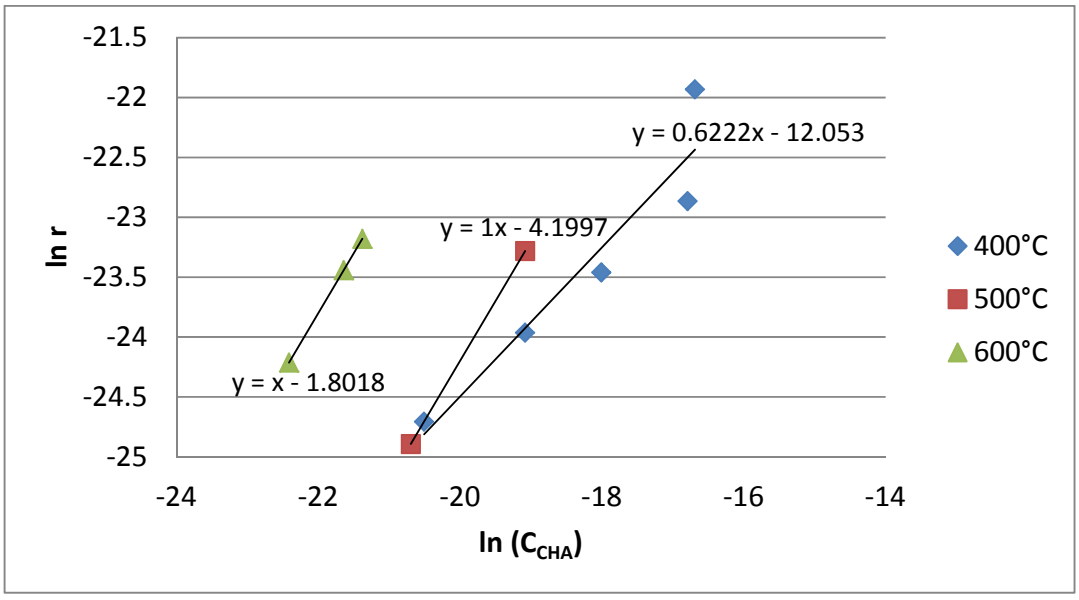

Figure 3-28. Determination of degradation order with CHA

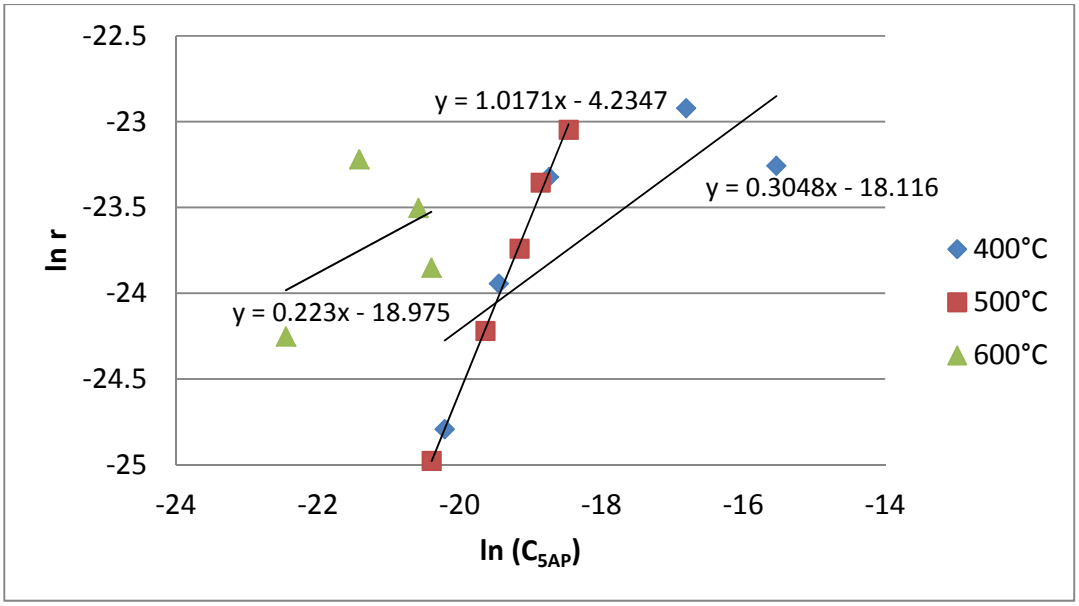

Figure 3-29. Determination of degradation order with 5AP

Table 3-7. Degradation order of organic amines

Temp. (°C)	MPH	MPA	CHA	5AP
400	1	0.44	0.62	0.3
500	-	1	1	1.02
600	1.66	1	1	0.22

3.4.3. Material Balance

Organic acids byproducts were analyzed by ion chromatography (IC). The byproducts were expected through literature studies (Shenberger et al., 1992; Klimas et al., 2003; Wesolowski et al., 2002) such as acetic acid (CH_3COOH), formic acid (HCOOH) and oxalic acid ($H_2C_2O_4$). These byproducts were discussed in Chapter 2.

Organic acids such as formic and acetic acids are neutral compounds under fossil plant operating conditions and are very volatile; however, any organic salts in steam

would exhibit lower volatility and could lead to a reduction of liquid film pH (Dooley et al., 2004).

Hydrolysis is the main reaction involved in degradation of all amine in supercritical conditions. Hydrolysis is a chemical process in which a water molecule is added to a substance resulting in the split into two parts. One fragment of the target molecule gains a hydrogen ion (H^+) while the other portion collects the hydroxyl group (OH^-).

Although various possible byproducts were evaluated based on literature in Chapter 2, degradation was assumed with only observed and measured chemicals through IC analysis. In addition, hydrolysis is assumed pseudo-first order reaction because of the relative small amount of amine (10ppm) in aqueous solution.

1) Ethanolamine:

$C_2H_7NO + H_2O \rightarrow NH_3 + C_2H_7NO + CH_3COOH + HCOOH + H_2C_2O_4 + H_2O$

2) Morpholine:

$C_4H_9NO + H_2O \rightarrow NH_3 + C_4H_9NO + CH_3COOH + HCOOH + H_2C_2O_4 + H_2O$

3) Cyclohexylamine:

$C_6H_{13}N + H_2O \rightarrow NH_3 + C_6H_{13}N + CH_3COOH + HCOOH + H_2C_2O_4 + H_2O$

4) 3-Methoxypropylamine:

$C_4H_{11}NO + H_2O \rightarrow NH_3 + C_4H_{11}NO + CH_3COOH + HCOOH + H_2C_2O_4 + H_2O$

5) 5-aminopentanol:

$C_5H_{13}NO + H_2O \rightarrow NH_3 + C_5H_{13}NO + CH_3COOH + HCOOH + H_2C_2O_4 + H_2O$

IC qualitative analysis was dependent on the retention time only, so retention time of all expected chemicals such as carboxylic acids had to be measured before the analysis. Ammonia was the most common amine. Acetate and formate were found but expected oxalate was not shown by IC analysis. Tables 3-8 to 3-11 show product concentrations after thermal degradation in supercritical water with material balances for carbon and nitrogen. The weight fraction of carbon and nitrogen were used to calculate the percentage loss, which means zero percent loss corresponds to the amount of initial carbon or nitrogen in each amine. In addition, the calculation is based on initial 10 ppm of aqueous amine.

In Table 3-8 to 3-11, it was assumed that the peak retention time between 3.8 and 4.0 minute corresponds to pure ammonia although the peak represents the mixture of ammonia and ethanolamine or other small amines such as methylamine, ethylamine or diethanolamine. Complete separation for these amines of small molecular weight through IC column was not possible. As a result, the nitrogen balance in the tables is based on ammonia and each amine only. With the assumption, a positive sign for loss corresponds to elements lost by thermal degradation; however, a negative sign for loss corresponds to element generation which is impossible. The peak is expected to contain the nitrogen complex with molecular weight larger than ammonia in the case of a negative sign for loss (%). Regarding material balance of carbon, the amount of carbon loss is increased at elevated temperature.

Table 3-8. Thermal degradation byproducts of MPH and material balance (Initial nitrogen and carbon concentration: 2.3 and 7.9 ppm)

Temp. (°C)	Press. (psi)	NH_3 (ppm)	MPH (ppm)	Acetate (ppm)	Formate (ppm)	Nitrogen (ppm)				Carbon (ppm)				
						NH_3	MPH	N Total	N Loss (%)	MPH	Acetate	Formate	C Total	C Loss (%)
300	1000	1.3	3.9	0.1	0.8	1.1	0.9	2.0	14.3	3.1	0.0	0.2	3.3	57.8
350	1000	2.2	0.6	0.6	0.3	1.8	0.1	1.9	15.0	0.5	0.2	0.1	0.8	89.9
400	5000	1.8	0.6	0.1	0.2	1.5	0.1	1.6	29.3	0.5	0.0	0.1	0.6	92.8
	4000	1.7	0.6	0.1	0.2	1.4	0.1	1.5	32.9	0.5	0.0	0.1	0.6	92.8
	3000	1.7	0.6	0.4	0.5	1.4	0.1	1.5	32.9	0.5	0.2	0.1	0.8	90.3
	2000	2	0.6	0.5	0.1	1.6	0.1	1.8	22.1	0.5	0.2	0.0	0.7	91.1
	1000	2	0.6	-	-	1.6	0.1	1.8	22.1	0.5	-	-	0.5	94.0
500	5000	2.1	-	-	-	1.7	-	1.7	24.5	-	-	-	0.0	100.0
	4000	2.2	-	0.2	-	1.8	-	1.8	21.0	-	0.1	-	0.1	99.0
	3000	2.3	-	-	-	1.9	-	1.9	17.4	-	-	-	0.0	100.0
	2000	2.3	0.6	0.8	-	1.9	0.1	2.0	11.4	0.5	0.3	-	0.8	89.9
	1000	1.5	-	-	-	1.2	-	1.2	46.1	-	-	-	0.0	100.0
600	5000	1.8	0.1	-	-	1.5	0.0	1.5	34.3	0.1	-	-	0.1	99.0
	4000	3.2	-	-	-	2.6	-	2.6	-15.0	-	-	-	0.0	100.0
	3000	1.8	-	-	-	1.5	-	1.5	35.3	-	-	-	0.0	100.0
	2000	1.2	0.1	-	-	1.0	0.0	1.0	55.9	0.1	-	-	0.1	99.0
	1000	1.5	0.2	-	-	1.2	0.0	1.3	44.1	0.2	-	-	0.2	98.0

Table 3-9. Thermal degradation byproducts of MPA and material balance (Initial nitrogen and carbon concentration: 1.6 and 5.4 ppm)

Temp. (°C)	Press. (psi)	NH_3 (ppm)	MPA (ppm)	Acetate (ppm)	Formate (ppm)	Nitrogen (ppm)				Carbon (ppm)				
						NH_3	MPA	N total	N Loss (%)	MPA	Acetate	Formate	C Total	C Loss (%)
300	1000	1.1	4.4	0.2	0.7	0.9	0.7	1.6	-1.7	2.4	0.1	0.2	2.6	51.1
350	1000	2	0.7	0.9	0.3	1.6	0.1	1.8	-11.9	0.4	0.4	0.1	0.8	84.9
400	5000	1	3.8	0.1	0.0	0.8	0.6	1.4	9.6	2.0	0.0	0.0	2.1	61.3
	4000	0.8	4.3	0.1	0.1	0.7	0.7	1.3	15.1	2.3	0.0	0.0	2.4	55.8
	3000	1.6	1	0.2	0.2	1.3	0.2	1.5	6.1	0.5	0.1	0.1	0.7	87.5
	2000	1.8	0.6	0.5	0.1	1.5	0.1	1.6	-0.4	0.3	0.2	0.0	0.5	89.8
	1000	1.6	0.7	0.3	0.1	1.3	0.1	1.4	9.1	0.4	0.1	0.0	0.5	90.3
500	5000	1.8	0.6	-	0.0	1.5	0.1	1.6	-0.4	0.3	-	0.0	0.3	94.0
	4000	1.8	0.6	0.3	0.1	1.5	0.1	1.6	-0.4	0.3	0.1	0.0	0.5	91.3
	3000	1.7	0.7	-	0.0	1.4	0.1	1.5	3.9	0.4	-	0.0	0.4	93.0
	2000	1.9	0.7	-	0.0	1.6	0.1	1.7	-6.6	0.4	-	0.0	0.4	93.0
	1000	1.8	0.6	-	0.0	1.5	0.1	1.6	-0.4	0.3	-	0.0	0.3	94.0
600	5000	0.1	0.1	-	-	0.1	0.0	0.1	93.8	0.1	-	-	0.1	99.0
	4000	1.2	0.1	-	-	1.0	0.0	1.0	36.1	0.1	-	-	0.1	99.0
	3000	1.3	0.1	-	-	1.1	0.0	1.1	30.8	0.1	-	-	0.1	99.0
	2000	0.7	-	-	-	0.6	-	0.6	63.3	-	-	-	0.0	100.0
	1000	0.7	-	-	-	0.6	-	0.6	63.3	-	-	-	0.0	100.0

Table 3-10. Thermal degradation byproducts of CHA and material balance (Initial nitrogen and carbon concentration: 1.4 and 7.3 ppm)

Temp. (°C)	Press. (psi)	NH_3 (ppm)	CHA (ppm)	Acetate (ppm)	Formate (ppm)	Nitrogen (ppm)				Carbon (ppm)				
						NH_3	CHA	N total	N Loss (%)	CHA	Acetate	Formate	C Total	C Loss (%)
300	1000	0.4	4.6	0.2	0.7	0.3	0.6	1.0	30.7	3.3	0.1	0.2	3.6	50.4
350	1000	0.7	2.5	0.3	0.3	0.6	0.4	0.9	34.2	1.8	0.1	0.1	2.0	72.3
400	5000	1.4	2.4	0.1	0.1	1.2	0.3	1.5	-5.7	1.7	0.0	0.0	1.8	75.1
	4000	1.1	4.2	0.2	0.1	0.9	0.6	1.5	-6.2	3.0	0.1	0.0	3.2	56.5
	3000	1.4	2.8	0.6	0.1	1.2	0.4	1.5	-9.7	2.0	0.2	0.0	2.3	68.3
	2000	1.7	1.8	0.9	0.1	1.4	0.3	1.7	-17.2	1.3	0.4	0.0	1.7	76.7
	1000	1.7	1	0.8	0.1	1.4	0.1	1.5	-9.2	0.7	0.3	0.0	1.1	85.2
500	5000	1.9	-	0.2	0.1	1.6	-	1.6	-10.8	-	0.1	0.0	0.1	98.5
	4000	2	1	-	-	1.6	0.1	1.8	-26.7	0.7	-	-	0.7	90.0
	3000	1.7	-	-	-	1.4	-	1.4	0.8	-	-	-	0.0	100.0
	2000	1.9	-	0.6	0.0	1.6	-	1.6	-10.8	-	0.2	0.0	0.2	96.7
	1000	1.3	1	-	-	1.1	0.1	1.2	14.2	0.7	-	-	0.7	90.0
600	5000	1.3	0	-	0.1	1.1	0.0	1.1	24.2	0.0	-	0.0	0.0	99.6
	4000	0.5	0.1	-	0.0	0.4	0.0	0.4	69.8	0.1	-	0.0	0.1	99.0
	3000	1.1	-	-	0.1	0.9	-	0.9	35.8	-	-	0.0	0.0	99.6
	2000	0.5	0.1	-	0.1	0.4	0.0	0.4	69.8	0.1	-	0.0	0.1	98.6
	1000	0	0	-	0.1	0.0	0.0	0.0	100.0	0.0	-	0.0	0.0	99.6

Table 3-11. Thermal degradation byproducts of 5AP and material balance (Initial nitrogen and carbon concentration: 1.4 and 5.8 ppm)

Temp. (°C)	Press. (psi)	NH_3 (ppm)	5AP (ppm)	Acetate (ppm)	Formate (ppm)	Nitrogen (ppm)				Carbon (ppm)				
						NH_3	5AP	N total	N Loss (%)	5AP	Acetate	Formate	C Total	C Loss (%)
300	1000	1.1	2.8	0.7	1.0	0.9	0.4	1.3	5.2	1.6	0.3	0.3	2.2	62.7
350	1000	0.5	1.4	0.7	0.2	0.4	0.2	0.6	55.7	0.8	0.3	0.1	1.1	80.3
400	5000	1.2	7.9	0.0	0.1	1.0	1.1	2.1	-51.8	4.6	0.0	0.0	4.6	20.6
	4000	1.4	4.3	0.1	0.2	1.2	0.6	1.7	-28.0	2.5	0.0	0.1	2.6	55.4
	3000	1.7	1.4	0.7	0.2	1.4	0.2	1.6	-17.2	0.8	0.3	0.1	1.1	80.3
	2000	2	1.3	0.3	0.0	1.6	0.2	1.8	-34.4	0.8	0.1	0.0	0.9	84.9
	1000	1.6	1.4	0.7	0.1	1.3	0.2	1.5	-11.1	0.8	0.3	0.0	1.1	80.7
500	5000	2	1.4	0.2	0.0	1.6	0.2	1.8	-35.4	0.8	0.1	0.0	0.9	84.6
	4000	2.1	1.3	-	-	1.7	0.2	1.9	-40.4	0.8	-	-	0.8	87.0
	3000	1.6	1.4	0.2	0.0	1.3	0.2	1.5	-11.1	0.8	0.1	0.0	0.9	84.6
	2000	2	1.4	-	0.0	1.6	0.2	1.8	-35.4	0.8	-	0.0	0.8	86.0
	1000	2	1.4	-	-	1.6	0.2	1.8	-35.4	0.8	-	-	0.8	86.0
600	5000	0.2	0.1	-	-	0.2	0.0	0.2	86.9	0.1	-	-	0.1	99.0
	4000	1.4	0.3	-	-	1.2	0.0	1.2	12.0	0.2	-	-	0.2	97.0
	3000	1.3	0.5	-	-	1.1	0.1	1.1	16.1	0.3	-	-	0.3	95.0
	2000	0.7	0.1	-	-	0.6	0.0	0.6	56.5	0.1	-	-	0.1	99.0
	1000	1.1	-	-	-	0.9	-	0.9	33.2	-	-	-	0.0	100.0

3.4.4. Discussion

Although there were many studies that evaluated amines degradation kinetic data, discussion is limited to word at high temperature and pressure.

This study explored thermal degradation of organic amines using the Arrhenius equation with pseudo first-order reaction in the range from 400 to 600°C and up to 5000 psi. Five organic amines (ETA, MPH, MPA, CHA and 5AP) were chosen from the amines currently used in power plants. Thermal degradation rates were found as functions of temperature as well as pressure. The pressure as a degradation factor can be considered from Le Chatelier's principle indicating that elevated pressure benefits the direction of reaction that results in the fewest number of molecules. All amines were completely degraded at the highest temperature. Ammonia, acetate and formate were measured as main products of thermal degradation of organic amines.

According to the Arrhenius plots, 5AP showed the lowest degradation rates followed by MPA and CHA over the experimental condition, however 5AP is still highly reactive. One of possibility is that heat energy is absorbed into high heat capacity of water instead of association with amine degradation so that rates for small amounts of amines in solution would depend on water heat capacity. ETA and 5AP have structure containing –OH groups. Since hydrogen bonding between water molecules and –OH is stronger than those between water and –NH, ETA and 5AP are postulated to have relatively lowest degradation rates corresponding strong hydrogen bonding with water. Degradation rates based on hydrolysis depend on the number of water molecules participating in the reaction.

The results for ammonia should be considered in more detail at this point. As mentioned at the experimental procedures, nitrogen gas was used to purge the reaction tubes thereby reducing oxidation. After the experimentation at said temperatures, all reaction tubes were cooled in iced water for 15 min to condense the samples. However, as noted, the remaining ammonia concentration at lower pressure was significantly lower than higher pressure. Two reasons can be considered for ammonia loss; including, different amines volatility at room temperature when the reaction tubes are opened and ammonia oxidation in contact with metal catalyst. Other high temperature ammonia reactions were not found in the literature.

Regarding relative volatility of selected alternative amines at Table 2-4, ammonia has the highest volatility at 25°C. So, it may be possible that the loss of ammonia and inaccurate measurement occur when the sample is collected and analyzed at the same temperature for all alternative amines.

Although oxidation was intended to be minimal, there are known reaction mechanisms. Ammonia loss is also possible by catalytic oxidation when ammonia contacts with metals in the degradation test in absence of oxygen. Shaw et al. (1991) reported that ammonia oxidation techniques have been used in removal of ammonia by decomposing into nitrogen and water using catalytic oxidation and production of pure nitrogen process. Nitrogen-containing compounds are converted to N_2 and N_2O under supercritical water oxidation conditions. Nitrous oxide (N_2O) can be eliminated by performing the oxidation at higher temperature. If the oxidation temperatures are lower (400-500°C), ammonia may form as intermediate which has been found to oxidize to N_2 at higher temperature (600°C)

Gang et al. (2001) studied the activities of metals and metal oxides for ammonia oxidation in the presence of metals like Pt, Pd, Cu, Ag, Ni, Au, Fe, W and Ti. They focused especially on the activity of ammonia oxidation in silver powdered catalyst. N_2 and N_2O are produced below 300°C and NO becomes one of the products instead of N_2O above 300°C from ammonia. In addition, NO can be produced even at room temperature regardless of temperature range and the final products of ammonia oxidation represent NO, N_2O, N_2 and H_2O.

Sazonova et al. (1996) reported the activity of various metal catalysts in ammonia oxidation at the temperature of 250-400°C. They showed the most active and selective catalysts are V/TiO_2, Cu/TiO_2 and Cu-ZSM-5. Wollner (1993) determined that high ammonia conversion of 80-100% was obtained over mixed copper-manganese oxides supported on Ti catalyst at temperature greater than 300°C. Segond et al. (2002) demonstrated mechanisms of ammonia oxidation in sub- and supercritical water.

$$2NH_4^+ + 2OH^- + 2O_2 \rightarrow N_2O + 5H_2O$$

$$NH_4^+ + 2OH^- + 2O_2 \rightarrow NO_3^- + 3H_2O$$

They suggested that it is hard to observe N_2O at the temperatures higher than 900K since N_2O reacts with ammonia to produce nitrogen. At atmospheric conditions, ammonia can be decomposed to nitrate and water by oxidation after contacting with metals based on the mechanisms. Cr, Ni, and Mo are the main metals which composed of 316 stainless steel used in amine degradation test. So, ammonia loss would occur in the area of reaction tube since ammonia oxidation occurs in presence of metal catalyst.

REFERENCES

Dooley, R.B. and Chexal, V.K. “Flow-Accelerated Corrosion” CORROSION 99, NACE International, Houston, 1999, Paper #347.

Domae, M. and Fujiwara, K. "Thermal Decomposition of 3-Methoxypropylamine as an Alternative Amine in PWR Secondary Systems," J Nucl. Sci. and Tech, 46(2) 210-215, 2009.

Fountain, M.J. “The use of amines to control two-phase erosion-corrosion in steam-raising plant.” Corrosion Prevention and Control (United Kingdom), 40 (5), 115-120, 1993.

Wilson, J. and Bates, J. “Evaluation of high cross linked cation gel resins in an MPA environment at Byron and Braindwood,” Proc. EPRI int. Water Chemistry of Nuclear Reactor Systems, San Francisco, USA, Oct. 11-14, 2004, Paper No. 5.9 (2005).

Nordmann, F. “Aspect on Chemistry in French Nuclear Power Plants.” J. Solution Chemistry 2003, 32 (10)

Millett, P.J. and Fruzzetti, K. “In Status of Application of Amines in US PWRs.” Proceedings of International Conference on the Interaction of Organics and Organic Cycle Treatment Chemicals iin Water, Steam and Materials, Stuttart,

Germany, October 4-6, 2005; Electric Power Research Institute (EPRI), Palo Alto, CA.

Gilbert, R. and Lamarre, C. "Thermal Stability of Morpholine Additive in the Steam-Water Cycle of CANDU-PHW Nuclear Power Plants," Can J Chem Engr., 67, 1989, 646-651.

Cobble, J.W. and Turner, P.J. "PWR Advanced All-Volatile Treatment Additives, By-Products and Boric Acid," EPRI report TR-100755, 1992.

Gronberg, L., Lovkvist, P., and Jonsson, J.A. “Measurement of aliphatic amines in ambient air and rainwater,” Chemosphere 1992; 24:1533-1540.

Tsukioka, T., Ozawa, H., and Murakami, T. “Gas chromatographic-mass spectrometric determination of lower aliphatic tertiary amines in environmental samples,” J. Chromatogr., 642, 395-400, 1993.

Saha, N.C., Jain, S.K., and Dua, R.K. "A Rapid Powerful Method for the Direct Gas Chromatography Analysis of Alkanolamines; Application to Ethanolamines," *Chromatographia*, 10, 368 (1977).

Sacher, F., Lenz, S., and Brauch, H.-J. “Analysis of primary and secondary aliphatic amines in waste water and surface water by gas chromatography-mass spectrometry after derivatization with 2,4-dinitrofluorobenzene or benzenesulfonyl chloride,” J. Chromatography A, 1997. 764(1): 85-93.

Vatsala, S., Bansal, V., Tuli, D.K., Rai, M.M., Jain, S.K., Srivastava, S.P., and Bhatnagar, A.K. "Gas Chromatographic Determination of Residual Hydrazine and

Morpholine in Boiler Feed Water and Steam Condensates," Chromatographia 38(7/8) 1994, 456-460.

Joseph, M., Kagdiyal, V., Tuli, D.K., Rai, M.M., Jain, S.K., Srivastava, S.P., and Bhatnagar, A.K. "Determination of Trace Amounds of Morpholine and its Thermal Degrdation Products in Boiler Water by HPLC, Chromatographia, 35(3/4), 1993, 173-176.

Davis, J. and Rochelle, G. “Thermal degradation of monoethanolamine at stripper conditions,” Energy Procedia 1 (2009) 327–333.

NIST (http://webbook.nist.gov)

McKay, M. “Morpholine Decomposition Studies in a Model Boiler at Dissolved Oxygen Concentration up to 500 ppb” presented at EPRI Workshop on Use of Amines in Conditioning Steam/Water Cycles, Sept. 25-27, 1990, Tampa, FL.

Foutch, G.L. and Johannes, A.H. “Reactors in Process Engineering,” Encyclopedia of Physical Science and Technology. 1992, Academic Press. 347-367.

Shenberger, D.M., Zupanovich, J.D., and Walker, J.L. “Loop testing of alternative amines for all-volatile treatment control in PWRs,” Electric Power Research Institute, Palo Alto CA., June 1992, TR-100756.

Wesolowski, D.J., Benezeth, P., Palmer, D.A., and Anovitz, L.M. “Protonation Constants of Morpholine, Dimethylamine and Ethanolamine to 290C and the Effect of Morpholine and Dimethylamine on the Surface Charge of Magnetite at 150-250C, Electric Power Research Institute, Palo Alto CA., TR-1003179, 2002.

Shaw, R.W., Thomas, B.B., Antony, A.C., Charles, A.E., and Franck, E.U. “Supercritical Water-A Medium for Chemistry” Chem. Eng. News 1991, 69(51), 26-39.

Gang L., Anderson B.G. Van Grondelle J. and Van Santen R.A., Low temperature selective oxidation of ammonia to nitrogen on silver-based catalysts. *Appl. Catal. B: Environ.,* 40, 101-110 (2003).

Sazonova, N.N., Simakov, A.V., Nikoro, T.A., Barannik, G.B., Lyakhova, V.F., Zheivot, V.I., Ismagilov, Z.R., and Veringa, H. “Selective catalytic oxidation of ammonia to nitrogen,” React. Kinet. Catal. Lett., 57 (1) 71-79 (1996).

Wollner, A., Lange, F., Schmelz, H., and Kniizinger, H. “Characterization of mixed copper-manganese oxides supported on titania catalysts for selective oxidation of ammonia,” Applied Catalysis A: General, 94 (1993) 181-203

Segond, N., Matsumura, Y., and Yamamoto, K. “Determination of Ammonia Oxidation Rate in Sub- and Supercritical Water,” Ind. Eng. Chem. Res., 2002, 41 (24), 6020–6027

CHAPTER IV

MIXED-BED ION EXCHANGE PERFORMANCE FOR SODIUM REMOVAL IN INCOMPLETE REGENERATION OF CATION RESIN

4.1. Introduction

A series of laboratory tests were performed to determine the sodium leakage from MBIE columns with different initial sodium loading on the cationic resin. Mixed bed ion exchange (MBIE) is the technology which consists of a mixture of spherical cationic and anionic resins in a column where cationic and anionic impurities are removed simultaneously. The application of MBIE was introduced by Kunin and McGarvey (1951). In ultrapure water production, the reason for mixing cationic and anionic resins is to obtain charge coupling and neutralizing reaction which would make the exchange process irreversible resulting in a fairly neutral effluent over a range of operating conditions. This was a giant step in water treatment capabilities, as it enabled the attainment of extremely low impurity levels with a neutralized effluent. Thus, MBIE is widely used in ultrapure water processes such as steam cycle condensate polishing,

microelectronics rinsewater and pharmaceutical water for injection because of an economic and efficient way to produce ultrapure water in parts per billion ranges.

The end of the service cycle is determined by monitoring the effluent concentration of a specific critical ion. The bed should be replaced or regenerated when the plant-defined concentration exceeds the industry specific limit (Chowdiah, 2003). In most industrial cases, the concentration of dissolved solids limit is to less than 1.0 ppb. These low impurities requirements have placed strict demands upon the performance of MBIE (Haub and Foutch, 1986).

An ion exchange column must begin an exchange cycle in a regenerated state. As the column is contacting with solution, the ion exchange resins exhausts, or converts, to another form. The exchange wave or boundary between unconverted and exhausted resins is not ideally sharp. Thus, when breakthrough occurs, the layers of resin at the exit end of the bed are not fully utilized. The degree of column utilization is the ratio of the capacity at breakthrough to the total resin capacity in the column. The end of the service cycle is when a defined effluent concentration of a critical ion – typically sodium – is anticipated. Operation may well stop short of this critical value in order to avoid the risk of exceeding it.

Incomplete regeneration also leads to ionic leakage from the MBIE into effluent. In general, the regeneration of H-form resin is performed for sodium removal by using HCl solution; however, incomplete regeneration results in a small amount of sodium exist in the resin. Typically sodium is the first ion to leave the bed and which contributes to erosion and corrosion problems within the steam cycle.

Many existing power plants have corrosion and erosion problems due to the contaminants present within process water (Sadler and Darvill, 1986). Control and monitoring of impurities and water chemistry in any steam cycle is important to long equipment life. Piping and tubes in power plants experience corrosion and erosion by impurities. Impurities sources arise from make-up water treatment, and chronic leakage, and the ion exchange resins themselves as a result of imperfect resin separation or regeneration.

Water purification, combining with pH control agents, can reduce erosion and corrosion. One method for improved corrosion control is the introduction of a weak base into the water to increase the pH which, in turn, reduces acidic corrosion of metallic surfaces. This work evaluated sodium leakage in feed solution containing high concentration of ammonium ion added for pH control.

4.2. Experimental Apparatus and Procedures

Overall apparatus was composed three one-inch diameters of columns, flow meters, a feed storage tank, feed pumps, and an injection pump at Figure 4-1. Cationic (DOWEX 650C-monosphere) and anionic (DOWEX 550A-monosphere) exchange resins were used in these tests and the properties of resins are addressed in Table 4-1.

All cationic and anionic resins were regenerated respectively and rinsed with DI water prior to mixing and loading into the beds at the required ratios and detailed steps were addressed in APPENDIX A.

Table 4-1. Physical properties of Dowex resins (Dowex)

Parameter	Cationic resin	Anionic resin
Name	Dowex Monosphere 650C (H)	Dowex Monosphere 550A (OH)
Type	Strong acid cation	Type 1 strong base anion
Functional Group	Sulfonic acid	Quaternary Amine
Capacity (eq/L)	2.0 (H^+ form)	1.1 (OH^- form)
Density (g/ml)	1.22	1.08
Diameter (μm)	650±50	590±50
Selectivity Coefficient (at 20 °C)	Na^+ 1.61 Ca^{2+} 4.44 Mg^{2+} 2.59	Cl^- 22.0 SO_4^{2-} 60 HCO_3^- 60 CO_3^{2-} 12
Water content (%)	46-51	55-65
Appearance	Hard, black, Spherical beads	Hard, white, Spherical beads

The initial sodium leakages from the laboratory test columns with different sodium loading were estimated. The initial sodium loading in the bed are listed in Table 4-2.

Table 4-2. Mixed bed ion exchange column initial compositions

Volumes (Liter)				Fractions				
anion	Cat H	Cat Na	Total	Anion	Cat H	Cat Na	Total Cat	Na load
0.115	0.1127	0.0023	0.23	0.5	0.4900	0.0100	0.5	0.0200
0.115	0.1106	0.0044	0.23	0.5	0.4809	0.0191	0.5	0.0383
0.115	0.1085	0.0065	0.23	0.5	0.4717	0.0283	0.5	0.0565
0.115	0.1065	0.0085	0.23	0.5	0.4630	0.0370	0.5	0.0739
0.115	0.1045	0.0105	0.23	0.5	0.4543	0.0457	0.5	0.0913

Three initially loading ratios with 2.00 %, 7.39 % and 9.13 % of sodium on the cationic sites were selected for evaluating ion exchange bed performance in a circulation

loop. Specific volume of hydrogen ions of DOWEX 650C were converted to sodium ions, then the cation resins were mixed with DOWEX 550A resins with 1:1 ratio.

The loop was constructed by PFA and PEX since PFA and PEX are superior to minimize ionic leaching from the tubing materials (ASTM D6071-96; ASTM D859-00; ASTM D4517-04; ASTM D4453-02). Water in the loop was allowed to circulate to save large amounts of ultrapure water required, so that ultrapure water quality was maintained in feed tank by installing 2500 ml of a MBIE (1:1 ratio of hydrogen form cation and hydroxide form anion resins) column between effluent loop and a feed tank. A feed solution was added by injection upstream of the three mixed beds operated at 760 ml/min each (2280 ml/min total). Flow to each bed was monitored by separate rotameters. Since we were looking for initial ionic leakage, the columns returned 18 mΩ water back to the recirculation tank. The flow rate maintained 2.5 cm/sec of superficial velocity (Noh, 1996) and the injection concentration was determined for total feed concentration as representing at Table 4-3. These concentrations give a calculated feed pH of 9.17 at 25°C.

The injection flow rate was fixed at 13.0 ml/min with a Walchem measuring pump into 2280 ml/min total flow. The concentrate was prepared by dissolving 0.1764 g of calcium carbonate, 0.2180 g of sodium metasilicate nonhydrate, 10.50 ml of ammonium hydroxide, 0.4798 g of ferrous sulfate and 0.2682 g of copper nitrate trihydrate in 20 liter of 18 mΩ pure DI water.

As each column broke through to 10 ppb sodium, they were turned off and the total and injection flow rates were adjusted to maintain their respective values.

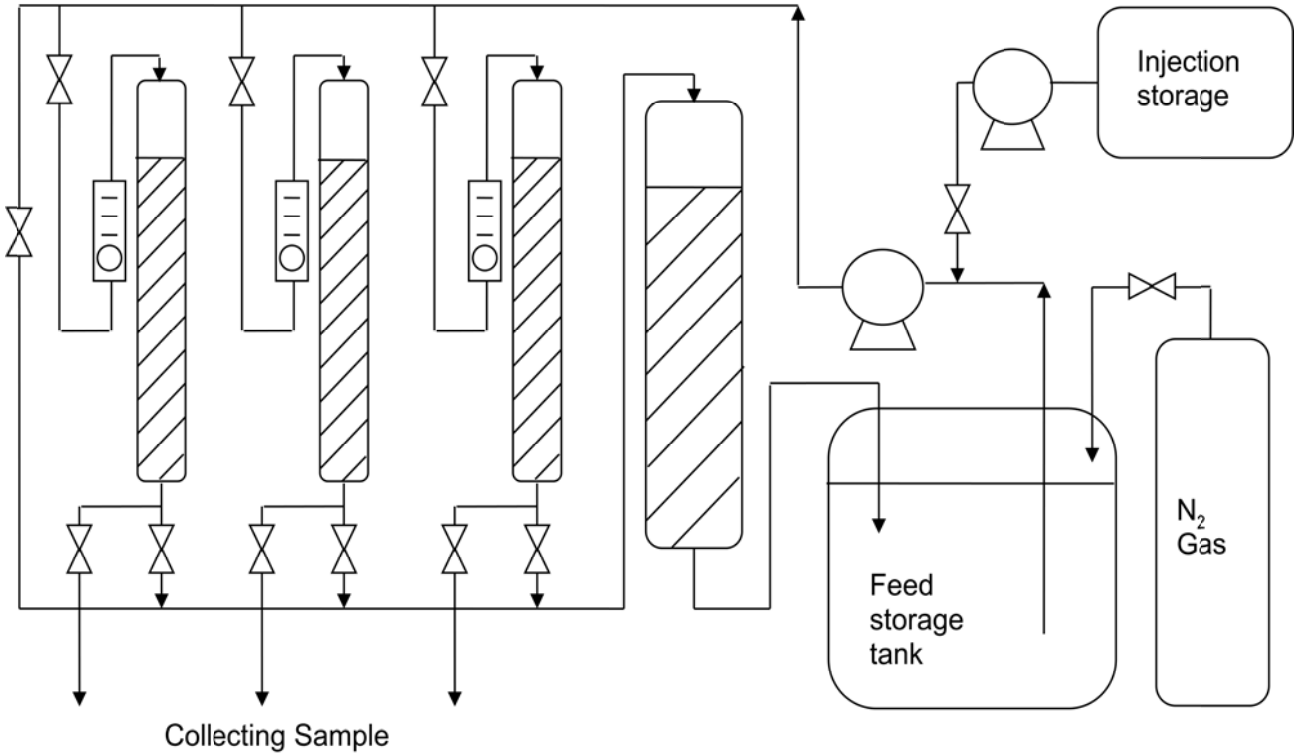

Figure 4-1. Schematic of multi-column test loop.

(The column bypass valve on the left was shut during operation.

The feed tank was blanketed with nitrogen gas to prevent CO_2 addition from the air)

Table 4-3. Injection composition and resulting column feed solution concentrations.

Ion	Injection concentration (ppb)	Feed concentration (ppb)
Carbonate (CO_3)	8820	50.0
Silica (SiO_2)	2300	13.1
Ammonia (NH_4)	70600	400.0
Iron (Fe)	882	50.0
Copper (Cu)	3540	20.0
Sodium (Na)	882	5.0
Calcium (Ca)	3532	12.3
Sulfate (SO_4)	14956	313.6
Nitrate (NO_3)	3441	7.5

A Waltron Aqualyzer 9031 Sodium analyzer equipped with a N3010-177 Sodium Measuring Electrode with a Di-Isopropylamine as a reagent was used to monitor sodium concentration. Additional analyses were obtained by a HACH sensIon5 conductivity meter, Oakton pHTestr 30 pH meter, Metrohm 790 personal cationic and anionic ion chromatographs were used to check measurements, as needed.

4.3. Performance Prediction by OSU MBIE

Application of the models for design of MBIE columns has been examined and the column model accounts for differing cationic and anionic resin properties and predicts effluent concentrations in the parts per billion ranges (ppb).

MBIE modeling is most accurately accomplished by integrating three mathematical models into a column material balance, which are the bulk neutralization of water, reaction equilibrium in ion exchange resins, and a diffusion model. Haub and

Foutch (1986) made the model for MBIE based on rate calculations. They developed the model for hydrogen cycle MBIE at concentrations below 1.0 ppb and considered the dissociation of water. The model was for the hydrogen cycle mixed bed with only two ions, Na^+ and Cl^-, considered for exchange with H^+ and OH^-, respectively. Zecchini (1990, 1991) expanded the model to manipulate a ternary system of monovalent ions and amines. This was the first attempt to simulate an amine cycle. Hussey (2000) developed a multi-component film controlled MBIE model and could reduce errors of column material balance significantly more than previous work.

The OSU mixed-bed ion exchange (OSUMBIE) simulation package was used to project the performance of the test columns to compare with experimental results. A description of the model details is in Yi and Foutch (2005). The program can handle any number of ions, including dissociative species. Simulations were performed with both equal volumes and equivalent volumes of DOWEX 650C and DOWEX550A on 18-inch deep beds (typical lab study). After the resin ratios, bed geometry and feed compositions were fixed. The only variable in the input data set was the fraction of cationic resin in the sodium form.

The sodium and ammonia concentrations, since these break first, along with pH, conductivity, copper and iron are presented about initial sodium loading of 9.13% in Table 4-4. Concentrations are in ppb.

Graphical representations of the results in Table 4-4 are in Figures 4-2 through 4-4. Figure 4-2 indicates that pH and conductivity deflect when sodium starts to break and that they would be good online indicators of breakthrough. However, in plant operation,

there are other contributors to changes in pH and conductivity that are not in Figure 4-2: primarily, the temperature effect of these variables in water.

Table 4-4. Effluent predictions of a mixed bed with an initial cationic sodium loading of 9.13%.

Time (day)	pH	Conductivity (25°C)	Total Ammonia	Sodium	Copper	Iron
0.0	7.03	5.47E-02	3.84E-05	1.31E-01	1.14E-02	2.01E-01
1.0	7.04	5.47E-02	8.55E-05	1.29E-01	1.38E-02	2.32E-01
2.0	7.05	5.47E-02	7.16E-04	1.28E-01	2.04E-02	3.15E-01
3.0	7.06	5.48E-02	9.22E-03	1.38E-01	2.58E-02	3.96E-01
4.0	7.08	5.51E-02	8.10E-02	2.03E-01	2.96E-02	4.59E-01
5.0	7.16	5.76E-02	5.05E-01	4.54E-01	3.20E-02	5.06E-01
6.0	7.45	8.56E-02	2.82E+00	1.33E+00	3.49E-02	5.77E-01
7.0	8.03	2.93E-01	1.55E+01	4.33E+00	4.05E-02	7.06E-01
8.0	8.60	1.08E+00	7.11E+01	1.34E+01	4.68E-02	8.62E-01
9.0	8.99	2.66E+00	2.22E+02	3.68E+01	2.48E-02	8.33E-01

Figure 4-3 shows the predicted concentrations of sodium and ammonia. These are presented in a log scale in order to show more sensitivity. Because of equilibrium leakage the sodium curve is flat to begin with and stays that way until sodium break. Ammonia was assumed not to be on the resin initially and remains below the detection limit until just after initial sodium break. Figure 4-4 shows a prediction of the time to 1.0 ppb sodium versus operating time. Even with an absolutely sodium free bed initially, because of the high feed concentration, the expected time to 1.0 ppb is extended by only a few days.

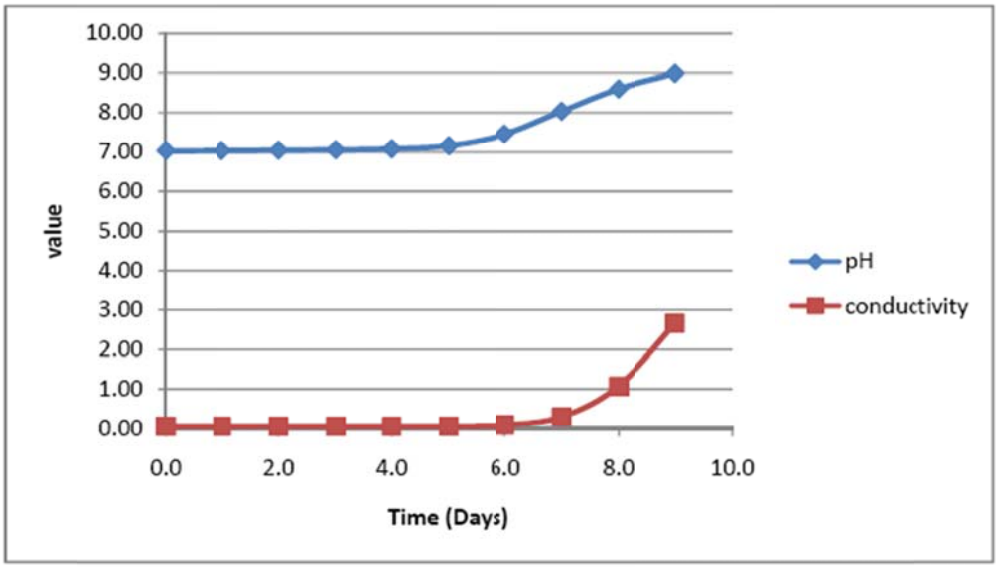

Figure 4-2. Prediction of pH and conductivity from a mixed bed with 9.13% of cationic sites in the sodium form.

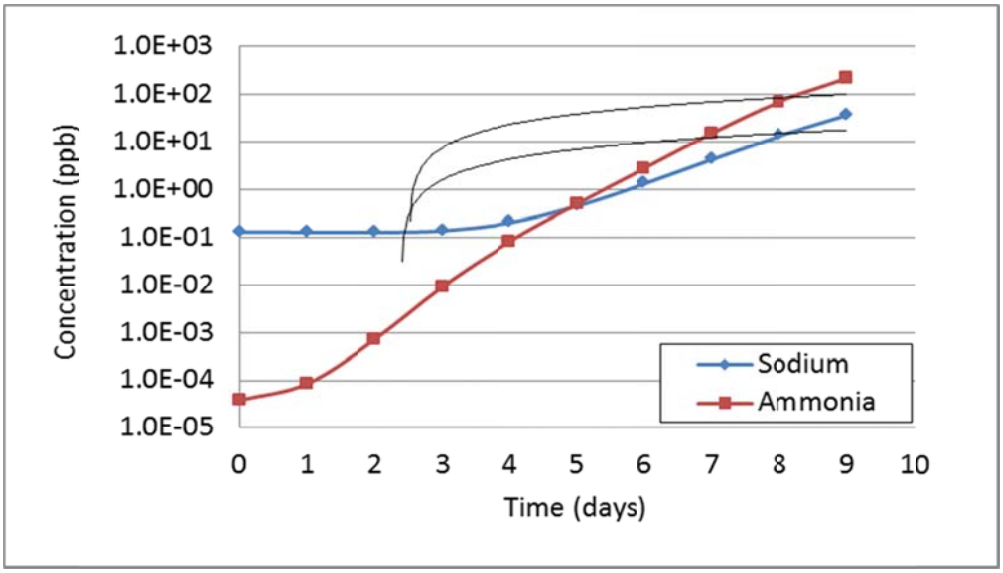

Figure 4-3. Concentrations of ammonia and sodium through the bed break for the case where 9.13% initial sodium is loaded on DOWEX 650C cationic resin in a mixed bed with DOWEX 550A.

In Figure 4-3, data are presented in a semilog plot, with linear relationships highlighted. The initial sodium predictions are expected to be reasonably accurate based on experience, especially since the cationic selectivity is well established. However, for

breakthrough the primary issue with the presence of ammonia is sodium throw that precedes the amine break. To estimate the sodium throw, full bed simulations are required. These give the sodium concentrations as a function of time so that threshold limits and maximum sodium throw can be determined. The driver for sodium breakthrough is the high concentration of ammonium from the use of ammonia as a pH control agent. Ammonium displaces sodium ions and "pushes" them down the column. Ammonia loading creates an enriched sodium region that is a combination of sodium displaced from the resin plus the sodium in the feed solution. When sodium ions leave the bottom of the bed they are either equilibrium leakage (from the resin) or kinetic leakage (from the feed). Kinetic leakage ahead of an ammonia front is typically described as "sodium throw". According to the simulation for initial sodium loading of 9.13 % in the sodium form, the time to achieve1.0 ppb sodium level is 5.8 days. Equilibrium leakage is fairly constant for a little more than 3 days before sodium concentration begins to rise.

Simulations were also performed with initial sodium loading of 0.00, 2.00, 3.83, 5.65, and 7.39 percent. The longest this column can operate at these high feed concentrations until a 1.0 ppb sodium effluent occurs is 10 days. As expected, the higher the initial loading the shorter the time until 1.0 ppb sodium effluent.

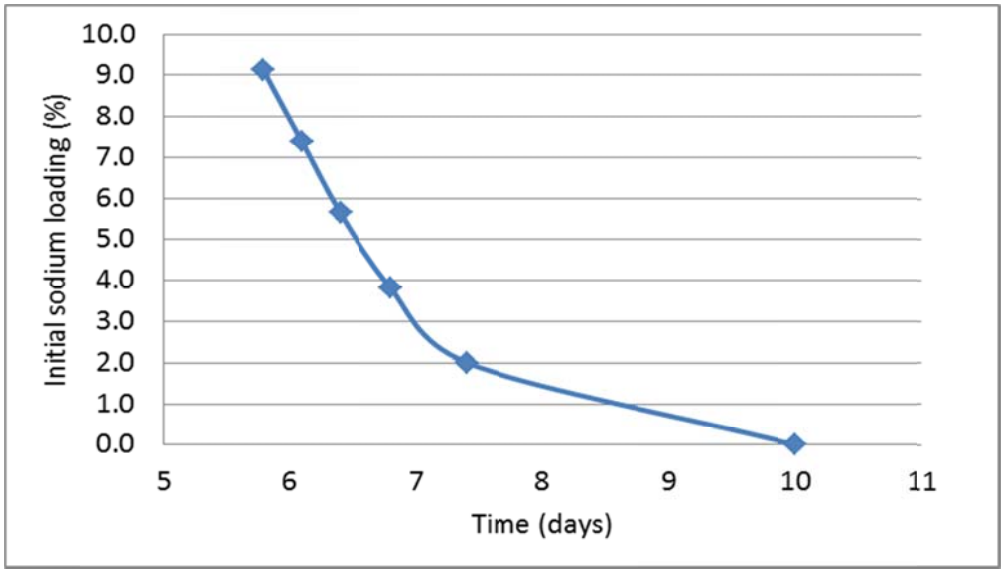

Figure 4-4. The relationship to initial sodium loading percentage on the cationic resin and the time until a 1.0 ppb sodium effluent concentration

4.4. Experimental Results and Discussion

Figure 4-5 presents the variation of sodium concentration at effluent from the series columns and the results of the first set of breakthrough curves. The results indicate that the time to breakthrough is extended with less sodium on the cationic resin. The initial leakage does not vary significantly. In all these cases, the initial sodium loading is distributed evenly throughout the entire column, so there is some sodium on the resin even in the bottom of the bed. In practice, this would result from inefficient resin separation prior to regeneration or from incomplete cationic regeneration. However, it is noteworthy that even with the 9.13% initial sodium bed we remain below 1.0 ppb sodium effluent past three operating days for these 18 inch test columns. The time to 1.0 ppb sodium increases about 0.3 day as the concentration is reduced from 9.13% to 7.39% initial loading, and then about 2 additional days for 2.00% (Table 4-5). In meter deep

commercial columns, the initial sodium effluent is not expected to change significantly, but the time to 1.0 ppb breakthrough would extend some number of days due to the total capacity of the resin in the bed and the shape of the breakthrough curve.

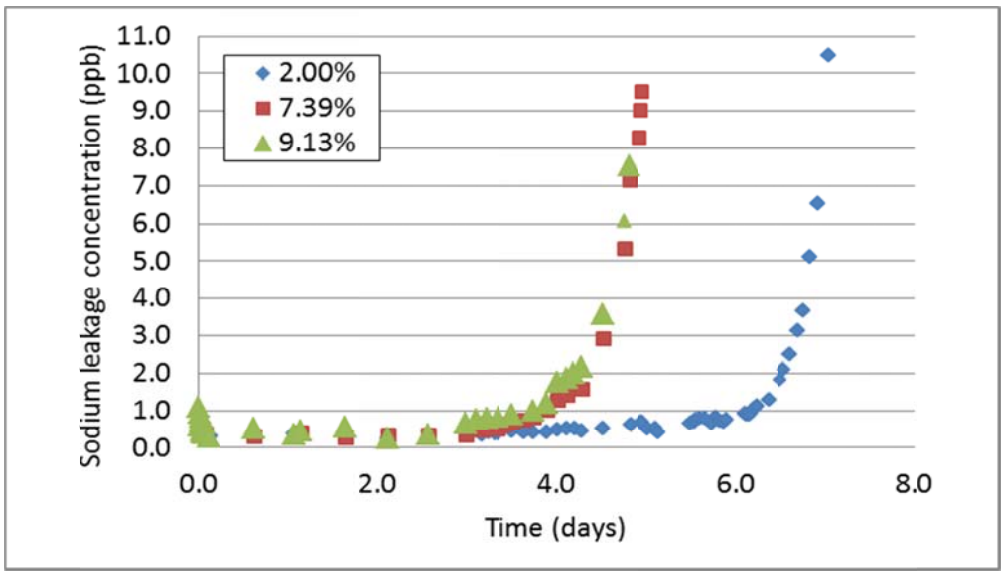

Figure 4-5. Sodium breakthrough curved with different initial sodium loading.

Table 4-5. Time (days) to 1.0 ppb sodium concentration as breakthrough for different columns.

Sodium ratio (%)	Experiment	MBIE prediction
9.13	3.8	5.8
7.39	4.0	6.1
2.00	6.2	7.4

Note in Figure 4-5 that the initial sodium concentrations being measured are about double those predicted by theory (~0.13 ppb). The initial sodium leakage concentration was 0.29 ppb after 170 min later from the beginning for 9.13% initial sodium ratio. The sodium effluent of 9.13% initial sodium bed was continuously higher than 7.13 % and 2.00 % initial sodium on column tests after 2.5 days. In practice, sodium is ubiquitous

and an experimental challenge to minimize from all possible sources. In addition, measurements are being made near the detection limits of the analytical equipment, so relatively high error bars may be expected.

Figure 4-6 shows that conductivities of three different columns have been keeping until each breakthrough. The conductivity of 2.00 % initial sodium loading was higher than 7.13 % and 9.13 % initial sodium on column test.

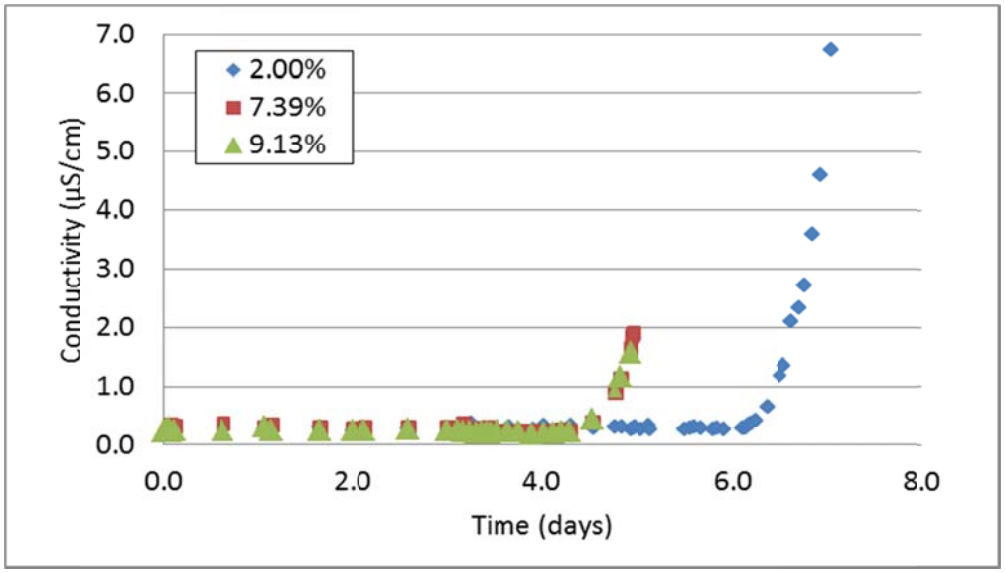

Figure 4-6. Effluent conductivity measurements with different initial sodium loading

Figure 4-7 shows effluent pH is constant until day 4 around pH 8 then increases toward 8.6 for 9.13 % and 7.39 % initial sodium loading and is constant until day 6.2 then increases for 2.00 % initial sodium loading. Although the order was not as predicted, the values are within experimental uncertainty.

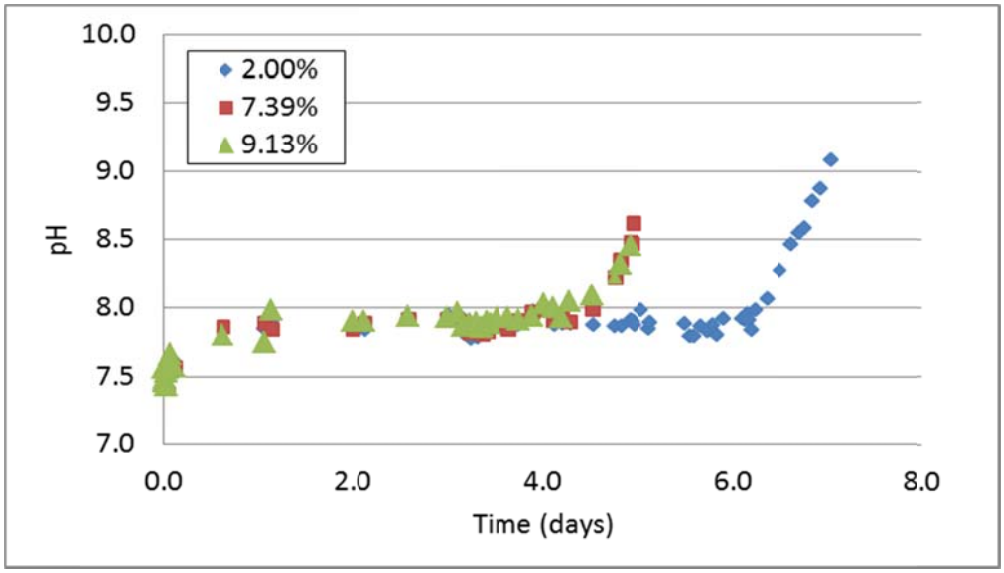

Figure 4-7. pH measurements of effluent with different initial sodium loading

In Figure 4-8, the model predicts ideal bed behavior. As a result, experimentation for 9.13 % initial sodium loading should generate a curve to the left of the prediction.

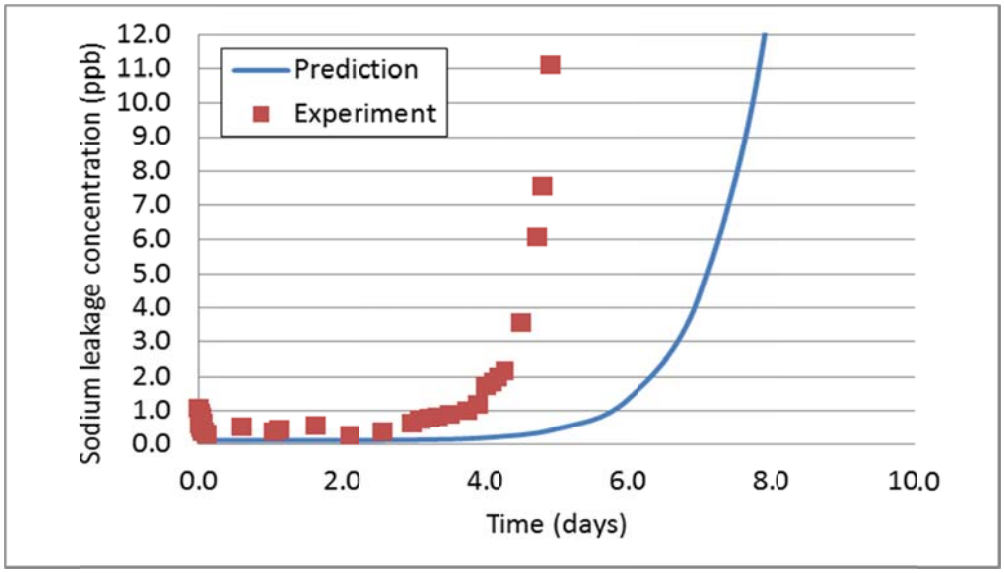

Figure 4-8. Comparing experimental and predicted breakthrough curves from ion exchange mixed beds using 9.13% initial sodium loading

In this case the difference from the 5.8 days to 1 ppb predicted compares with 3.8 days from experimentation is larger than expected. Most likely this is due to laboratory experimentation issues and operation near the detection limits of our sensors.

Figure 4-9 presents the time to reach 1.0 ppb between column experimentation and the prediction at different initial sodium loadings. It shows the time of the experimental results is significantly less than prediction; about 2 days earlier for 9.13 % and 7.39 % initial sodium bed and 1 day earlier for 2.00 % initial sodium bed. The difference between prediction by MBIE package and column test was large for higher initial sodium concentration bed but trends of all different initial sodium loading are similar to prediction. The difference between the curves can be attributed to analytical error bars and the contribution of experimental error from all sources. The actual time will always be less than the predicted case at specific conditions. However, the difference between actual and predicted time can be adjusted from the solubility of feed solution.

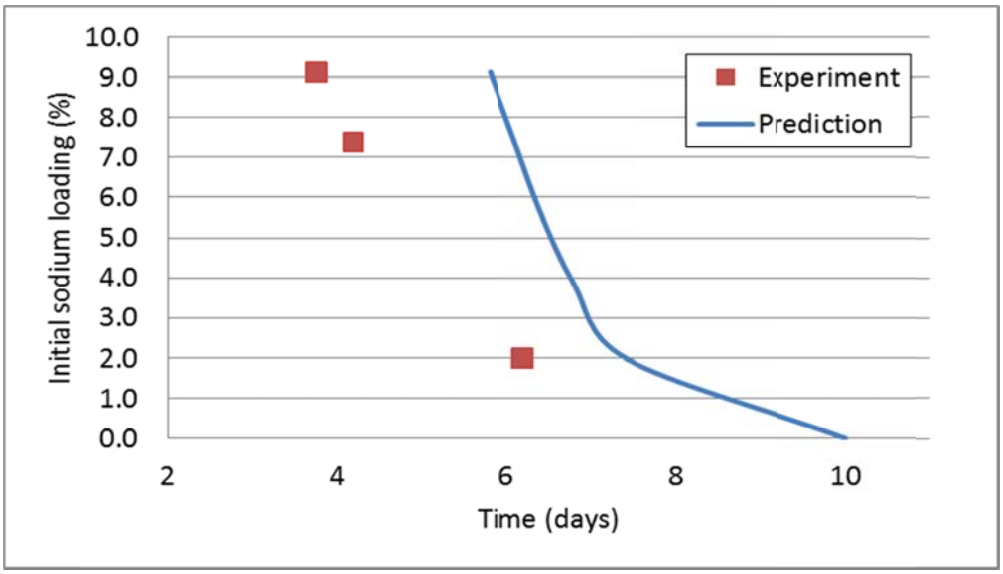

Figure 4-9. The times until 1.0 ppb sodium for both predicted and experimental cases.

4.4.1. Discussion

Mixed-bed ion exchange (MBIE) technology uses a mixture of cationic and anionic resins in a fixed column. The operation period is determined the time until the bed has ionic breakthrough. Regeneration efficiency and mass-transfer properties are the keys to effluent water purity. Inefficient regeneration leads to ionic leakage from the bed. Typically, sodium is the first cation to leave the bed and may contribute to materials problems within the steam cycle.

The driver for breakthrough is the very high concentration of ammonium ions from the use of ammonia as a pH control agent. Under these conditions, ammonium displaces sodium ions and "pushes" them down the column. This is easily seen by the fact that the feed concentration to the columns is 5.0 ppb sodium, yet each test column operation was stopped when sodium concentration reaches 10 ppb. Just ahead of the ammonia loading profile is an enriched sodium region that is a combination of displaced sodium initially on the resin plus the sodium in the feed. When sodium ions leave the bottom of the bed they are either equilibrium leakage (from the resin) or kinetic leakage (from the feed). The higher the initial sodium loading, the more significant equilibrium leakage is in the effluent. After ammonia breakthrough has stabilized the sodium effluent would match the 5 ppb feed concentration.

In order to evaluate the impact of partial bed regeneration, a series of column experiments were performed with different initial sodium loading. Results indicate that time to reach 1.0 ppb sodium leakage is 3.8 days for 9.13 % of cationic sites in the sodium form, 4.0 days for 7.39 %, and 6.2 days for 2.00 %, respectively.

The time to reach breakthrough was shorter with higher sodium loading. Because measurements are made near the minimum detection limit of the analytical equipment, relatively high uncertainty may be expected. Experimental breakthrough occurred sooner than predicted by the more ideal simulation results although the trends were similar, as expected.

REFERENCES

Kunin R., and McGarvey, F. ”Mixed bed deionization,” 1951, United States Patent #2578937.

Chowdiah, V.N., Foutch, G.L., and Lee, G.C. ”Binary Liquid-Phase Mass Transport in Mixed-Bed Ion Exchange at Low Solute Concentration,” Ind. Eng. Chem. Res, Vol.42, 1485-1494 (2003).

Haub, C.E. and Foutch, G.L.” Mixed-Bed Ion Exchange at Concentrations Approaching the Dissociation of Water. 2. Column Model Applications” Ind. Eng. Chem. Fundam., Vol 25, 381-385 (1986).

Sadler, M.A. and Darvill, M.P. “Condensate Polishers for Brackish Water-Cooled PWR’s,” 1986, EPRI NP-4550, Project 1571-5.

ASTM D6071-96, “Standard Test Method for Low Level Sodium in High Water by Graphite Furnace Atomic Absorption Spectroscopy”, Annual Book of ASTM Standards, 1996.

ASTM D859-00, “Standard Test Method for Silica in Water”, Annual Book of ASTM Standards, 2000.

ASTM D4517-04, “Standard Test Method for Low-Level Total Silica in High-Purity Water by Flameless Atomic Absorption Spectroscopy”, Annual Book of ASTM Standards, 2004.

ASTM D4453-02, “Standard Practice for Handling of Ultra-Pure Water Samples”, Annual Book of ASTM Standards, 2002.

Noh, B.I., Yoon, T.K., and Moon, B.H. “The Mixed-Bed Ion Exchange Performance at Ultralow Concentrations: 1. Variable Feed Concentration and Incomplete Mixing of Resins,” Korean J. of Chem. Eng., 13(2), 150-158 (1996).

Zecchini, E.J. "Solutions to Selected Problems in Multicomponent Mixed-Bed Ion Exchange Modeling,” Ph.D. Dissertation, Oklahoma State University, Stillwater, Oklahoma, 1990.

Zecchini, E.J. and Foutch, G.L. ”Mixed-Bed Ion-Exchange Modeling with Amine Form Cation Resins,” Ind. Eng. Chem. Res., Vol. 30, 1886-1892 (1991).

Hussey, D.F. “Development of a multicomponent film diffusion controlled mixed bed ion exchange column model applicable to variable influent systems,” Ph.D. Dissertation, Oklahoma State University, Stillwater, Oklahoma, 2000.

Yi, J. and Foutch, G.L. “True Multicomponent Mixed-Bed Ion-Exchange Modeling,” Reactive Polymers, Invited paper in an issue honoring Michael Streat, Vol 60C, p121-135 (2004).

CHAPTER V

CONCLUSIONS AND RECOMMENDATION

Specific issues in water chemistry for the coal-fired power plant steam cycle system were discussed such as thermal degradation of corrosion inhibitors in supercritical water and sodium removal performance of incomplete cation regeneration.

Chapter 3 presented thermal degradation of amines at supercritical conditions in laboratory scale. The results show all organic amines are not stable at supercritical conditions. Ammonia, acetic acid and formic acid were the main thermal degradation byproducts of all selected organic amines. Unknown nitrogen complexes beside ammonia were expected from the nitrogen balance.

As degradation parameters, temperature and pressure effects were evaluated in supercritical conditions; however pressure was not a significant parameter at elevated temperature, especially the highest temperature. Thermal degradation of amines was dominated by temperature. 5AP shows the slowest thermal degradation rate over the entire range of experimental conditions however it is still highly reactive. No organic amine tested is acceptable for use at supercritical operating conditions. Therefore,

inorganic pH control agents like buffer solutions should be investigated for supercritical conditions.

Chapter 4 presented mixed-bed ion exchange performance for sodium removal in incomplete cation regeneration. Laboratory scale column tests and the mixed bed ion exchange simulation package were used to determine the breakthrough of sodium from MBIE columns with three different initial sodium loadings on the cationic resin. Sodium concentration, conductivity and pH with time were measured for three different columns. Breakthrough times of three different initial sodium loadings were significantly less than the predicted values; however, the trends are in the same order. Differences are likely explained by large error bars for the analytical equipment as a result of operation at very low concentrations and experimental difficulties. According to the results, the time to reach breakthrough was shorter in beds with a higher sodium load.

For the advanced amine selection as a corrosion inhibitor, three main parameters were compared such as stability, volatility and basicity. However volatility of amines may not have an impact in supercritical condition. The investigation of basicity in supercritical may be needed to determine the acid-base behavior.

The reaction experiments define the kinetic constants for amines at supercritical conditions. However, an analysis of the byproducts was limited due to the analytical equipment. Should knowledge of the reaction products be required additional experimentation using more accurate analytical equipment would be needed.

APPENDIX A

EXPERIMENTAL PROCEDURES

Detailed procedures of the amine degradation experiments; amine aqueous solution preparation for the operation of the gas chromatography, the liquid chromatography and the ion chromatography, and sodium effluent experiments: the preparation of inefficient cation regeneration, the preparation of feed solution, the operation sodium analyzer; are given in this section.

Aqueous Amine Solution Preparation

18 mΩ of DI water was prepared and there were 100 ml of glass volumetric flasks used for storage and dilution. All 10 ppm of aqueous amine solution was diluted from 1000 ppm of stock aqueous amine solution first at every experiment as follows Table A-1

1. A hundred ml of volumetric flask was prepared for 1000 ppm of aqueous amine solution. For example, 1000 ppm of aqueous amine was prepared by pipeting 0.115 ml of concentrated ethanolamine with 18 mΩ DI water in 100 ml of volumetric flask. 10

ppm of aqueous amine solution was prepared by pipeting 1 ml of the solution from 1000 ppm of amine solution and adding into 100 ml of volumetric flask with DI water.

Table A-1. The properties of alternative amines

Amine	Manufacturer	Molecular weight (g/mol)	Density (g/ml)	10 ppm (ml)	1000ppm (ml)
Std Ammonia, 10ppm (NH4Cl)	Ricca Chemical Company	53.49	1.53	-	-
Morpholine (MPH)	Acros Organics	87.12	0.99	0.001	0.101
Cyclohexylamine (CHA)	Acros Organics	99.18	0.87	0.001	0.115
Ethanolamine (ETA)	Acros Organics	61.08	1.012	0.001	0.099
3-Methoxypropylamine (MPA)	Aldrich Chemical Company	89.14	0.87	0.001	0.115
5-aminopentanol (5AP)	Aldrich Chemical Company	103.17	0.949	0.003	0.263

2. The actual volume was measured for calculation of accurate amount of aqueous amine solution.

3. Ten ppm of aqueous amine solution was added into the reaction tube as following;

1) Connect tubes for vacuum and nitrogen gas with a reaction tube. Note all valves were closed.

2) Install calculated amount of amine solution into the injection syringe. Check no bubble inside the syringe.

3) Open the valve of nitrogen gas cylinder and purge into the reaction tube for 2 minutes to avoid oxidation.

4) Close the valve of nitrogen and sealed on the cap of a reaction tube.

5) Open the valve of vacuum pump and turn on the vacuum pump with 13.7 psig of capacity.

6) Close the valve of vacuum tube and turn off the pump.

7) Open the valve of injection tube quickly. Thus aqueous amine solution was installed into the reaction tube by vacuum force.

8) Close cap of the reaction tube.

Derivatization Method of Gas Chromatography

Modified derivatization method using benzensulfonyl chloride (BSC) reagent was performed and the procedures were as follow;

1. One ml conical vials with Teflon-lined screw caps were cleaned well, rinsed at least three times with methylene chloride and dried in on oven at temperature greater than 120°C.

2. Samples were stored in the vials and their weights recorded.

3. A 0.2 gram 1M NaOH solution was added to the vials and 50 µl of BSC was added.

4. Vials were placed and shaken for 5 minutes.

5. Vials were placed on a shaker for at least 8 hours.

6. After 8 hours, an additional 0.2 gram 1M NaOH solution was added and the vials placed in an oven at 80°C for at least 8 hours with occasionally shaking.

7. At the end of 8 hours, the samples were inspected for homogeneity. If not homogenous, they were placed in an oven to completely react with unreacted BSC.

8. After cooling in iced water for 5 minutes, 100 µl of methylene chloride was added and vials were shaken vigorously for 5 minutes.

9. A clean syringe was used to select 5 µl of sample for gas chromatography-mass spectrometer (GC/MS) analysis.

10. After sampling, the syringe needle should be clean with a Kimwipe to remove water on the external surface before GC/MS injection.

Sodium Analyzer Operation Procedures

1. Place low concentration solution (100 ppb) and high concentration solution (1 ppm) in the container CAL1 and CAL2, respectively.

2. Perform calibration process with 2-point calibration method.

3. Rinse a polyethylene grab sample bottle well with 18 mΩ of DI water.

4. Fill the sample in the grab sample bottle and place it in container.

5. Select “Grab Sample” option by arrow key.

3. Read sodium concentration after 2 minutes for completely stabilization.

Inefficient Cation Regeneration of Mixed-Bed Ion Exchange

1. Dowex monosphere 650C (H^+ form) and 550A (OH^- form) were prepared and were placed in different plastic containers.

2. Cation and anion resins were washed by 18 mΩ of DI water to ensure removal of impurities on the surface and regenerated by 5% of H_2SO_4 and 6% NaOH aqueous solution, respectively.

3. After regeneration, all resins were washed 8-10 times by 18 mΩ of DI water until conductivity was closed to 18 mΩ of conductivity.

4. A hundred ml of cation resin (H^+ form) was regenerated by 6% NaOH solution and was stirred by plastic stick well. The resins with NaOH solution was keeping in overnight.

5. NaOH solution was removed and cation resin was washed by DI water several times until sodium analyzer indicated almost zero sodium concentration.

6. After regeneration and washing by DI water, 0.115 ml of OH form anion resin was added in 50 ml of mass cylinder and DI water was added at the same time for precipitation or packing well. H form cation resin was also added in the mass cylinder with same way. Calculated volume of Na form cation resin was added to make inefficient cation ratio.

7. Mixed resins were moved into plastic beaker and mixed with plastic stick for complete mixing.

8. Mixed resin of different cation ratio was moved to test columns.

APPENDIX B

THERMAL DEGRATION OF AMINES FROM LIQUID-VAPOR TO SUPERCRITICAL CONDITIONS

The thermal degradation test between 348 to 577°C, representing vapor phase and supercritical phase, about eight kinds of initial 10 ppm aqueous amines; morpholine (MPH), cycloehexylamine (CHA), ethanolamine (ETA), 3-methoxylpropylamine (MPA), dimethylamine (DMA), 5-aminopentanolamine (5AP), N,N-diethylpropylamine (DEEA), and N,N-dimethylpropylamine (DMEA).

Five ml 316 stainless steel tubes also served as reaction chamber. The experimental conditions are following;

B.1. Experimental condition

The inside volume of all tubes was measured initially so that the volume of amine solution could be compensated in the mass measurement. The filled tubes were placed in the oven at an isothermal temperature within the 348 to 577°C range for 10 minutes. After cooling at room temperature the tubes were placed in iced water for at least 10 minutes to ensure sample condensation. Tubes were opened, samples were removed and

analyzed. For MPH, CHA and DMA derivatization for was performed for gas chromatography MSD (GC/MS). For the other amines, samples were analyzed by LC/MS without derivatization.

Table B-1. Amount of amine samples for each operating temperature added to each 5 ml tube.

Desired Temperature (°C) (Actual Temperature)	Mass (g) at 1000 psi (P actual)	Mass (g) at 2000 psi (P actual)	Mass (g) at 3000 psi (P actual)
300 (257)	0.1660 (648, 66% quality)		
400 (348)	0.1230 (896)	0.2841 (1704)	0.5350 (2327)
500 (462)	0.1022 (942)	0.2180 (1863)	0.3523 (2754)
600 (577)	0.0884 (971)	0.1833 (1936)	0.2855 (2893)

B.2. Analysis Devices

B.2.1. Gas chromatography MSD

An Agilent 6890 series gas chromatography and Agilent MSD 5973 mass selective detector of 70eV ionization voltage (MSD) were used and Restek Rtx-5 (30m×0.25mm ID×0.25μm thickness) capillary column for amine analysis. High quality (>99%) helium served as the carrier gas at 1 ml/min. The temperature of MS Source and MS Quad were 230°C and 150°C, respectively. The injection temperature was 250°C, detection and oven temperatures were programmed as 140°C at 3 min, increasing

3°C/min to 210 and increasing 10°C/min to 300°C and remained constant for the final 5 min. Data were evaluated by Agilent MSD Chemstation G1701EA software.

B.2.2. Liquid chromatography MSD

A Shimadzu DGU-20AS liquid chromatography consisted of LC-20AD pump and LC/MS-201D EV were used for some amines analyses. CTO-20A HPLC column (10 cm×4.6mm ID×3µm particle diameter) packed with premier cyano phase was used for separation. CDL temperature was 250°C and oven temperature was set as 40°C. A 0.2% acetic acid solution was used to protonate amines and serve as carrier through the column at 0.3 ml/min. The detector voltage was 1.5kV. For amine analysis, LC/MS solution ver.3 was used.

B.3. Arrhenius Plots

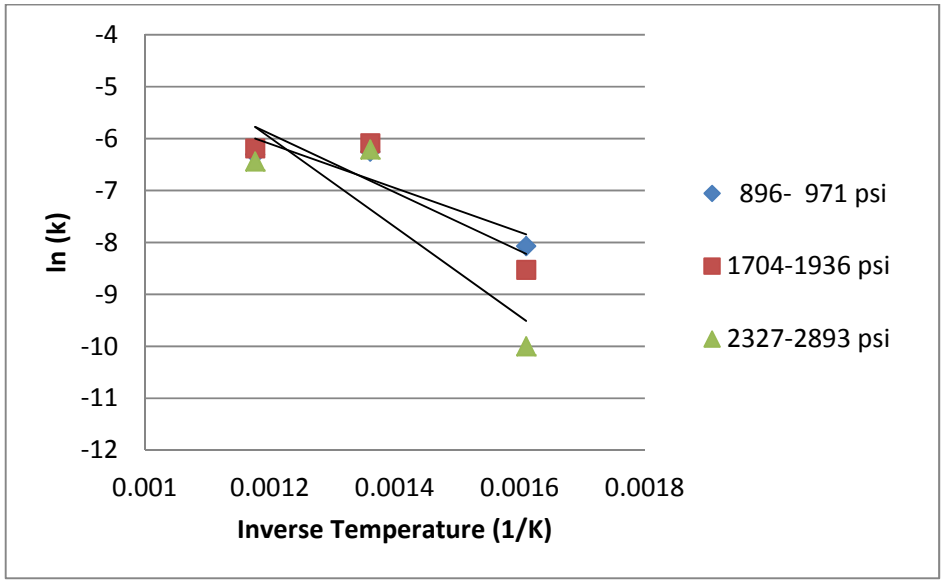

Figure B-1. MPH Arrhenius plots (Temperature from 348 to 577°C)

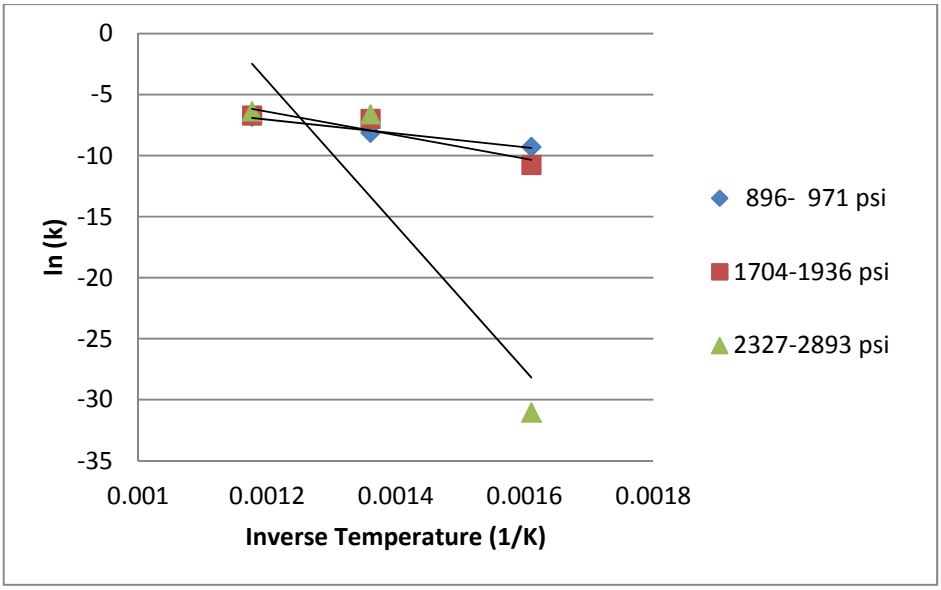

Figure B-2. CHA Arrhenius plots (Temperature from 348 to 577°C)

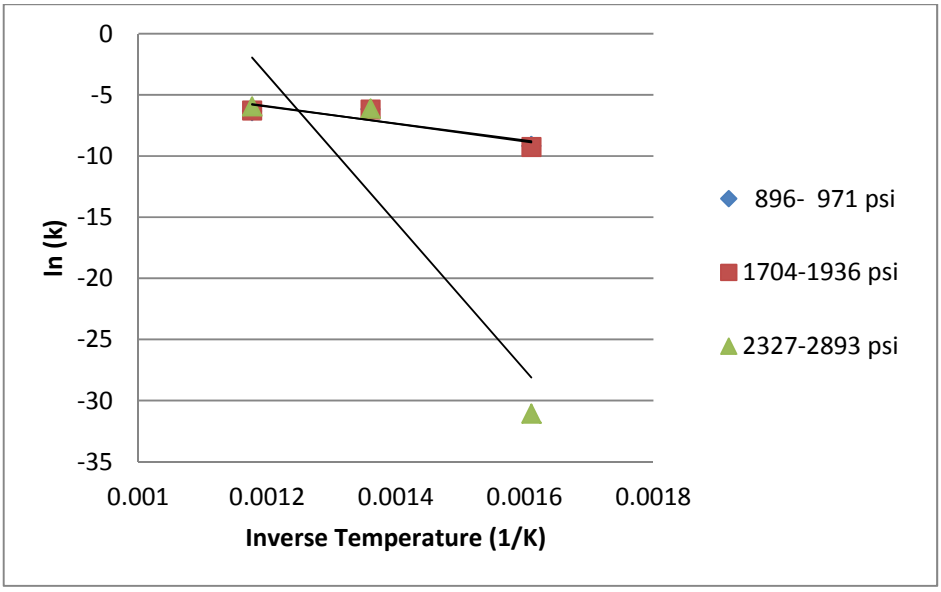

Figure B-3. DMA Arrhenius plots (Temperature from 348 to 577°C)

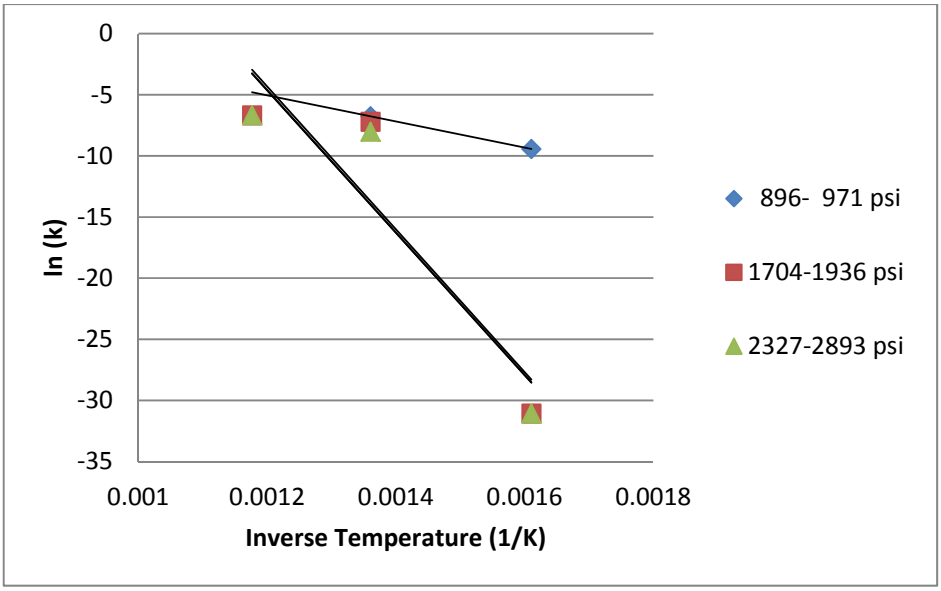

Figure B-4. ETA Arrhenius plots (Temperature from 348 to 577°C)

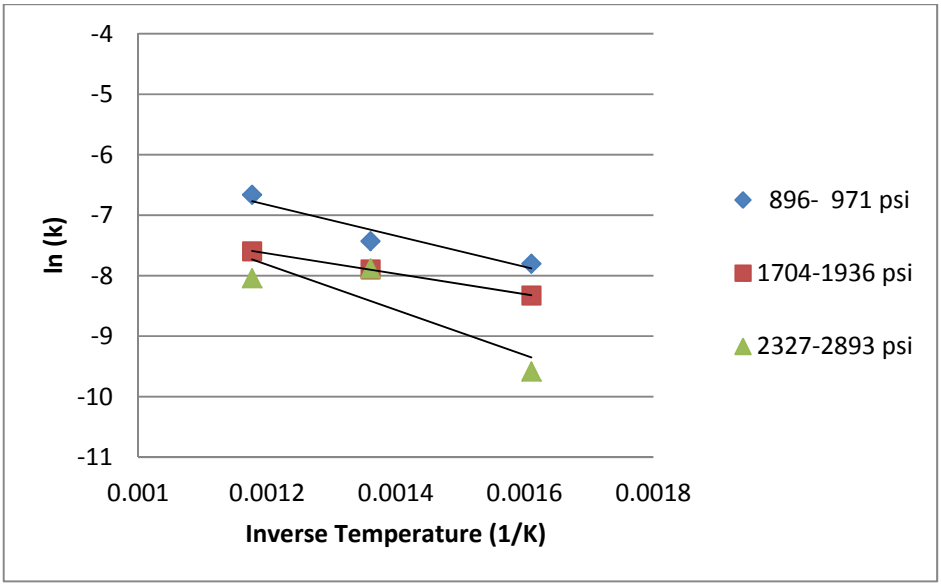

Figure B-5. MPA Arrhenius plots (Temperature from 348 to 577°C)

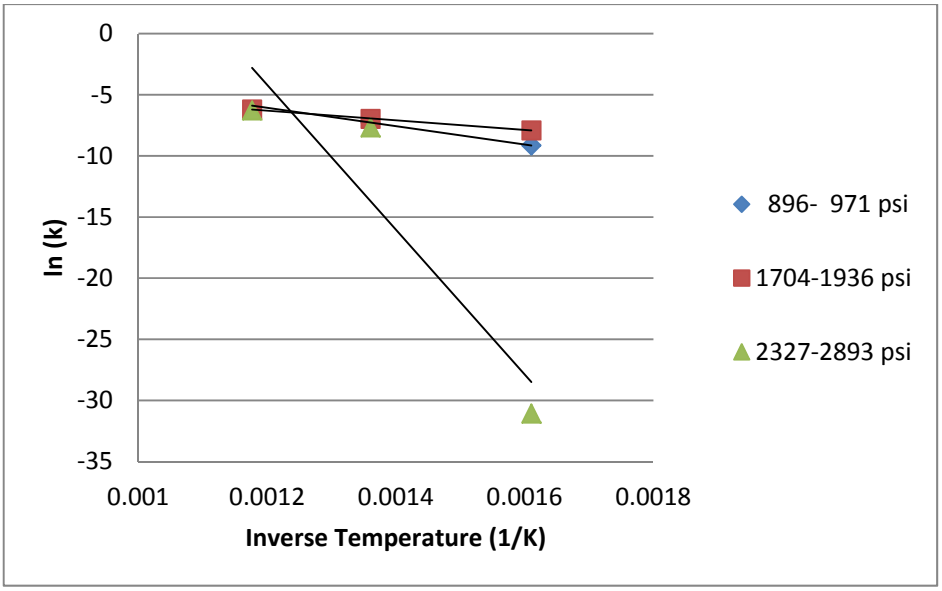

Figure B-6. 5AP Arrhenius plots (Temperature from 348 to 577°C)

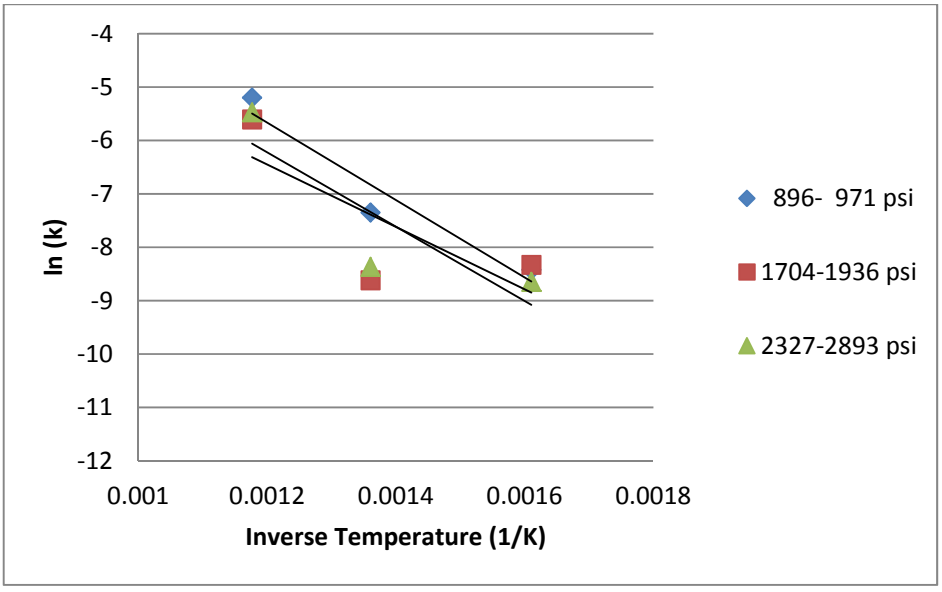

Figure B-7. DEEA Arrhenius plots (Temperature from 348 to 577°C)

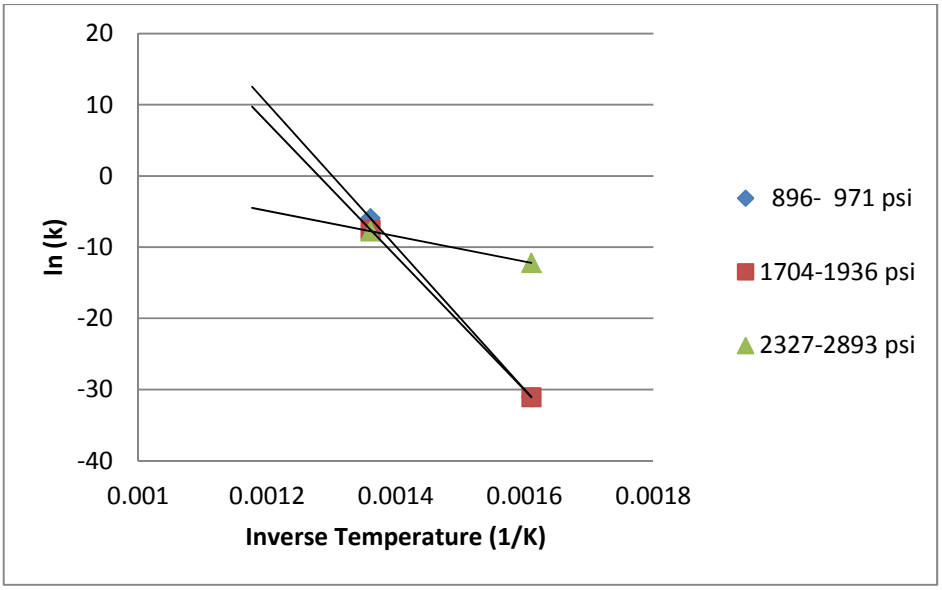

Figure B-8. DMEA Arrhenius plots (Temperature from 348 to 577°C)

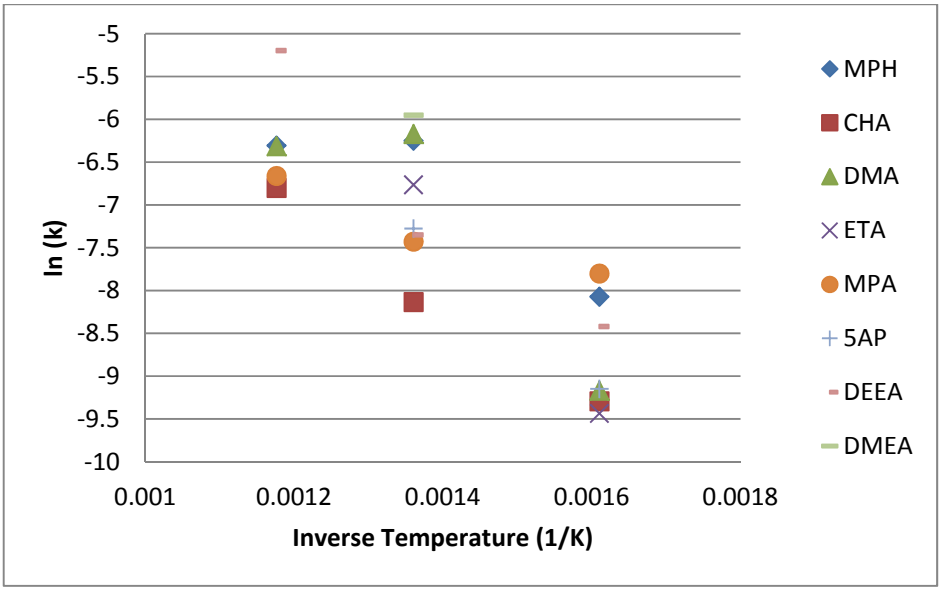

Figure B-9. Arrhenius plots in the range of 896 to 971 psi

(Temperature from 348 to 577°C)

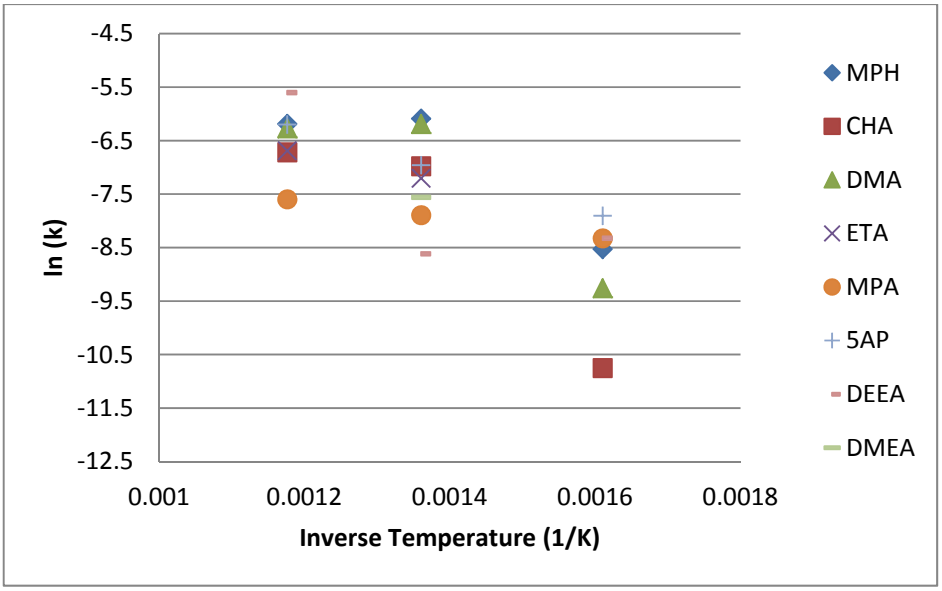

Figure B-10. Arrhenius plots in the range of 1704 to 1936 psi

(Temperature from 348 to 577°C)

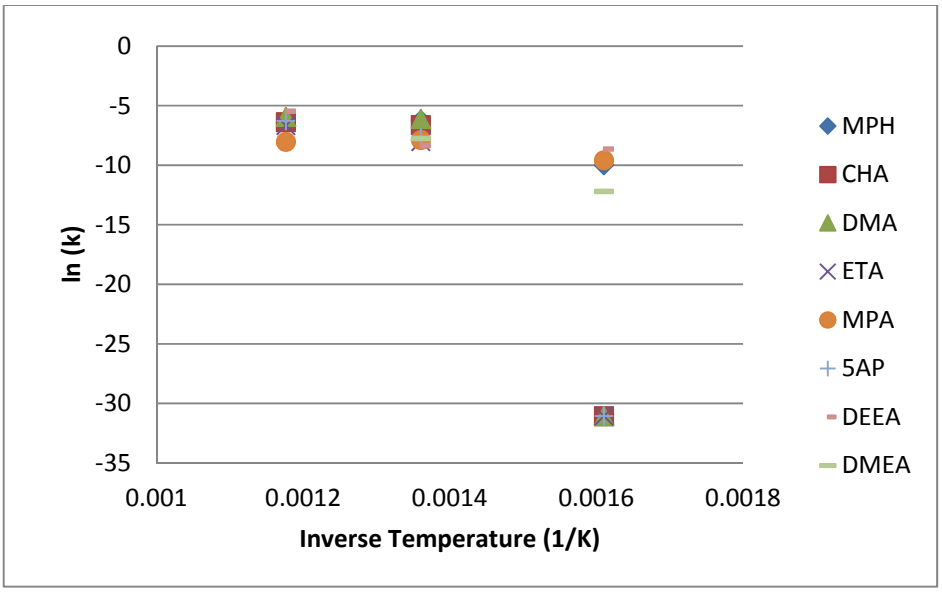

Figure B-10. Arrhenius plots in the range of 2327 to 2893 psi

(Temperature from 348 to 577°C)

VITA

Joonyong Lee

Candidate for the Degree of

Doctor of Philosophy

Thesis: COAL FIRED POWER PLANT WATER CHEMISTRY ISSUES: AMINE SELECTION AT SUPERCRITICAL CONDITIONS AND SODIUM LEACHING FROM ION EXCHANGE MIXED BEDS

Major Field: Chemical Engineering

Biographical:

Personal Data: Born on April 22, 1972 in Incheon, Korea.

Education:

Completed the requirements for the Doctor of Philosophy in Chemical engineering at Oklahoma State University, Stillwater, Oklahoma in May, 2012.

Completed the requirements for the Master of Science in Chemical engineering at Kangwon National University, Chuncheon, South Korea in February, 1997.

Completed the requirements for the Bachelor of Science in Chemical engineering at Kangwon National University, Chuncheon, South Korea in February, 1997.

Experience: Military service, Final Rank; First Lieutenant, Military Officer of 105 mm artillery, 61 Division, South Korea, July 1998 to October 2001

Name: Joonyong Lee Date of Degree: May, 2012

Institution: Oklahoma State University Location: Stillwater, Oklahoma

Title of Study: COAL FIRED POWER PLANT WATER CHEMISTRY ISSUES: AMINE SELECTION AT SUPERCRITICAL CONDITIONS AND SODIUM LEACHING FROM ION EXCHANGE MIXED BEDS

Pages in Study: 133 Candidate for the Degree of Doctor of Philosophy

Major Field: Chemical Engineering

Scope and Method of Study: This study evaluated thermal degradation kinetics of neutralizing amines in steam cycle coal fired power plants operating supercritical conditions as functions of temperature and pressure. The loading amounts of amines into the reaction tube were evaluated by vapor liquid equilibrium (VLE) data from NIST database and the temperature ramp up and down inside tube was applied for evaluation of Arrhenius constants.

Findings and Conclusions: Thermal degradation of neutralizing amines over a range of supercritical temperature (300-600ºC) and pressure (1000-5000 psia) in laboratory scale and found no clear preference based on degradation rates since all neutralizing amines are not stable at high temperature. Ammonia, acetic acid and formic acid were the main thermal degradation byproducts of all selected neutralizing amines and unknown nitrogen complexes beside ammonia were expected from the nitrogen balance. Thermal degradation was dominated by temperature significantly; however pressure effect has an even weak influence on the degradation at the higher temperature. 5AP shows the slowest thermal degradation rate however it is still highly reactive. Hence, no neutralizing amine tested is acceptable for use at supercritical operating conditions.

ADVISER'S APPROVAL: Dr. Gary L. Foutch